EVALUATION OF METHODS USED TO ESTIMATE THE REQUIRED THRUST FORCE FOR DIRECT PIPE INSTALLATION WITHIN CLAYEY SOIL BASED ON CASE STUDIES

by

Stefan J.B. Goerz

A thesis submitted in partial fulfillment of the requirements for the degree of

Master of Science

in

Geotechnical Engineering

Department of Civil and Environmental Engineering
University of Alberta

ABSTRACT

There is a unique technology called Direct Pipe Installation™ (DPI) developed by Herrenknecht Tunnelling Systems (Herrenknecht) which is becoming more a prominent construction method in the pipeline crossing industry. This construction technique is completed by connecting a micro tunnel boring machine (MTBM) to a section of welded pipeline and utilizing a thruster on surface to push the pipeline through the ground while excavation of the soil by the MTBM commences. Evaluation of the total thrust force required to advance the MTBM during DPI construction in clayey soil is the focus of this research.

The current state of practice calculation method was developed by Herrenknecht (Pruiksma, Pfeff, & Kruse, 2012), utilizing concepts from both horizontal directional drilling (HDD) and conventional micro-tunnelling theories. Following extensive review of the calculation method, the most sensitive parameters were determined. Among the most sensitive were the soil to pipeline interface friction, the roller to pipeline interface friction, the coefficient of horizontal earth pressure, and the applied pressure above minimal pressure. Using the data obtained from four DPI construction projects, and geotechnical information from the site characterization documents, total realized thrust was compared to the current state of practice calculation. The calculation over predicted the realized thrust in three case studies (maximum average percent error of 319%), and under predicted in a single case study (minimum average percent error of 9%) while tunnelling in cohesive soil conditions.

Current calculation methods show that friction generation is the main contribution to the total thrust force; however, findings from this research show that the soil reaction at the cutting face is underestimated, and the frictional component may be severely over estimated. Using linear regression analysis for specific sections of the DPI tunnel alignment, the pipeline roller interface,

lubrication and pipeline to soil interface friction values were estimated. As well, the realized front cutting face force determined from the analysis was larger than the predicted value at the same location along the tunnel alignment. As suggested in this research, after decreasing the frictional resistance and increasing the front cutting face force in cohesive soil, it is expected that the total thrust calculation will more closely predict the realized thrust force on future DPI projects.

ACKNOWLEDGEMENTS

I wish to express gratitude to my supervisors, Dr. Michael Hendry and Dr. Alireza Bayat, for their support and assistance during the course of this research. The work presented herein would not have been possible without their guidance.

I would also like to thank Mr. Brent Goerz and Mr. David Dupuis of CCI Inc. for providing financial and technical assistance for this research. The contributions from CCI Inc. were of utmost importance for this research, which could not have proceeded without it, and are appreciated immensely.

Additionally, I would like to thank Dr. Gerhard Lang of Herrenknecht Tunnelling Systems for the conversations and exchange of information exchange during this research. He provided insight that helped with diagnosing some of the information used in this thesis.

Finally, I would like to thank my family for their support, especially the support my wife Samantha Goerz. The positivity and assistance I received was very important to the completion of this thesis work.

TABLE OF CONTENTS

LIST OF TABLES

LIST OF FIGURES

LIST OF SYMBOLS AND ABBREVIATIONS

D_o: outer diameter of pipeline [m]

$D_{o,m}$: outer shield diameter of the micro-tunnelling machine [m]

EI: bending stiffness of pipeline [Nmm^2]

E_o: applied pressure above minimal pressure [kPa]

f_1: frictional coefficient between pipeline and surficial rollers [ ]

f_2: frictional coefficient between pipeline and lubricant fluid [N/m^2]

f_3: frictional coefficient between soil and pipeline interface [ ]

F: total thrust prior to buckling of pipeline [kN]

F_{buckle}: Friction due to buckling of the pipeline [kN]

F_f: front force [kN]

F_{lb}: frictional force between pipeline and lubricant fluid [kN]

F_{mec}: required mechanical force [kN]

F_p^0: frictional force prior to curved section [kN]

F_p^{end}: frictional force following curved section [kN]

F_r: roller friction force [kN]

g_{eff}: buoyant weight of pipeline per unit length [N/m]

g_{opw}: upward force of the pipeline [N/m]

g_p: weight of pipeline per unit length [N/m]

k: soil stiffness [MPa]

K: horizontal earth pressure coefficient [ ]

L: total pipeline length [m]

L_b: length of pipeline inside of borehole [m]

L_{out}: length of pipeline outside of borehole [m]

L_t: length of pipeline inside borehole over which there is no contact with tunnel wall [m]

q: soil reaction perpendicular to pipeline [kN]

q_{max}: maximum soil reaction near the end of the bend [Pa]

R: design radius of curved tunnel alignment [m]

r_e: outer radius of pipeline [m]

ROA: rate of advance [mm/min]

r_{tunnel}: radius of tunnel [m]

s: distance along tunnel alignment [m]

u: pore pressure [kPa]

w_{gap}: width of overcut between tunnel wall and pipeline [m]

α: angle change along curved section [radians]

ΔF_p^{bend}: frictional force at beginning or end of curve [kN]

ΔF_w: frictional force of straight section [kN]

γ_b: bulk unit weight of soil [kN/m^3]

γ_{fl}: unit weight of lubricant fluid [kN/m^3]

μ: frictional coefficient between soil and pipeline interface (*analogous to* f_3) [ ]

Ø' : effective friction angle of soil [degrees]

$\sigma'_{h,min}$: minimum horizontal earth pressure [kPa]

σ_{sup}: required support pressure [kPa]

CHAPTER 1. INTRODUCTION

1.1 BACKGROUND

1.1.1 General

There are various construction methods which utilize a Micro Tunnel Boring Machine (MTBM) to install medium to large diameter utilities by trenchless underground excavation. Some of these methods may include Pipe Jacking, Pilot Tube Micro Tunnelling, or a more recently developed construction method called Direct Pipe Installation™ (DPI). In all these construction methods, a thrust/jacking force is required to progress the MTBM while it excavates the soil or rock ahead. The magnitude of thrust force in cohesive soil may be dependent on geological, machine or operational dependant factors. DPI methods are the main source of information referenced in this document for reasons outlined in the following sections.

1.1.2 Direct Pipe Installation™

DPI, developed by Herrenknecht Tunnelling Systems (Herrenknecht), is a method of installing steel pipeline crossings, ranging in diameter from 914.4 mm to 1524 mm (36” to 60”), by thrusting a guidable, slurry supported MTBM along a pre-determined path (Pfeff D. , 2013). An illustration of a typical DPI launch area is shown on Figure 1.1, below.

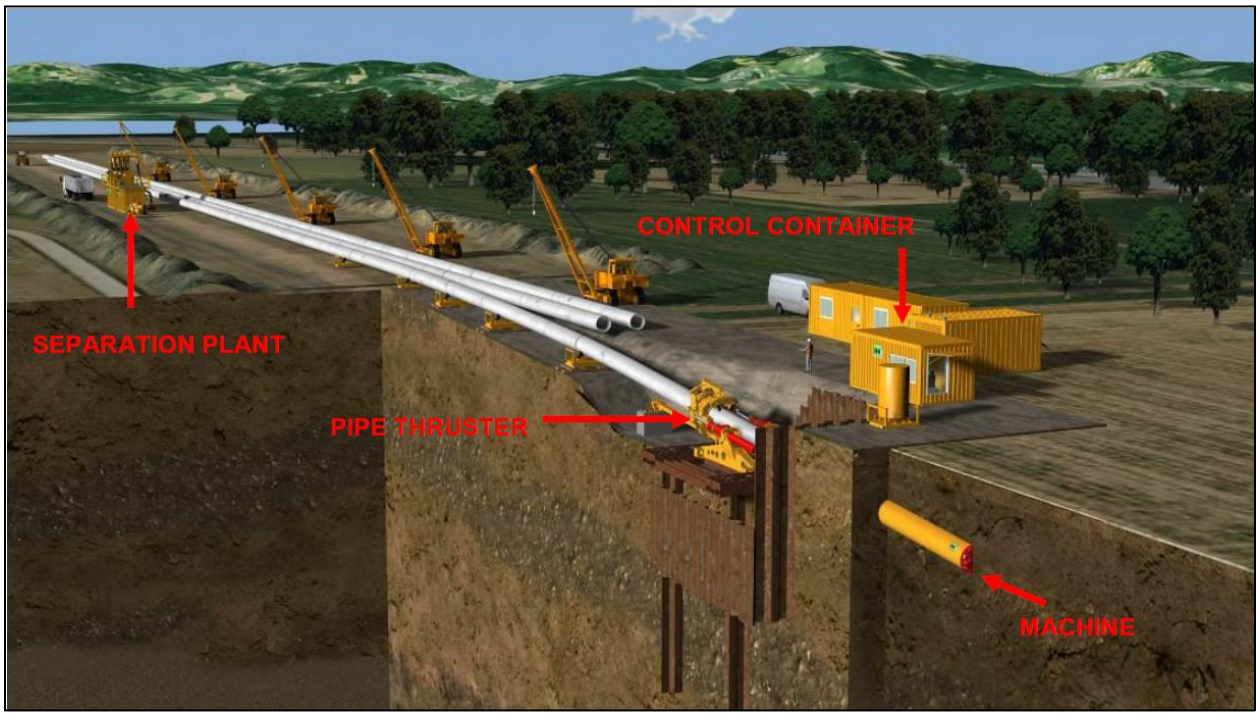

Figure 1.1: Typical DPI worksite showing equipment at the launch area (Pfeff D. , 2013).

The product pipeline section is prepared, welded to the proper length, and laid on surface. The MTBM is connected to the front of the pipeline section. The MTBM is typically 25 mm larger, radially, than the product pipeline creating an overcut. A stationary thruster, developed by Herrenknecht, is situated at a launch location where the MTBM and pipeline are threaded through the clamping inserts of the thruster at the design angle. The vulcanized rubber clamping inserts grab the outer surface of the pipeline and push the MTBM and pipeline section forward. Additionally, the DPI system uses a bentonite fluid injected within the annular space created by the overcut. The bentonitic fluid is under pressure, intended to support the soil along the borehole wall and provide lubrication during tunnelling operations.

Although construction costs are currently higher than other pipeline crossing methods, DPI is gaining industry-wide traction because of its versatility in all soil types. Additional benefits of this method include a smaller work space, shorter timelines for project completion, and shallower depth of cover requirements for installation.

1.2 PROBLEM STATEMENT

DPI is becoming a highly sought-after option for constructing pipeline crossings. Designers facing the challenges of engineering this recently developed construction method need to ensure overstressing of the pipeline does not occur. In addition, proper equipment needs to be selected for a successful project completion. There are various components which complicate the design of a DPI project, one being the estimation of the total thrust force required. All of these factors contribute to a successful operation of this prospering technology.

Many engineers' experience is required to make sure that a certain technology is working in order for others to benefit from it. For instance, Pruiksma, Pfeff, & Kruse (2012) have developed a guideline for calculating the required thrust force using conventional theories from micro-tunnelling and horizontal directional drilling, herein referred to as the current state of practice calculation method. This calculation method is used by designers all over the world to evaluate the required thrust force during DPI.

The aforementioned method has so far proved to be successful. However, the current state of practice for estimating the total thrust force during DPI construction relies heavily on recommended frictional coefficients. Using these recommended coefficients, in combination with the estimate of force at the MTBM cutting face, the current state of practice does not predict the realized thrust force accurately throughout the entire tunnel alignment.

1.3 RESEARCH PURPOSE

The purpose of this research is to evaluate the calculation method used to estimate the total required thrust force in DPI and compare the estimate with realized values during case studies. The amount of frictional resistance and cohesive soil reaction at the cutting face of the slurry supported micro tunnel boring machine in DPI. This in turn helped to better understand the effects that soil properties, machine parameters, and design geometry have on the thrust forces. It is important to understand the required thrust forces in order to prevent damage to the product pipeline during installation, as well as to ensure suitable equipment for construction. Additionally, a better understanding of the factors influencing the rate of tunnel advance while tunnel boring within cohesive soil strata should allow both designer and contractor to strive for optimum project success. Finally, both cost and other additional risks associated with DPI projects would be reduced as more information detailing thrust forces becomes available.

1.4 HYPOTHESIS

It follows from the previous section that the coefficients and the force on the MTBM cutting face can be improved to estimate the thrust force more reliably through the entire tunnel alignment in DPI construction.

Anecdotal evidence from discussions with operators, construction specialists, and attending various DPI presentations lead the author to the following hypothesis:

The frictional contribution is overestimated, and the amount of resistance from the force at the MTBM cutting face is underestimated, in cohesive soil using the recommended parameters for calculating the total thrust force in the current state of practice calculation method.

1.4.1 Research Objectives

To support my hypothesis, the objectives of the research contained in this thesis are as follows:

- Review and evaluate the current state of practice calculation method for estimating total thrust force during DPI construction, and determine which parameters have the greatest influence on the result;
- Compare the amount of total thrust force realized during DPI construction to the estimate and evaluate discrepancies;
- Assess and evaluate the contribution of the frictional components to the total thrust force, including modification of the frictional coefficients;
- Assess the contribution of the force at the MTBM cutting face to the total thrust force and evaluate and quantify the differences from realized DPI construction data.

1.5 THESIS STRUCTURE

This thesis is organized according to the following structure:

Chapter 1. Introduction: This chapter presents the purpose of the thesis, background of the DPI construction methods, and the importance of more accurately predicting the total thrust force.

Chapter 2. Literature Review: This chapter reviews findings from literature pertaining to the application of DPI.

Chapter 3. Case Study Review - This chapter reviews and describes findings from four case studies forming a basis for the data used and conclusions derived from this research.

Chapter 4. Evaluating the Current State of Practice Calculation Method and Comparison to Realized Thrust during Case Studies - This chapter reviews the current state of practice calculation method and compares the calculated total thrust to the realized thrust from case study data. Additionally, evaluation of the data fit using percent error analysis is completed.

Chapter 5. Evaluating Contribution of the Total Thrust Force Components - This chapter evaluates the frictional and the force at the MTBM cutting face components of the current state of practice calculation method using the information obtained from the case studies.

Chapter 6. Results and Discussion - This chapter summarizes the findings obtained from the previous sections and provides commentary on the results.

Chapter 7. Conclusions and Recommendations - This final chapter summarizes the entire body of research, lists the main conclusions and contributions of the thesis, and suggests recommendations for future research on this subject.

CHAPTER 2. LITERATURE REVIEW

2.1 INTRODUCTION

Pruiksma, Pfeff, & Kruse (2012) investigated the thrust force in DPI using ABAQUS finite element software package. The authors found that, according to the software, the five (5) mechanisms that contribute to the thrust force are as follows: friction behind the thruster on rollers, friction between the pipeline and lubricant fluid, front force at the MTBM face, friction between the pipeline and tunnel wall, and friction due to buckling. This coincides with the focus of this thesis; the frictional effects from the pipeline soil, pipeline lubricant fluid, and pipeline roller interfaces as well as the front force at the MTBM cutting face.

2.2 FRICTIONAL RESISTANCE

During DPI, frictional forces develop along the length of tunnel alignment as the MTBM advances. The magnitudes of frictional forces are dependent on the interface shear of the pipe material, and the soil type along the tunnel sidewall. Interface shear characteristics were examined by Iscimen (2004) for multiple curved materials representing pipes. Surface roughness of Hobas™ FRP, polycrete, steel, wet-cast concrete, Packerhead™ concrete, and vitrified clay were examined, and the frictional resistance between these materials and both Ottawa and Atlanta blasted sands was determined. This research provides evidence that surface roughness of pipe material has a large influence on the amount of frictional resistance. Additionally, Iscimen suggests a “bi-linear” friction envelope is present where the interface friction is unable to increase past the internal friction angle of the soil with which the material is in contact, providing insight into maximum frictional resistance in unlubricated sections of DPI alignments. The relationship is shown on the illustration in Figure 2.1, below.

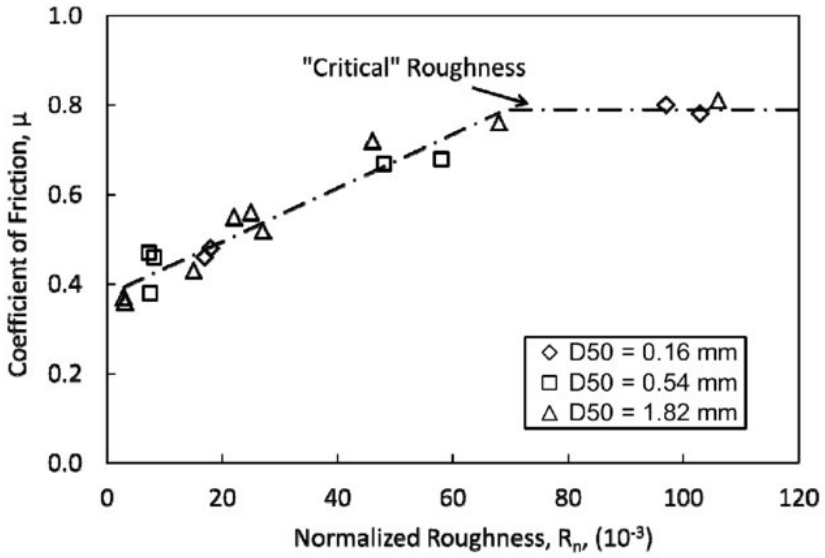

Figure 2.1: Illustration of the Bi-Linear relationship between coefficient of friction and surface roughness (Uesugi & Kishida, 1986) (Iscimen, 2004) .

The residual friction angle to be used in the jacking or thust force calculations for the soil which contacts the pipe is recommended by Bennett and Cording (2000) and Staheli (2006). Using the residual friction angle to calculate the fricitonal resistance along the DPI alignment lowers the amount of friction obtained in an unlubricated section. However, it is expected that in cohesive soil most, if not all, of the tunnel drive is lubricated in a mass lubrication scenario. Marshall (1998) suggests that, depending on its stability, lubrication introduced in cohesive soil can work its way over the whole pipe surface, resulting in reduced friction along the entire length. His findings indicate that the average frictional resistance drops rapidly once bentonite lubrication is introduced; the decrease was found to be between 44% and 90% in Marshall's research. Additionally, the friction angles in cohesionless soils were 38 degrees and 37.5 degrees, respectively, falling to 14 degrees when bentonite fluid is injected as jacking forces become excessive, which is also known as partial lubrication. When using mass lubrication, where bentonite fluid is injected into the overcut continuously, results in friction angles close to zero.

Staheli (2006) replicates these findings in her Ph.D thesis. She provides evidence in various case studies that there is marked difference in frictional resistance for lubricated versus non-lubricated intervals. Review of the case study information revealed that by applying mass lubrication, 90% reduction in jacking forces were observed in sandy soils. The information from case studies reviewed by both Marshall (1998) and Staheli (2006) reveal that mass lubrication techniques used in DPI likely reduce the amount of pipe to soil interface frictional resistance by up to 90%.

Extensive monitoring of lubrication pressure in the annulus of the tunnel provides valuable information during DPI construction. The effect of lubrication pressure was examined by Namli & Guler (2017), and their work suggests that the benefits of bentonite application under constant pressure can be achieved with minimal injection pressures. Namli & Guler suggest that it is not the amount of pressure that reduces pipe-soil friction to 10% of its original value; the mere presence of pressure ensures that bentonite is coating the entire pipe surface area. If pressure is present in the DPI machinery lubrication chamber, it is likely that the entire surface area is coated in lubrication, and the interface friction is comprised entirely of pipe-bentonite, rather than pipe-soil (Namli & Guler, 2017). A pipe to soil interface comprised entirely of bentionite reduces the frictional resistance immensely.

A document completed in 2013 by Herrenknecht examines data from multiple case studies of DPI construction and compares their maximum jacking loads per total length of alignment (Pfeff D. , 2013). In this study, Pfeff compiles the total thrust data and both the maximum thrust and the thrust at the end of alignment for various diameters of pipeline that were previously recorded. Following, she computed the resistance force per length and resistance force per surface area. The frictional data compiled in this document considers the total thrust data as the frictional resistance and does not separate force originating from the face and force from frictional

resistance. Additionally, the document separates and reviews the frictional resistance calculated using this methodology for projects constructed within various geotechnical conditions. Interestingly, the total force per meter length in the case studies of primarily clay strata were among the lowest maximum thrust forces, as well as the lowest thrust at the end of the alignment, ranging from 2.64 kN/m to 3.47 kN/m, and 1.80 kN/m to 2.78 kN/m, respectively. The data reviewed and completed by Pfeff in 2013 is represented in Table 2.1 below.

Table 2.1: Realized thrust data from previously completed DPI projects (Pfeff D. , 2013)

Case No.	Geotechnical Conditions	Diameter (in.)	Length (m)	Push Max. (kN)	Absolute Max. Push (kN/m)	Max. Friction (kN/m^2)	Push force at end of alignment (kN)	Average Push at end of alignment (kN/m)	Friction at end of alignment (kN/m^2)
1	Sand/Gravel	48	464	2256.3	4.86	1.27	981.00	2.11	0.55
2	Sand	48	362	1569.6	4.34	1.13	1275.30	3.52	0.92
3	Sand	48	435	1765.8	4.06	1.06	1471.50	3.38	0.88
4	Sand	48	545	3041.1	5.58	1.46	2354.40	4.32	1.13
5	Sand	48	516	1814.85	3.52	0.92	1569.60	3.04	0.79
6	Clay	48	394	1177.2	2.99	0.78	784.80	1.99	0.52
7	Clay	48	600	2060.1	3.43	0.90	1667.70	2.78	0.73
8	Clay	48	372	981.0	2.64	0.69	735.75	1.98	0.52
9	Clay	48	707	2452.5	3.47	0.91	1275.30	1.80	0.47
10	Sand	48	248	882.9	3.56	0.93	784.80	3.16	0.83
11	Mixed Soft Soils	56	860	5395.5	6.27	1.40	4414.50	5.13	1.15
12	Mixed Soft Soils	56	860	6867	7.98	1.79	4905.00	5.70	1.28
13	Clay (with silt and stones)	42	471	1765.8	3.75	1.12	1373.40	2.92	0.87
13	Clay (with silt and stones)	42	680	2060.1	3.03	0.90	1471.50	2.16	0.65
13	Clay (with silt and stones)	42	570	2403.5	4.22	1.26	1471.50	2.58	0.77
13	Clay (with silt and stones)	42	718	2550.6	3.55	1.06	1962.00	2.73	0.82
13	Clay (with silt and stones)	42	654	2354.4	3.60	1.07	1765.80	2.70	0.81
13	Clay (with silt and stones)	42	622	3825.9	6.15	1.84	3531.60	5.68	1.69
14	Clay (with Rock and Gravel)	42	410	1765.8	4.31	1.29	588.60	1.44	0.43

The document by Pfeff D. (2013) also suggests that the total force per unit of pipe surface area, which Pfeff defines as friction, should range between 0.7 kN/m^2 and 0.9 kN/m^2.

2.3 FRONT FORCE AT MTBM CUTTING FACE

In DPI, the calculation considers the front face force analogous to the face pressure required to stabilize the excavated soil. Various models describe the “lower bound”, or required support pressure, at the tunnel face. To form a basis for face support pressure calculations, the at rest earth pressure coefficient is used to quantify the horizontal stress acting on the tunnel face (Babendererde & Elsner, 2014). This model was improved to act as a sliding wedge, which reduced the face pressure in front of the tunnel because of wedge movement. The value of the coefficient of earth pressure at rest was modified to reflect this assumption by instead including the active coefficient of earth pressure. Babendererde & Elsner (2014) also suggested that through construction experience, tunnel engineers soon realized that required face pressure was much lower than these model calculations, even when active earth pressure calculation was considered. Using these models to calculate the amount of force on the MTBM face adds to the total thrust force required during DPI construction.

Other methods to calculate the required face pressure for use in DPI construction estimate the front face force are present in the industry. Zizka & Thewes (2016) recommend calculating face support pressure during shield tunnelling by using limit equilibrium methods (Horn,1961) to find the required face support pressure based on assumptions about the contact area by using a square of side length equal to the shield diameter (Jancsecz & Steiner, 1994) or a square of equal area to the shield (Anagnostou & Kovari, 1994). Figure 2.2, below, shows the first limit equilibrium failure mechanism suggested by Horn (1961), that assumes a sliding wedge in front of the tunnel face loaded by a rectangular prism.

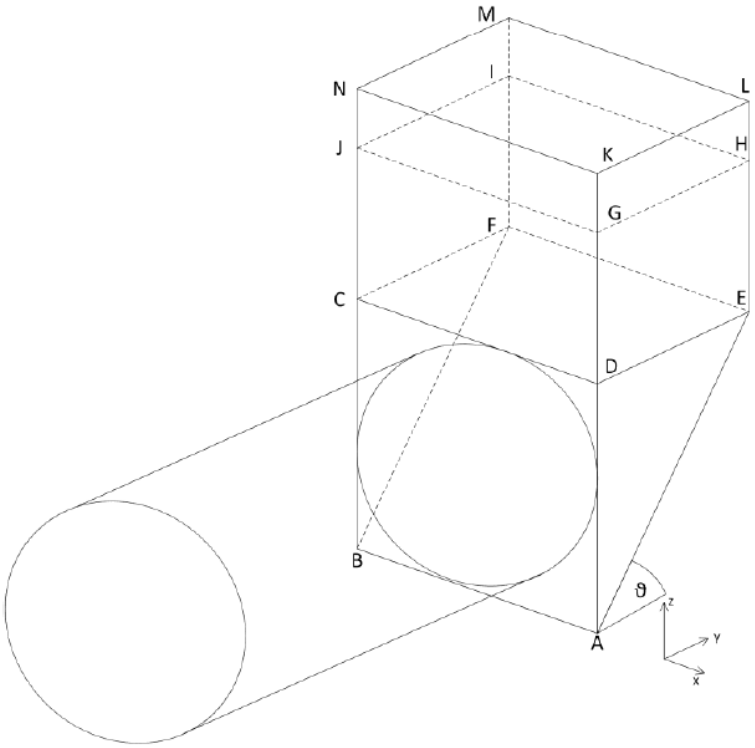

Figure 2.2: Horn's limit equilibrium failure mechanism as represented by the wedge (ABCDEF) and prism (CDEFKLMN) considering groundwater level (GHIJ) (Zizka & Thewes, 2016).

Zizka and Thewes (2016) also suggest empirical stability ratios as a means of calculating the face support pressure. According to the authors, the stability ratio method for calculating the required face pressure generally produces a more realistic value for tunnel drives in clayey soil. However, using these methods to determine face pressure for DPI tunnel diameter sizes does not provide reasonable results.

The reduction in required face pressure is best explained using Terzaghi's arching theory (Terzaghi, 1936), which proves a reduction in earth pressure occurs at depth. In his famous "Trap-Door Experiment", Terzaghi quantified the arching phenomenon for the first time by measuring the load on a trap door in both dry and saturated sands during mobilization. His results showed

that the effect of arching was prominent in both dense and loose sand. The reduction in earth pressure following soil mobilization indicates that the required face pressure in DPI may not be the largest contributor to the force at the cutting face, but that the amount of additional force required to advance the machine could be a more substantial component.

2.4 SUMMARY

The literature relating to the calculation of the required thrust force for the DPI method have been reviewed in this chapter. The conclusions of the literature review include:

- The mechanisms within the current state of practice calculation method were identified by Herrenknecht (Pruiksma, Pfeff, & Kruse, 2012) using finite element analysis performed in ABAQUS for the DPI method. The numerical model suggested that five mechanisms contribute to the total thrust force and can be grouped into frictional and front cutting face force components. An analytical calculation for DPI was developed using the information from the numerical model to provide designers with a means for estimating the total thrust force. At the present time, this analytical method is considered the industry state of practice.
- Experimental results of soil pipeline interface friction suggest a bi-linear frictional envelope, where the frictional coefficient is limited to the soil friction angle (Iscimen, 2004). These findings are useful for assessing the maximum frictional resistance generated from unlubricated sections of the DPI alignment.
- Residual soil friction angles provide a reasonable assessment of the frictional resistance in unlubricated or dry sections of tunnel drives (Bennett & Cording, 2000) (Staheli, 2006).
- For tunnel alignments passing through cohesive soil, it is likely that lubrication surrounds the entire pipe surface, thus the frictional effects of the soil along the tunnel wall are

reduced (Marshall, 1998). Additionally, application of mass lubrication techniques, similar to those used in DPI construction, reduce the jacking force by up to 90% (Staheli, 2006), and it is not necessarily the lubrication pressure that reduces the frictional resistance, but the mere presence of the bentonite lubrication adhering to the soil on the tunnel wall (Namli & Guler, 2017) .

- Total thrust force compiled for DPI construction is smaller in clayey soil than in granular soil (Pfeff D. , 2013) ranging from 2.64 kN/m to 3.47 kN/m, and 1.80 kN/m to 2.78 kN/m for maximum thrust forces and thrust at the end of the alignment, respectively. Additionally, the frictional resistance as defined by Pfeff ranges from 0.7 kN/m^2 to 0.9 kN/m^2 for the case studies examined.

- The active earth pressure model (Babendererde & Elsner, 2014), or limit equilibrium methods (Zizka & Thewes, 2016) are used to calculated the required face pressure to stabilize the cutting face. For large diameter tunnel drives in cohesive soil the use of stability ratio methods is recommended (Zizka & Thewes, 2016), however the empirical stability ratio method does not work well for DPI tunnel diameters.

- Reduction of the of the active earth pressure calculation incorporating arching theory (Terzaghi, 1936) provides the best estimate of required face pressure to stabilize the cutting face (Babendererde & Elsner, 2014).

CHAPTER 3. CASE STUDY REVIEW

3.1 INTRODUCTION

This chapter presents DPI case studies obtained for review and evaluation. The review describes the specific project alignment, geotechnical considerations, and considerations during construction to provide background information and form a basis for the evaluation of thrust information contained in the following chapters.

3.2 CASE STUDY 1 - AKA “THE FLAT TYPICAL DPI”

3.2.1 Project Description and Design

The first case study examined was a DPI crossing located in Ontario, Canada. The project depicted in this case study was a crossing of a future development area with relatively level to gently sloping terrain and no water body influence. A 1066.8 mm (42 inch) diameter pipeline was installed within an 1110 mm (43.7 inch) diameter tunnel. The designed length of the tunnel alignment was 286 m, however due to excavation placements and field decisions; the final tunnel length was 266 m long. This alignment included a launch angle of 5 degrees, approximately 11.5H : 1V slope. A 38 m length of 1524 mm (60 inch) diameter steel surface casing, lined with High Density Poly Ethylene (HDPE), was installed to ensure proper depth of soil cover was maintained during the beginning of the drive. The steel casing was HDPE lined, to ensure the final product pipeline was not damaged. This curved drive had geometric changes of a 1100 m radius that connected the initial launch slope to a horizontal baseline. Following the horizontal baseline, an additional curved section with a 1100 m radius was required, connected to a final tangent at an angle of 6 degrees, or 9.5H : 1V, exiting into the receiving pit. The maximum depth

of tunnel crown below ground surface for the “as-constructed” tunnel was about 8.7 m below ground surface. All curved portions of the tunnel drive were vertical, and no horizontally curved segments were planned. A pictorial representation of the DPI alignment is shown in Figure 3.1, below.

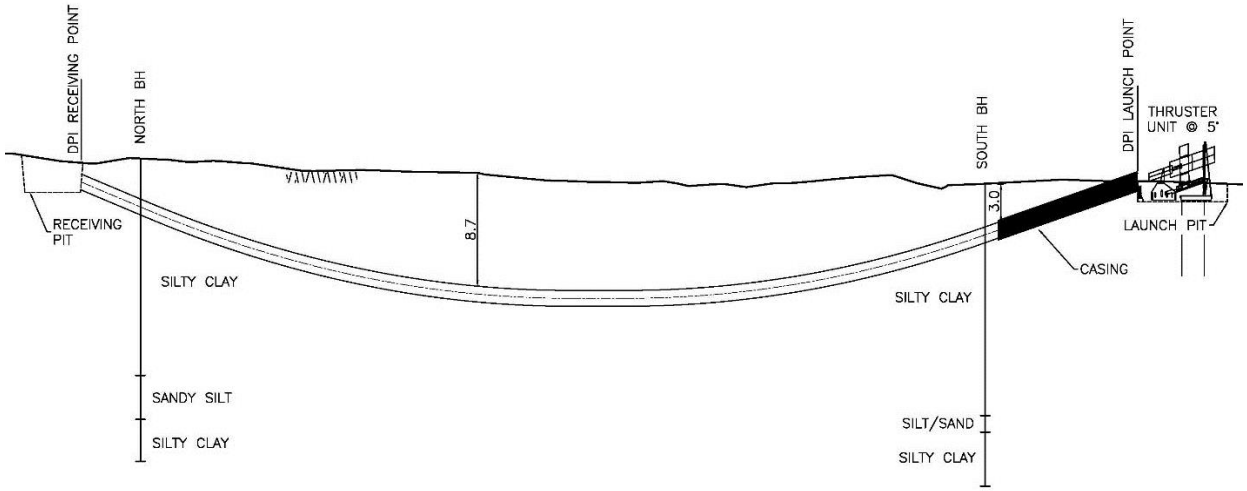

Figure 3.1: Pictorial representation of the Flat Typical DPI alignment. Adapted from case study design drawing prepared by CCI Inc.

The drawing in Figure 3.1 was based on a combination of factors, including surface geometric constraints, pipeline stress considerations, factors associated with constructability, and geotechnical considerations.

3.2.2 Geotechnical Conditions along Alignment

The Flat Typical DPI was a tunnel constructed primarily through silty clay north of Toronto, Canada. A geotechnical evaluation of site conditions was completed by the consultant for the project and geotechnical information contained in that report has been used for the case study analysis.

Two boreholes were completed to depths of 20.4 m located near the launch and receiving locations of the tunnel drive as shown on the drawing in : . Beneath 0.60 m of topsoil on the south side and 0.15 m of topsoil to the north lay 1.0 m of silt and sand, then silty clay to a depth below the pipeline alignment. Grain size analysis and hydrometer testing showed the samples collected comprised 5% gravel, 10% sand, 85% silt and clay sizes. The Atterberg limits of the silt and clay size fractions were tested to assist in classification and determination of mechanical properties of the soil. Testing showed the silty clay had liquid limits and plastic limits ranging from 23% to 37% and 12% to 17%, respectively, which indicate clay of low to medium plasticity. The chart in Figure 3.2, shown below, demonstrates the variation of water content with depth, and shows the Atterberg limits of the silty clay.

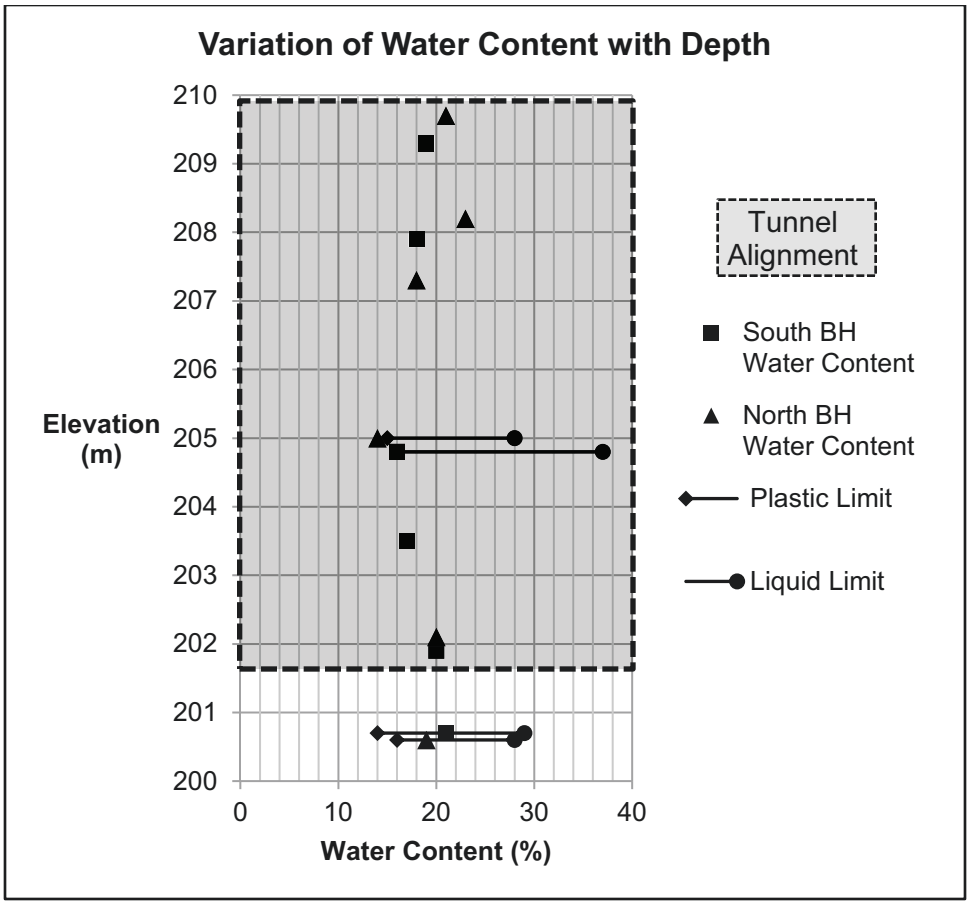

Figure 3.2: Variation of water content with depth, and Atterberg limits of cohesive soil

As shown in Figure 3.2, the water content of the clay varies between 14% and 23%. Generally, these values fall near or above the plastic limit, and below the liquid limit. Lower moisture content values that fall near the soil's plastic limit indicates the clay is over consolidated.

Standard Penetration Testing (SPT) was completed throughout the drilling of each borehole. SPT "N Values" of 3 to 20 were achieved, indicating a soft to very stiff consistency. The lower SPT N Values were achieved both near surface and at lower elevations, between 201 m and 197 m, geodetic datum. The chart in Figure 3.3 below demonstrates the consistency of the soil with depth in each borehole.

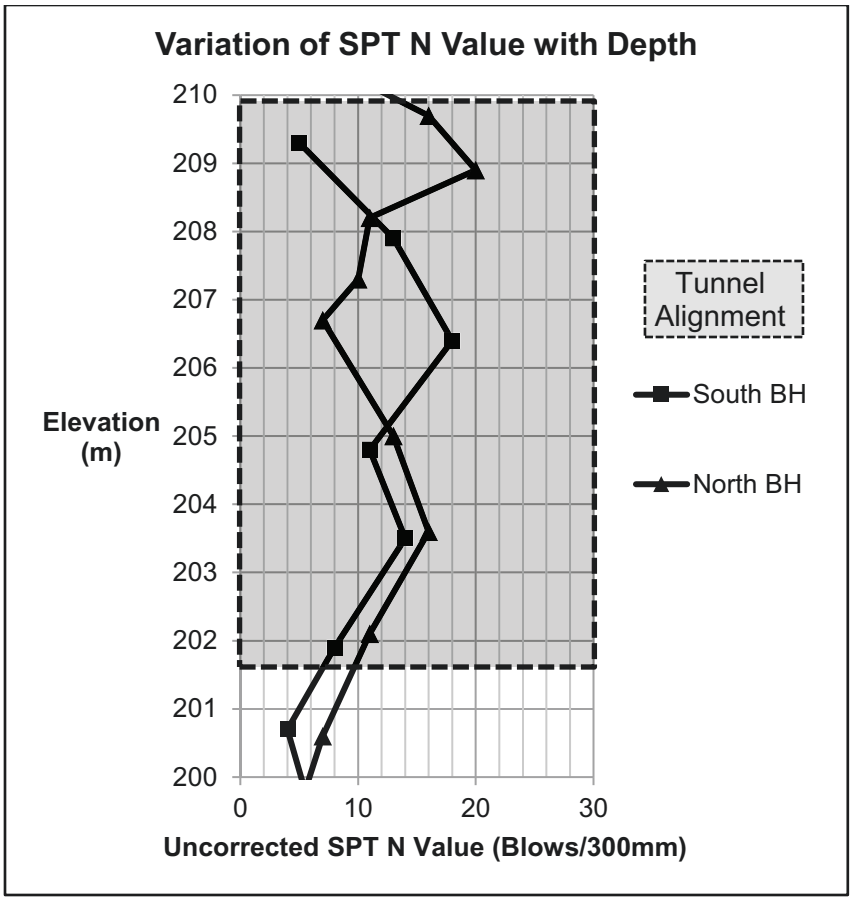

Figure 3.3: Variation of uncorrected SPT N-Value with depth.

The SPT "N-Values" shown in Figure 3.3 show the soil is largely stiff to very stiff at the elevation of the tunnel alignment. These correlated stiffness values are consistent with the moisture contents obtained from laboratory testing.

Although both boreholes were observed to be dry on completion, the geotechnical information contained within this case study assumed groundwater may establish equilibrium at approximately 2 m depth.

Through review of the site investigation and the soil parameters established by the geotechnical consultant, representative parameters for the use in the current state of practice calculation. This

thesis investigates both drained and undrained soil conditions in the analysis. The soil parameters chosen for use in both the drained and undrained analyses are shown in Table 3.1 below.

Table 3.1: Properties used in the evaluation of the total thrust force for the Flat Typical DPI Crossing

PARAMETER	SILTY CLAY
Drained Friction Angle (Ø')	25 Degrees
Undrained Horizontal Earth Pressure Coefficient (K)*	1
Stiffness (k)	20 MPa
Bulk Unit Weight (γ_b)	18.5 kN/m^3

*Ø' = 0 analysis undertaken, assuming isotropic stress state

3.2.3 Construction Considerations

Some mechanical issues during construction lead to progress stoppages. These stoppages were considered when looking at the data provided from the MTBM. Located below, Figure 3.4 shows the location along the tunnel alignment where major delays in progress had occurred during construction.

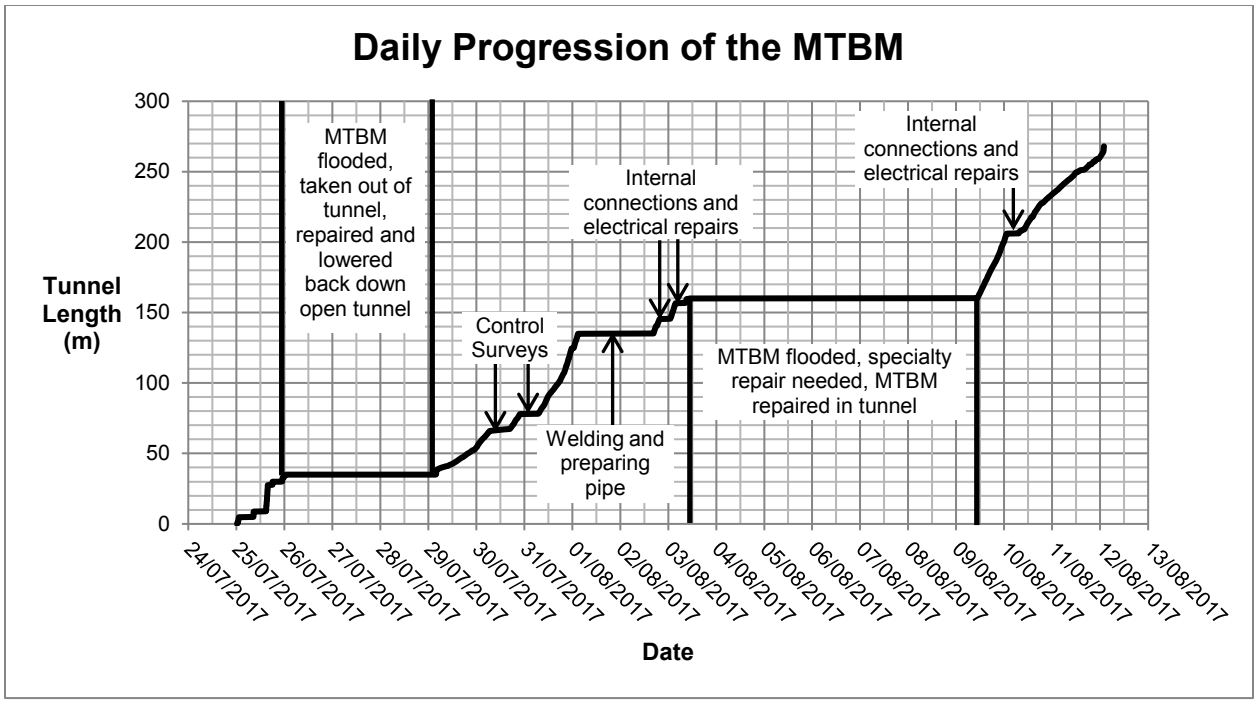

Figure 3.4: Daily progression of the MTBM, showing the delays in progress which occurred during construction.

Horizontal portions of the progression line on the chart in Figure 3.4 indicate no forward progress over time; thus, considered stoppages. These stoppages were confirmed with the construction reports provided by CCI Inc. and the reasoning is labeled on the above chart. The initial flooding of the MTBM provided an opportunity to analyze data while the MTBM was lowered into the tunnel after it was repaired.

3.3 CASE STUDY 2 - AKA “THE TRAIL DPI”

3.3.1 Project Description and Design

Case Study 2 was a DPI crossing of a highway located in north-central Alberta, Canada. The north to south crossing alignment comprised a 1219.2 mm (48 inch) diameter pipeline that was

installed within a 1325 mm (52.2 inch) diameter, 208 m long tunnel. The launch angle was about 3 degrees, an approximately 1V : 19H slope. The curved drive began with a radius of about 1200 m, connecting the launch tangent to a horizontal baseline segment. The horizontal section was 114 m long and led into the second curved segment, with a radius of 1200 m, exiting into the receiving pit at a 2 degree or 1V : 28H slope. The maximum depth of the tunnel crown below ground surface was 6.6 m, which was located under the highway crossing. The thruster was situated within a 4.5 m deep launch shaft, and the elevation on the launch location of the MTBM was 944.6 m, geodetic. The pictorial representation of the DPI alignment is shown in Figure 3.5, below.

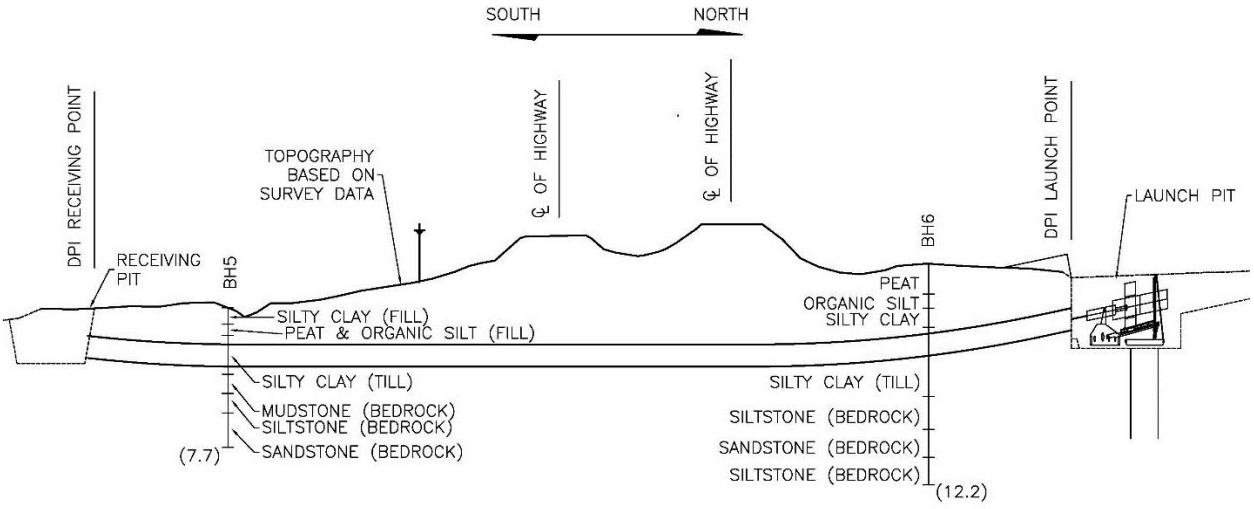

Figure 3.5: Pictorial representation of the Trail DPI alignment. Adapted from case study design drawing prepared by CCI Inc.

The drawing in Figure 3.5 shows a profile view of the tunnel alignment. The design is based on a combination of factors, including surface geometric constraints, pipeline stress considerations, factors associated with constructability, and geotechnical considerations.

3.3.2 Geotechnical Conditions along Tunnel Alignment

Located along the crossing alignment as described in the case study, boreholes BH5 and BH6 were drilled using solid stem auger techniques to depths of 7.7 m and 12.2 m, respectively, which was greater than the “as-constructed” profile. Boreholes BH5 and BH6 were situated at elevations of 945.2 m and 947.4 m , geodetic, drilled to depths of 7.7 m and 12.2 m on the south and north sides of the crossing, respectively. This indicates a topography sloping gently downward towards the south. Information from both boreholes indicated that fill and organic material extend to depths of 1.5 m to 3.5 m, overlying silty clay (till) about 1.6 m to 3.6 m thick at the crossing location. Bedrock, comprised of mudstone and siltstone, was encountered at elevations of 940.1 m and 941.6 m, geodetic, on the north and south sides of the crossing, respectively.

The Trail DPI was mined mainly through silty clay (till) due to the elevation of the launch location and the excavation at the receiving pit. The clay (till) encountered at the site is comprised of a heterogeneous mixture of soil grain sizes deposited as glacial drift. Additionally, cobbles or boulders could have been encountered during tunnelling operations. Based on SPT N Values ranging between 3 and 33, the clay (till) encountered at the site was described as soft to very stiff. The variation of SPT N-value with depth is shown on the chart in Figure 3.6, below.

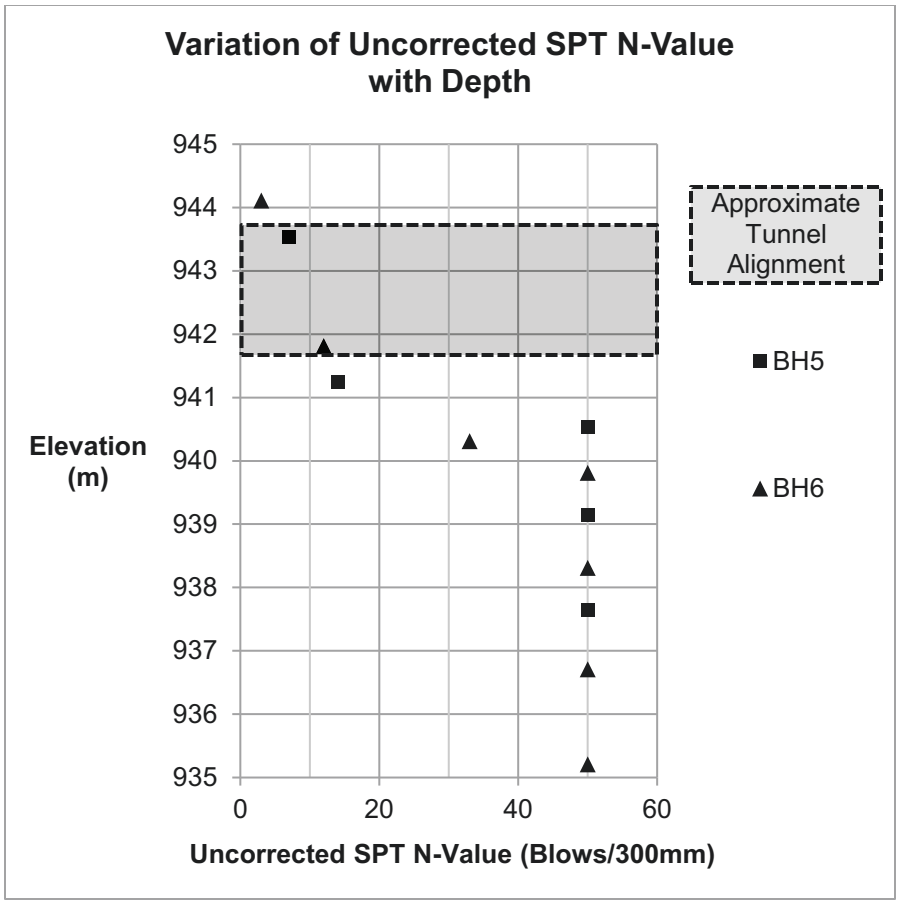

Figure 3.6: Variation in SPT-N Value with depth at the Trail DPI location.

Laboratory testing was completed on the split spoon, auger grab, and thin walled tube soil samples obtained from the geotechnical investigation. Grain Size testing on the soil indicates that the silty clay (till) comprised from about 23.7% to 28.4% sand, 35.8% to 46.4% silt, and 29.9% to 35.8% clay at the project location. Atterberg limit testing was performed on the silt and clay size fraction of the material. The test results yielded values for liquid limit and plastic limit to range from 39% to 48% and 18% to 21%, respectively, indicating a soil of medium plasticity. The variation of moisture content and Atterberg limits with depth is shown on the chart located in Figure 3.7, below.

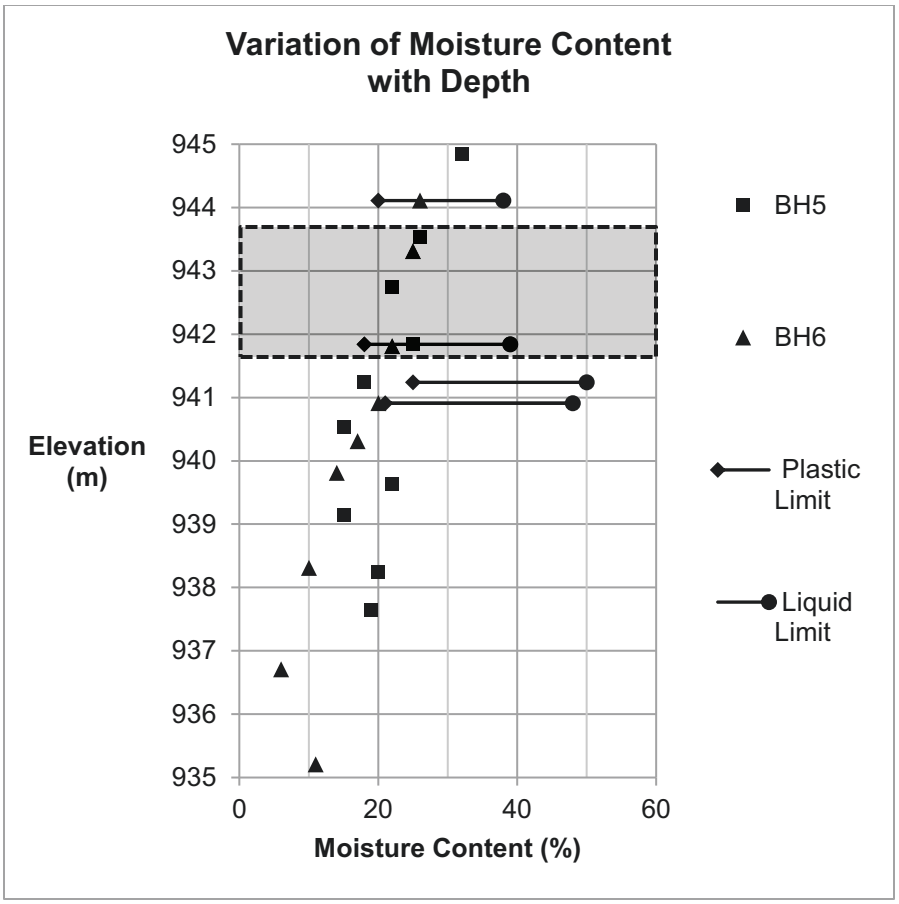

Figure 3.7: Variation in moisture content and Atterberg limits with depth in Boreholes 5 and 6 at the Trail crossing location.

The geotechnical assessment also provides estimated parameters based on site specific information and consultant experience with similar soils for the silty clay (till). The dry and bulk unit weights considered for the silty clay (till) soil are 16 kN/m^3 and 20 kN/m^3, respectively. The friction angle and cohesion of the till were estimated to be 28 degrees and 5 kPa, respectively. Additionally, the upper completely weathered bedrock dry unit weight and bulk unit weights were estimated to be 18 kN/m^3 and 22 kN/m^3, and friction angle and cohesion were estimated to be 32 degrees and 20 kPa, respectively.

Geotechnical parameters were established after review of the information from the data obtained from the site investigation, with consideration given to the suggested parameters from the site-specific geotechnical report. This thesis investigates both drained and undrained soil conditions and the soil parameters chosen for use in the analyses are shown in Table 3.2 below.

Table 3.2: Properties used in the evaluation of the total thrust force for the Trail DPI Crossing

PARAMETER	SILTY CLAY (TILL)
Drained Friction Angle (Ø')	28 Degrees
Undrained Horizontal Earth Pressure Coefficient (K)*	1
Stiffness (k)	52 MPa
Bulk Unit Weight (γ_b)	20 kN/m^3

*Ø' = 0 analysis undertaken, assuming isotropic stress state

3.3.3 Construction Considerations

Case study 2 detailed a relatively short drive completed under the proposed schedule. The rising upper bedrock surface had forced the MTBM higher in elevation than originally planned. It stands to reason that the rising upper bedrock surface was encountered during construction at a small angle, approximately 33 m from the end of the tunnel alignment. The encounter with the upper bedrock surface deflected the tunnel alignment higher than anticipated and the author expects this to have had an impact on the data obtained. Additionally, this higher tunnel alignment resulted in a heave, and bentonite, or slurry fluid, was released to surface in a ditch located south of the highway. The depth of cover where the release occurred was 0.9 m in the ditch adjacent to the highway. The topography continued to heave for about 30 m to the location of the receiving pit, where the MTBM exited the ground. The chart in Figure 3.8, below, demonstrates the daily progression of the MTBM.

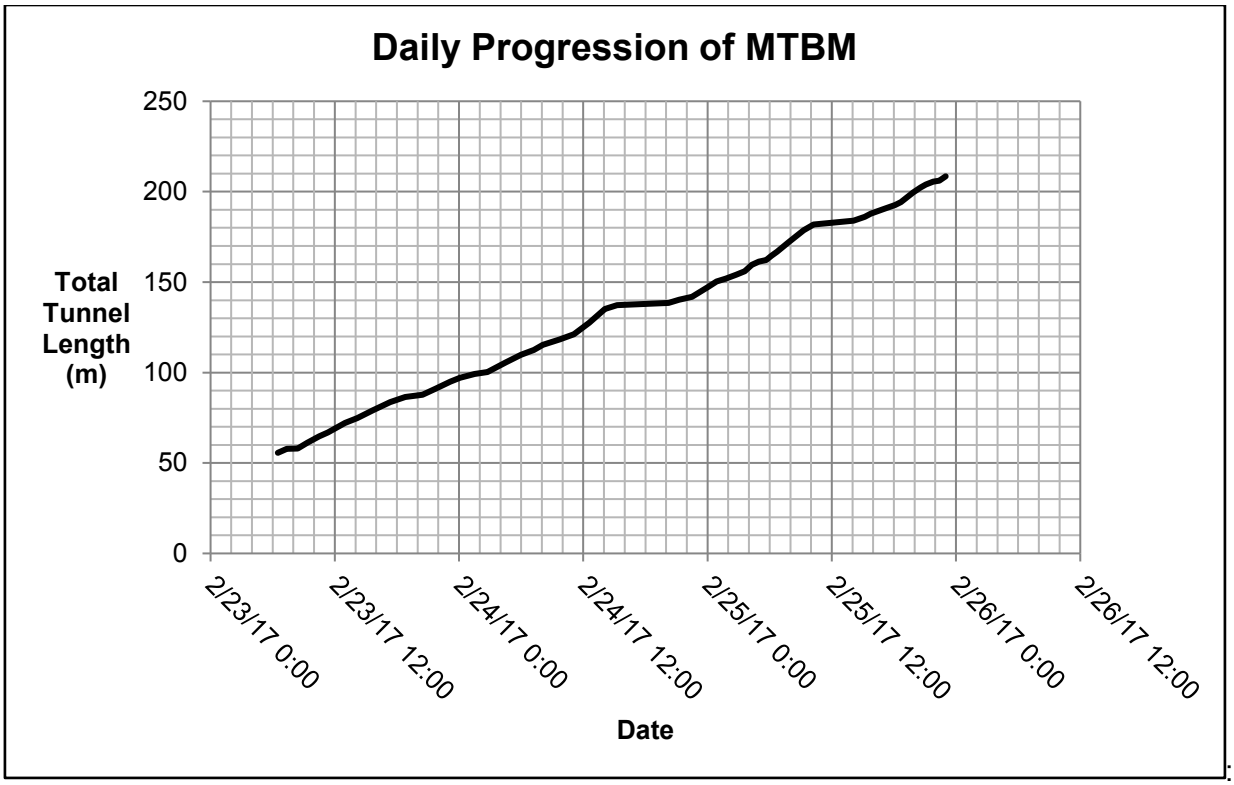

Figure 3.8: Daily progression of the MTBM during the Trail DPI

The Trail DPI did not experience any lengthy delays during construction. However, the rate of advancement (ROA) did slow after the MTBM encountered the rising upper bedrock surface (about 10:00 on February 25, 2017).

3.4 CASE STUDY 3 - AKA “THE LLR DPI”

3.4.1 Project Description and Design

The LLR DPI crossing was located in Ontario, Canada. The project depicted in this case study was a long crossing of two rivers, the terrain sloping gently to moderately. A hill approximately 30 m tall separated the two rivers.

A 1066.8 mm (42 inch) diameter pipeline was installed within an 1110 mm (43.7 inch) diameter, 796 m long tunnel. This alignment included a launch angle of 10 degrees, an approximately 5.5H : 1V slope. The large launch angle was necessitated by the approximately 7 H: 1V, slope on which the launch excavation was located. A 20 m length of 1524 mm (60 inch) diameter steel surface casing lined with HDPE was installed to ensure proper depth of soil cover was maintained in the beginning of the drive. This curved drive had geometric changes of an 1100 m radius, connecting the initial launch slope to a horizontal baseline. An additional curved section with a 1100 m radius was required following the horizontal baseline, connecting to a final tangent at an angle of 7 degrees, or 8.1H : 1V, exiting into the receiving pit. The maximum depth of tunnel crown below ground surface for the “as-constructed” tunnel was about 53 m; however, the depth of the alignment was only 15.2 m below the main river channel. Figure 3.9, below, shows the design of the DPI tunnel alignment.

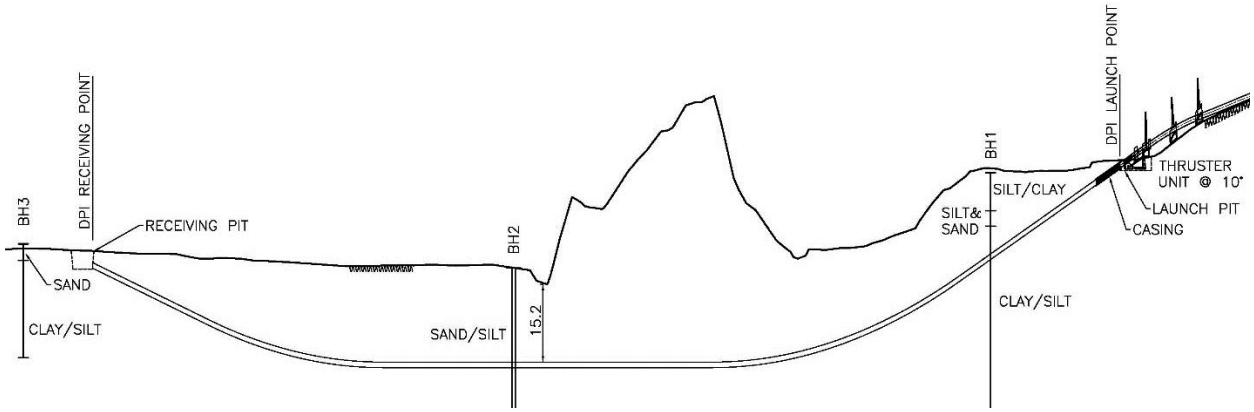

Figure 3.9: Pictorial representation of the LLR DPI alignment. Adapted from the case study design drawing prepared by CCI Inc.

The drawing in Figure 3.9 shows a profile view of the tunnel alignment. The design is based on a combination of factors, including surface geometric constraints, pipeline stress considerations, factors associated with constructability, and geotechnical considerations.

3.4.2 Geotechnical Conditions along Tunnel Alignment

Geotechnical data was obtained at three boreholes for this crossing location. Borehole 1, located on the northeast, and Boreholes 2 and 3, located on the southwest approach, were drilled to depths deeper than the designed tunnel alignment.

Nearest the DPI launch pit, low to medium plastic soft to hard silty clay, containing trace to some sand and trace gravel extending to 13.3 m was encountered in Borehole 1. A 3 m thick layer of very dense silt and sand was encountered within the clay unit at a depth of 7.3 m. Silt of slight plasticity was encountered underlying the silty clay, extending to a depth of 21.2 m, overlying another silty clay layer, which extended below the depth of the tunnel alignment. The lower silty clay was described as stiff to hard, with trace to some sand and cobbles.

Beneath 0.6 m of topsoil in Borehole 2, “sand”, “silty sand”, and “silt and sand” extended to 11.4 m depth below ground surface. The sand, with varying silt content, was described as very loose near surface and compact at depth. Non-plastic silt was encountered underlying the sand extending to a depth of 17.8 m, underlain by silty sand. The silty sand extended below the maximum depth of the tunnel alignment.

Nearest the DPI receiving pit, beneath 0.6 m of topsoil, Borehole 3 encountered 2.6 m of loose to compact silty sand, with trace gravel and fines, overlying “silty clay to clayey silt” extending to 14.9 m depth below ground surface. The “silty clay to clayey silt” was described as very soft to hard, with trace sand and gravel, and underlain by sandy silt extending beyond the final depth of

investigation. The sandy silt was described as non-cohesive and very loose to dense, with trace plastic fines.

In situ stiffness of the silty clay and density of the sandy soil at the LLR DPI crossing location were inferred using the SPT method. SPT N-values ranged from 97 to 6, 28 to 2, and 54 to 0 (Weight of Hammer) in Boreholes 1, 2 and 3, respectively. The SPT N-Value of “zero” in Borehole 3 suggests that there are layers of very loose and saturated cohesionless soil nearest the DPI receiving pit. The variation of uncorrected SPT N Value with depth for Boreholes 1, 2, and 3 are shown on the chart in Figure 3.10 below.

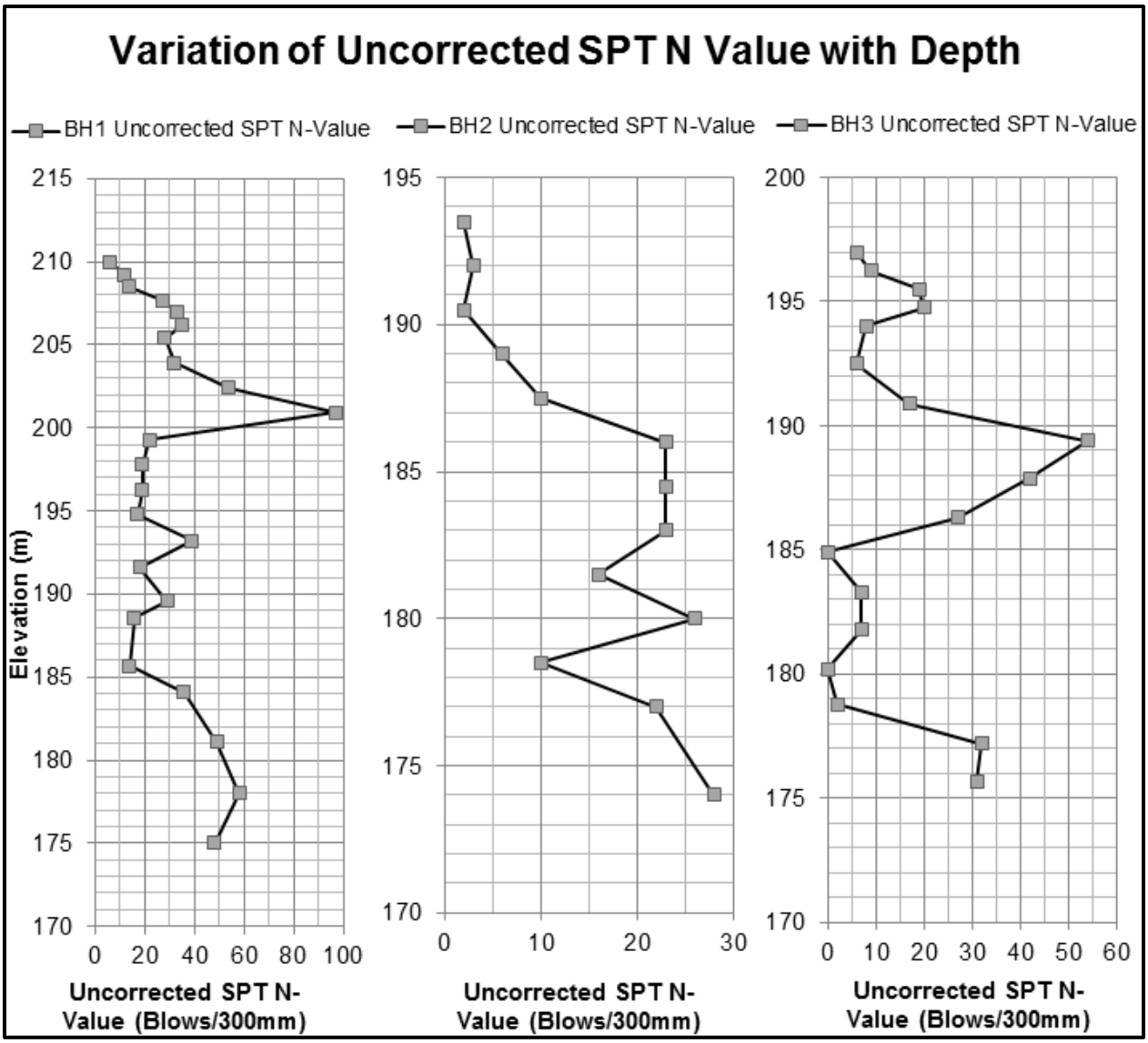

Figure 3.10: Variation of Uncorrected SPT N-Value with depth at the LLR DPI Crossing Location.

Atterberg limit testing was performed on various samples obtained during the geotechnical investigation. The silt and silt to sand encountered at the site had liquid and plastic limits ranging from 19% to 16% and 16% to 11%, respectively. The silty clay formation Atterberg limit testing revealed that liquid and plastic limits ranged from 29% to 16% and 19% to 11%, respectively. The

soil exhibited moisture contents generally between the liquid and plastic limits, however dryer than the plastic limit in some cases. The variation of water content and Atterberg limits with depth are shown on the chart in Figure 3.11 below.

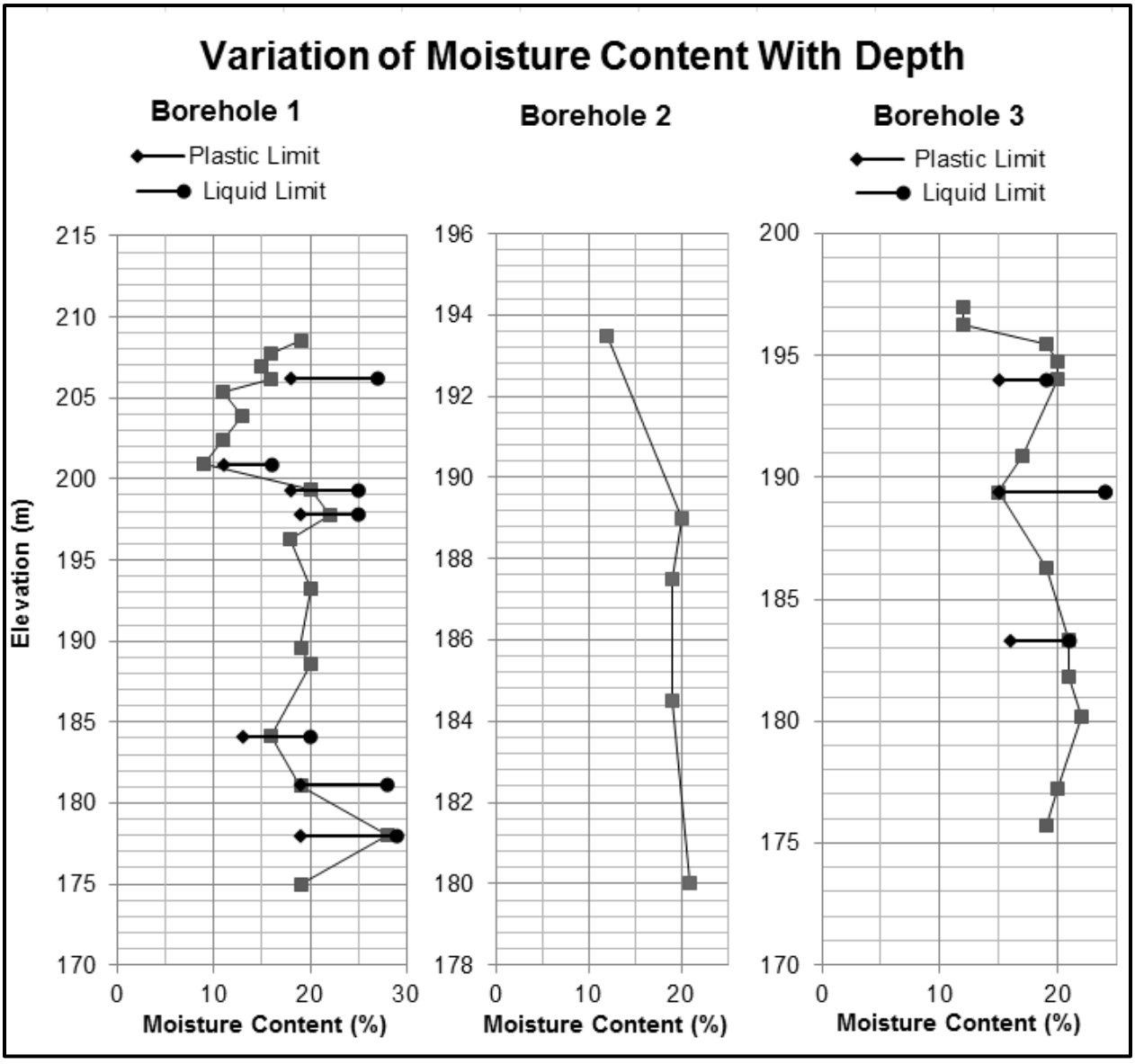

Figure 3.11: Variation of moisture content and Atterberg limits for Boreholes 1, 2 and 3 at the LLR DPI crossing location.

The site characterization documents completed by the consultant had established geotechnical parameters for the crossing location. This thesis evaluates drained conditions for the silt and sand, and undrained soil conditions for the silty clay encountered at the crossing location. The soil parameters chosen for use in both the drained and undrained analyses are shown in Table 3.3 below.

Table 3.3: Properties used in the evaluation of the total thrust force for the LLR DPI Crossing

PARAMETER	SILT and SAND	SILTY CLAY
Drained Friction Angle (ø')	28 Degrees	N/A
Undrained Horizontal Earth Pressure Coefficient (K)*	N/A	1
Stiffness (k)	20 MPa	15 MPa
Bulk Unit Weight (γ_b)	20 kN/m^3	18.5 kN/m^3

*ø' = 0 analysis undertaken, assuming isotropic stress state

3.4.3 Construction Considerations

Construction of the LLR DPI crossing was in accordance with the proposed schedule, in general, however, the MTBM malfunctioned at a tunnel length of approximately 40 m and was raised to surface for repair. After repair, the MTBM was lowered back through the open tunnel and recording of data from the thruster and the MTBM began at this time. The project continued without major delay following the MTBM malfunction. The chart in Figure 3.12, shown below, details the construction schedule.

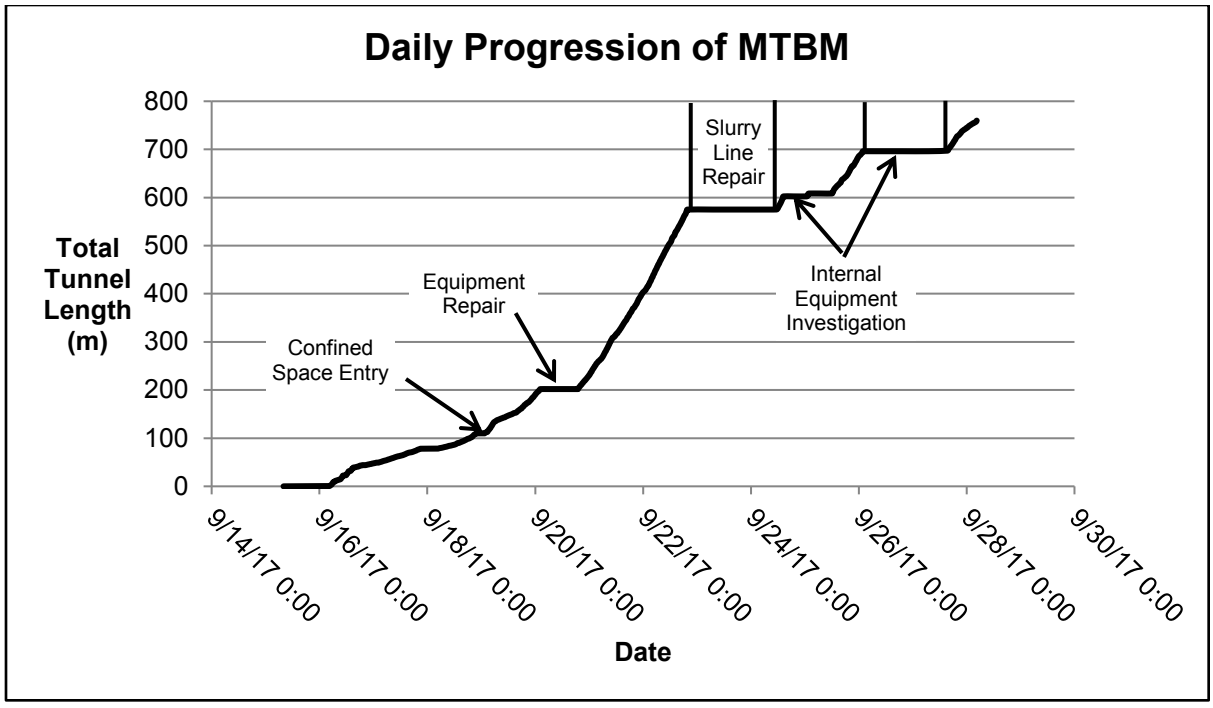

Figure 3.12: Daily progression during the LLR DPI for the duration of the project.

As shown on the chart in Figure 3.12, the project progressed rapidly. The middle section, where the MTBM was mining mainly granular soil, had the quickest daily progression, as evidenced by the steeper trend of the data. Additionally, near the beginning and end of the tunnel alignment, where geotechnical conditions were mainly cohesive, the MTBM progressed less rapidly. Finally, it should be noted that the horizontal trends in the data reflect construction stoppages.

3.5 CASE STUDY 4 - AKA “THE SPIRIT DPI”

3.5.1 Project Description and Design

The Spirit DPI crossing was in Saskatchewan, Canada where the 914.4 m (36 in) diameter pipeline was installed within a 975 mm (38.4 in) diameter tunnel. The 261 m long tunnel drive had a launch angle of 7 degrees, or a 1V : 8H slope from surface. NPS 42 casing, 20 m long, was

installed from surface to ensure at least 3 m of soil overburden cover was maintained throughout the drive. The launch tangent was 27 m long, shifting to a curved section with an approximate radius of 900 m. A short 10 m long horizontal baseline, located at a depth of 5.5 m under the river, connected the initial curved section to the exit curved section, also with a 900 m radius. The DPI path exited at a 7 degree, 1V : 8H slope, into a 3.8 m deep receiving pit where the machine was disassembled. The drawing in Figure 3.13 below shows the designed tunnel alignment.

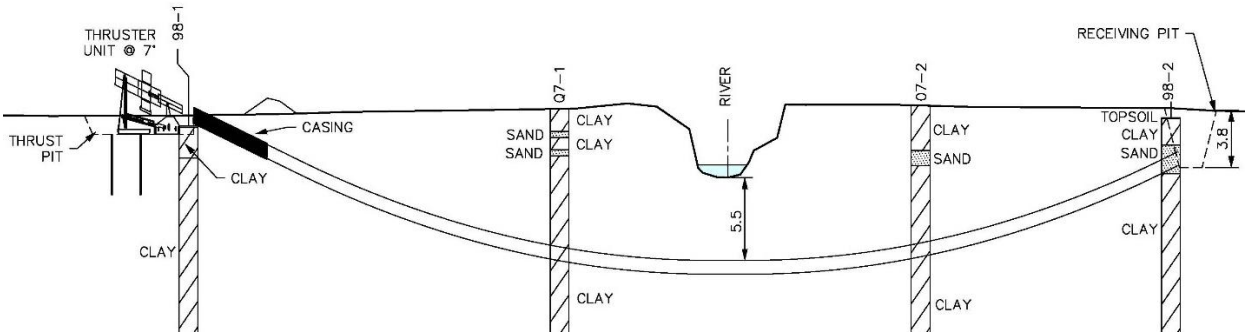

Figure 3.13: Pictorial representation of the Spirit DPI alignment. Adapted from case study design drawing prepared by CCI Inc.

The drawing in Figure 3.13, above, shows the profile view of the tunnel alignment. The design is based on a combination of factors including surface geometric constraints, stress considerations, factors associated with constructability, and geotechnical considerations.

3.5.2 Geotechnical Conditions along Tunnel Alignment

The tunnel alignment was located within the floodplain contained by a large valley. The terrain in the alignment area was relatively level to very gently sloping and flat with local depressions. Four (4) boreholes were drilled and sampled along the tunnel alignment. Boreholes 98-1 and 98-2 were completed in 1998, 07-1 and 07-2 in 2007, to depths ranging from 18.2 m to 30 m below ground surface. The tunnel alignment was constructed within 11 m from the ground surface. Two (2)

boreholes, 15-1 and 15-2, were also completed more recently; however, these boreholes were drilled greater than 200 m from the “as-constructed” tunnel. More extensive testing was completed in these recent boreholes; therefore, consideration has been given to the laboratory testing results from similar materials encountered in Boreholes 15-1 and 15-2.

Beneath a thin veneer of topsoil, clay of medium to high plasticity and wet sand layers were encountered extending to a maximum depth of 4.6 m. The sand layers were described as loose, silty, and containing clay layers. Underlying the upper clay and sand, high plastic clay extended to depths below the tunnel drive alignment. The thick, high plastic clay unit contained some medium plastic clay layers, and some wood fragments were discovered at depths exceeding 10 m below ground surface.

Undrained shear strength and compressive strength estimates values were obtained with consideration given to SPT and laboratory testing. In Boreholes 07-1 and 07-2, SPT N-Values ranged from 5 to 13 and 6 to 11, respectively, indicating the clay was generally firm to stiff, with undrained shear strengths ranging from 25 kPa to 100 kPa (Sivrikaya & Togrol, 2006). Additionally, in Boreholes 98-1 and 98-2, Shelby tube samples were collected and unconfined compressive strength (UCS) testing was completed in selected samples. UCS values obtained range from 50 kPa to 150 kPa in both boreholes, indicating undrained shear strength of the clay from 25 kPa to 75 kPa. These values agree well with the SPT values collected in Boreholes 07-1 and 07-2. Below, the variation of uncorrected SPT N-Value with depth is shown on Figure 3.14.

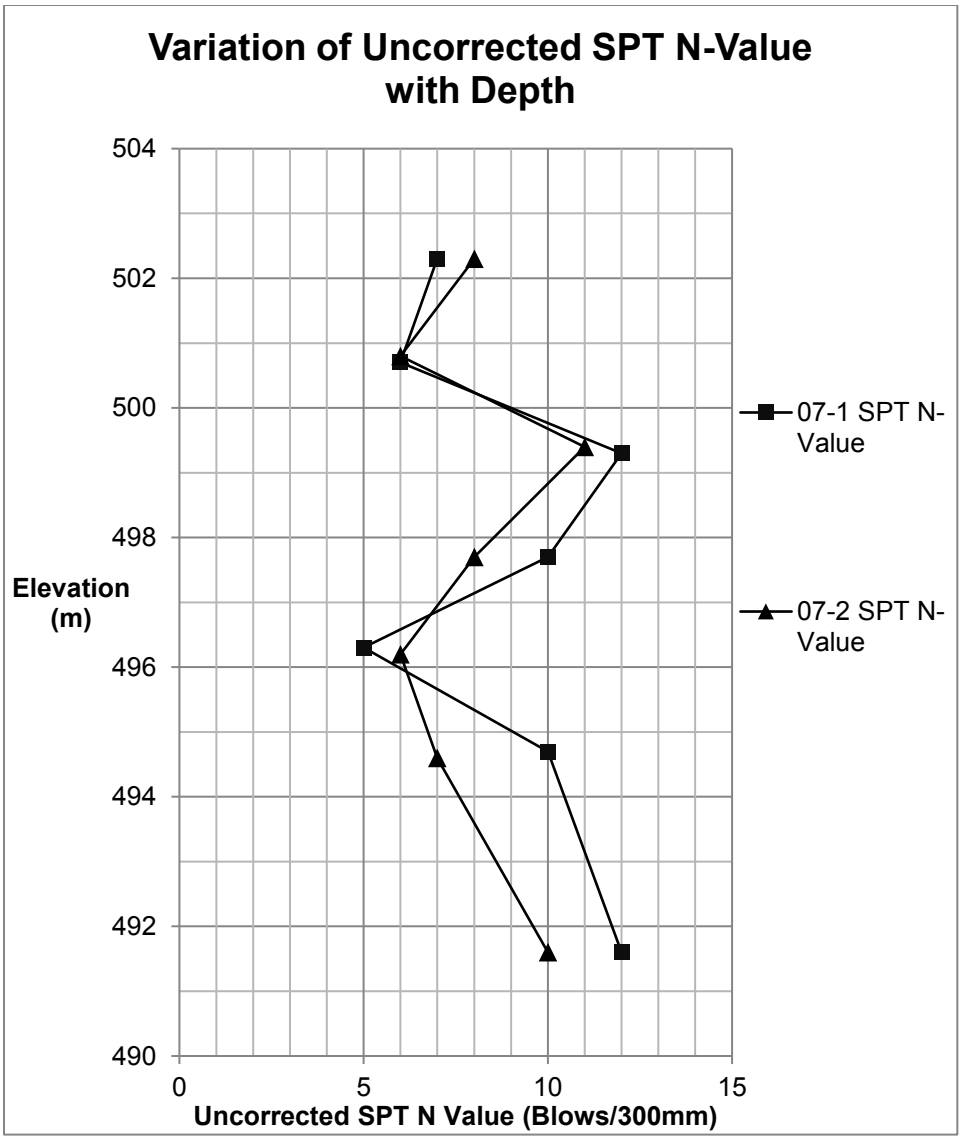

Figure 3.14: Variation of uncorrected SPT N-Value at the Spirit DPI location for Boreholes 07-1 and 07-2.

This geotechnical summary considers data from boreholes that are more recent, however completed some distance from the tunnel alignment that include laboratory testing within similar soil strata. Grain size analyses and hydrometer testing within the clay show that 23% to 40% silt and 60% to 77% clay sizes were present. There was no gravel or sand detected in the grain size

analysis testing within the high plastic clay formation at depths where the tunnel was constructed. Atterberg limit testing within the high plastic clay show the liquid and plastic limits may range from 66% to 77%, and 19% to 22%, respectively. Additional testing at depths greater than the “as-constructed” tunnel alignment, show that liquid and plastic limits may be about 39% and 16%, respectively, within the medium plastic clay layers. The variations of moisture content for Boreholes 07-1 and 07-2 with depth are shown in Figure 3.15 below.

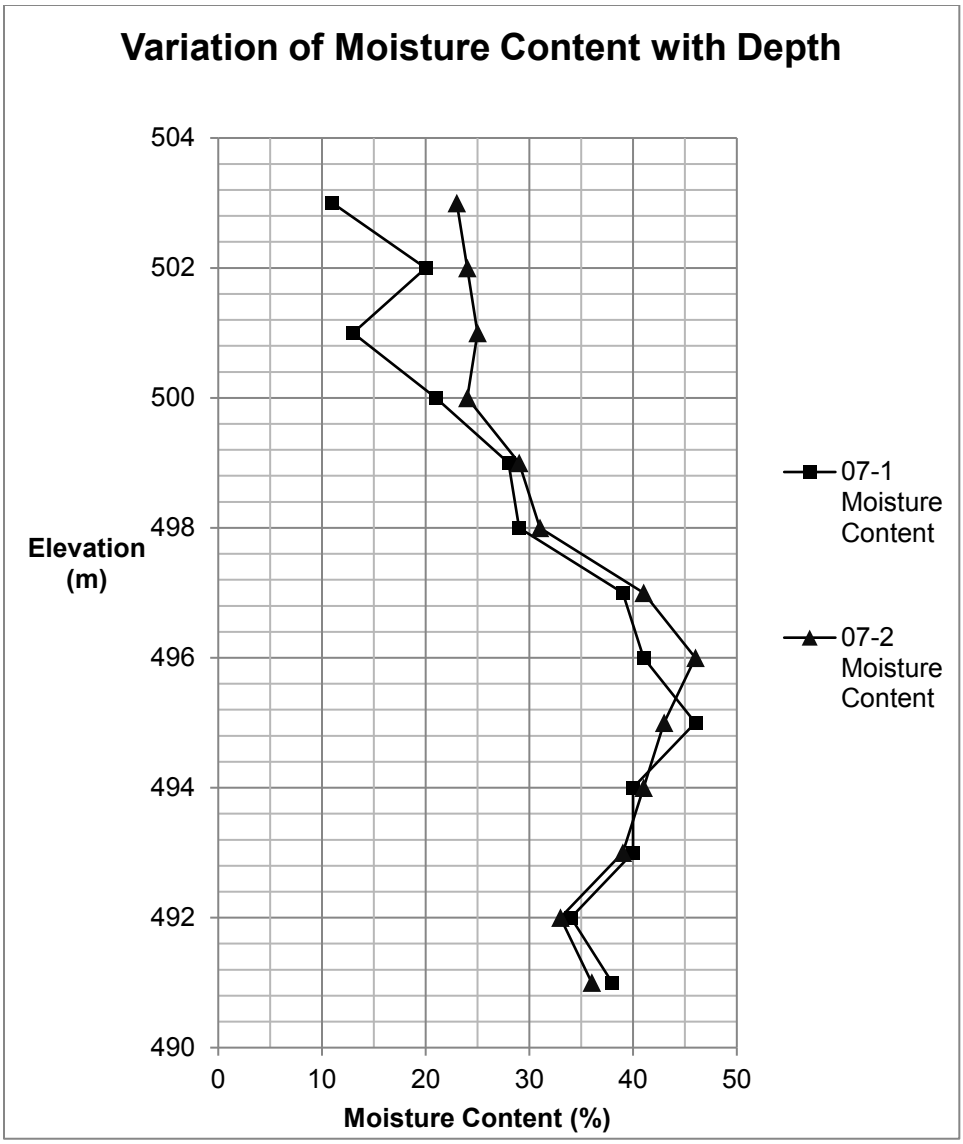

Figure 3.15: Variation of moisture content at the Spirit DPI for Boreholes 07-1 and 07-2.

Geotechnical parameters were established after review of the data obtained from the site investigation described above and consideration given to parameters suggested by the consultant. This thesis evaluates both drained and undrained conditions for the upper clay and the lower clay units. The evaluation also considers drained soil conditions in the sand separating

the two clay units. The soil parameters chosen for use in both the drained and undrained analyses are shown in Table 3.4 below.

Table 3.4: Properties used in the evaluation of the total thrust force for the Spirit DPI Crossing

PARAMETER	UPPER CLAY	SAND	LOWER CLAY
Drained Friction Angle (Ø')	15 Degrees	28 Degrees	17 Degrees
Undrained Horizontal Earth Pressure Coefficient	1	N/A	1
Stiffness (k)	10 MPa	15 MPa	15 MPa
Bulk Unit Weight (γ_b)	18.5 kN/m^3	20.0 kN/m^3	18.5 kN/m^3

3.5.3 Construction Considerations

3.5.3.1 General

Construction of the Spirit DPI proceeded according to the planned schedule without many significant issues. Considered "average" for the geology through which the tunnel is aligned, the ROA during construction was about 15 to 30 mm/min. The MTBM operator indicated that some clogging of the MTBM face was occurring, and therefore the slurry flow rates and ROA required adjusting. To assist in freeing the cutters from clogged soil, by saturation and abrasion, and allow the slurry to carry the muck out of the tunnel the operator lowered the ROA.

Space limitations during construction necessitated the lift section be separated into two sections. The joining of the two pipeline sections initiated a stoppage in tunnelling progress. Three days were required to attach the second pipe section and associated hoses. The daily tunnel progression is shown on the chart in Figure 3.16 below.

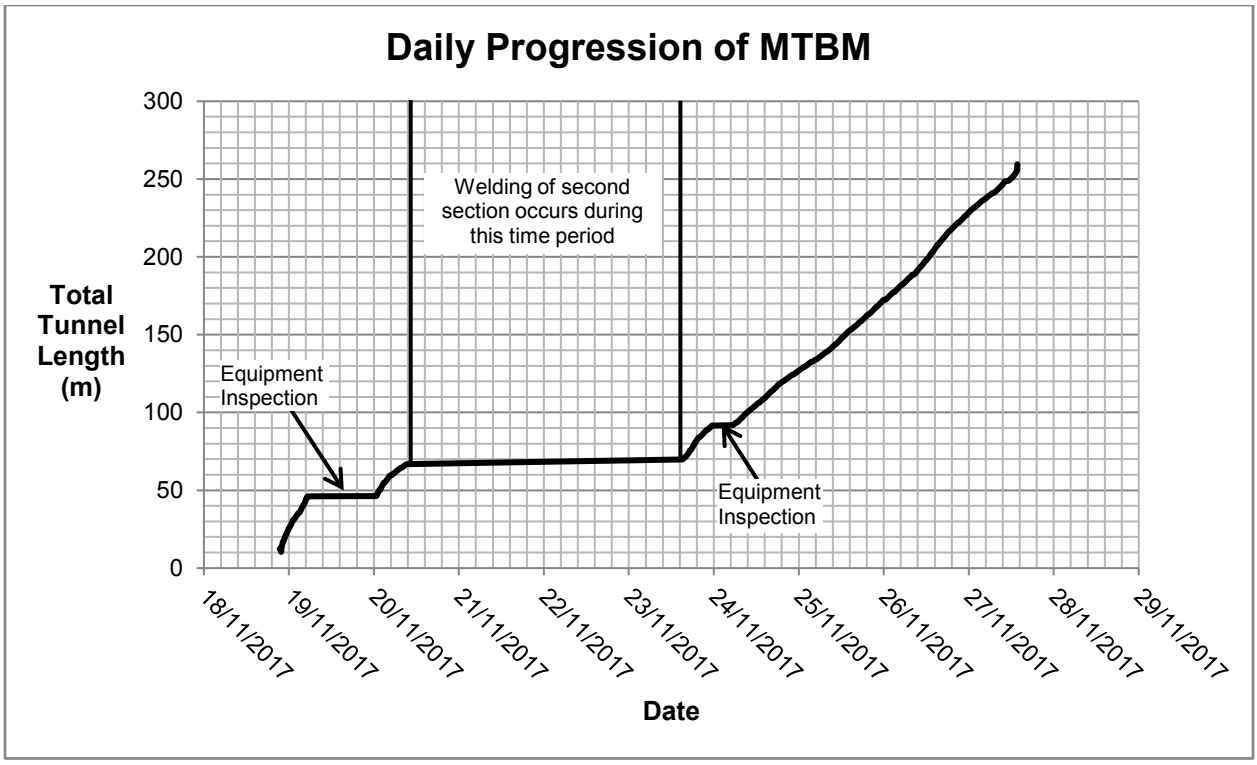

Figure 3.16: Daily progression of MTBM during construction of the Spirit DPI

Daily progression was rapid following the installation of the second pipeline section. The ROA did not slow as the tunnel progressed to the receiving pit at the end of the alignment. This suggests that length of DPI drive and ROA may not have a significant correlation in clayey soils.

3.5.3.2 Field Observations

During research for use in this thesis, the author had the opportunity to observe the Spirit DPI drive during construction. The observations are detailed as follows:

- During the tunnelling process, a long stoppage in progression was required due to logistical issues. The stoppage during construction was approximately 42 hours. An initial surge in thrust force occurred upon completion of this stop, however, the thrust force did not markedly increase for the remainder of the tunnel drive. This suggests the amount of

lubrication pressure in the annulus of the tunnel was sufficient to both support the formation and resist any swelling effect of the formation. This is interesting because, at the design stage, the expectation was that a stoppage in MTBM movement would result in higher frictional forces continuing for the duration of the tunnel drive.

- Throughout the timeline of the project, the amount of frictional resistance between the pipeline and soil appeared to be low, and the ROA did not appear to change significantly throughout the alignment.
- Operators can influence the required thrust force during DPI construction by modification of the machine parameters. When achieving an optimum mining operation through modification of the MTBM and thruster controlled parameters, the thrust forces seemed to become less erratic and more predictable.

The observations made by the author during the construction of the Spirit DPI provided supporting evidence of the necessary adjustment engineers can use at the design stage to better predict thrust force during construction.

3.6 SUMMARY

This chapter examined four DPI case studies to form a basis for the information used hereafter. The review of the case studies included the following:

- Geotechnical conditions along the DPI alignment were reviewed for each case study. Reports prepared by consultants for each case study evaluated subsurface conditions and, based on their experience, provided soil parameters for pipeline crossing construction. The reports evaluating subsurface conditions were assessed, and drained and undrained soil properties were obtained based on the data obtained in the geotechnical reports.

- Construction considerations for each case study were reviewed to provide insight into the schedule, rate of advance, and issues which may affect the data provided. These items were assessed using construction reports written by CCI inspection personnel and confirmed any anomalies in the realized total thrust data used in this thesis.
- On site experience of the author during DPI construction of a single case study provided invaluable insight into the construction process. Findings from the onsite experience had indicated that frictional resistance tended to be small, and lengthy stoppages in construction did not seem to influence the total thrust force. Additionally, it was determined that the machine operator can influence the required thrust force to a large extent during the construction process.

CHAPTER 4. EVALUATING THE CURRENT STATE OF PRACTICE CALCULATION METHOD AND COMPARISON TO REALIZED THRUST DURING CASE STUDIES

4.1 INTRODUCTION

In this chapter, extensive review and evaluation of the current state of practice calculation method for estimating total thrust force is completed. The evaluation includes sensitivity analysis of the parameters in the calculation to determine which have the greatest influence on the result. In addition, the chapter compares the calculated total thrust and the realized thrust magnitude obtained from each case study described in Chapter 3, including evaluation of any discrepancies.

4.2 REVIEW OF THE CURRENT STATE OF PRACTICE FOR ESTIMATING THE TOTAL THRUST FORCE

To determine the mechanisms contributing to the total thrust force in DPI, ABAQUS Finite Element software was used by the equipment manufacturer (Pruiksma, Pfeff, & Kruse, 2012). According to the finite element analysis completed, there are five mechanisms that contribute to the total thrust force including:

- Surficial frictional effects between the roller to pipeline interface behind the thruster as it moves forward. This portion of the total thrust is dependant on the lift section design and layout. A free body diagram of the surficial friction is shown in Figure 4.1, below.

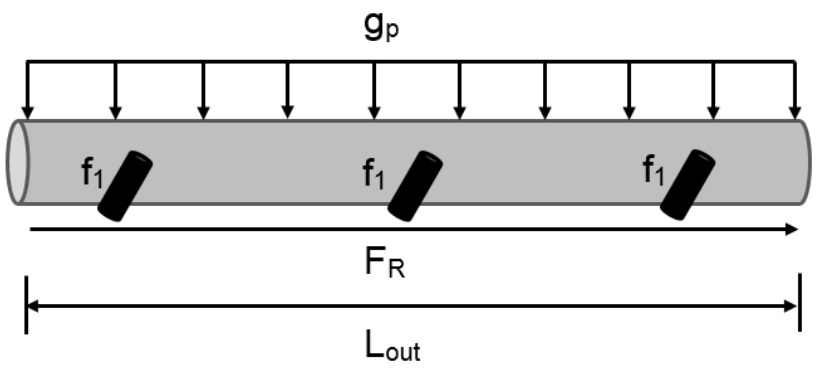

Figure 4.1: Free body diagram showing forces contributing to the roller to pipeline interface friction

- The frictional effects between the pipeline and lubricant fluid. A free body diagram showing the forces contributing to the pipeline lubrication friction is shown in Figure 4.2, below.

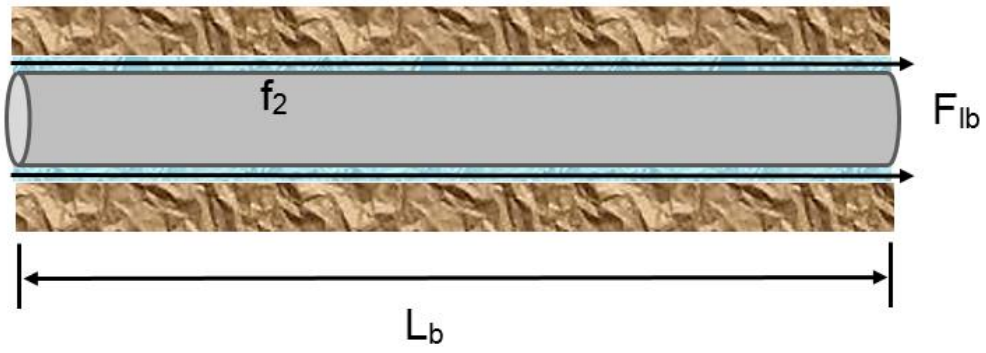

Figure 4.2: Free body diagram showing the forces contributing to the pipeline to lubrication interface friction

- The front force at the MTBM cutting face also contributes to the total required thrust force. This contribution is calculated from on the earth pressure acting on the cutting face, and the required force to advance the tunnel. A free body diagram showing the forces contributing to the force at the MTBM cutting face is shown in Figure 4.3, below.

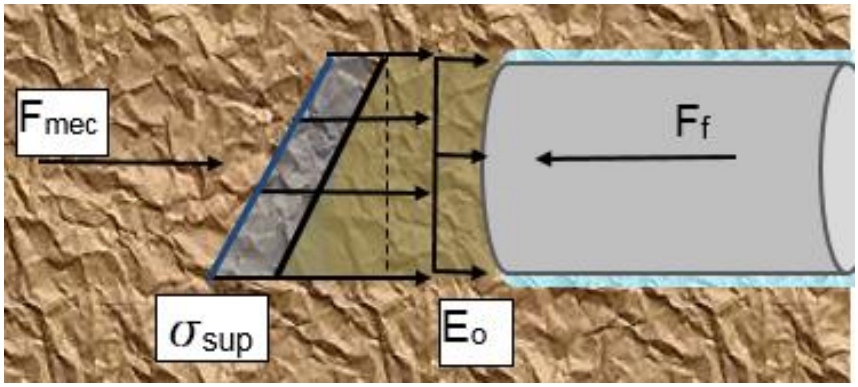

Figure 4.3: Free body diagram showing the forces contributing to the force at the MTBM cutting face.

- The friction between the pipeline and soil interface at the tunnel wall also contributes to the total required thrust force. This component depends on the geometry of the tunnel alignment, as well as the frictional coefficient between the pipeline and soil. The free body diagram showing forces contributing to the pipeline to soil interface friction is shown in Figure 4.4, below.

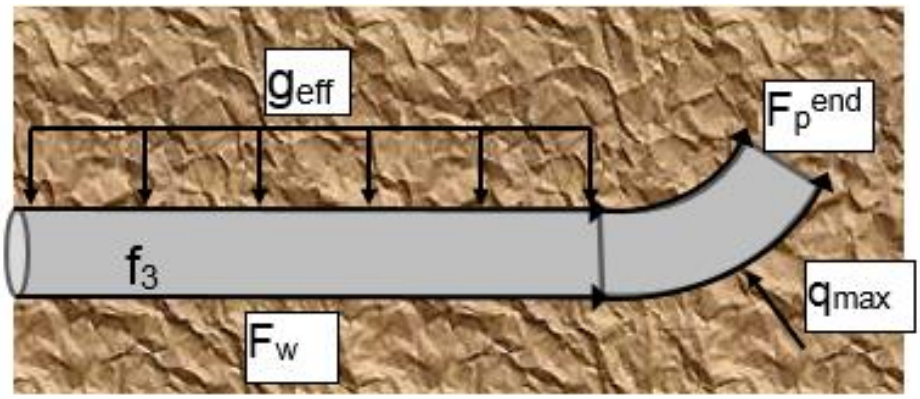

Figure 4.4: Free body diagram showing the forces contributing to the soil to pipeline interface friction along the tunnel alignment.

- The final mechanism contributing to the total thrust is additional friction due to buckling of the pipeline, inducing additional normal force to the tunnel wall. This value is dependant on the thrust applied and the flexural stiffness of the pipeline. A free body diagram of the forces contributing to the friction due to pipeline buckling is shown in Figure 4.5, below.

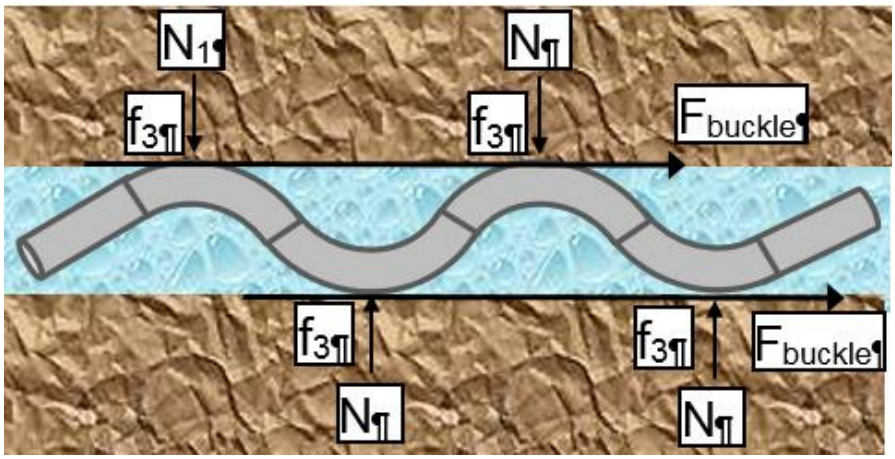

Figure 4.5: Free body diagram showing the forces contributing to the additional friction due to pipeline buckling.

The calculations within the current state of practice approach include a combination of Horizontal Directional Drilling (HDD), and conventional micro-tunnelling theories, and have been developed to represent a simplified approach to estimate the total thrust force.

Surficial friction of the pipeline to roller and cradle interface is the first component of the total thrust force calculation. The calculation is shown in equation (4.1) below.

$$F_R = L_{out}\, g_p\, f_1 \tag{4.1}$$

Additionally, the bentonite lubrication that surrounds the pipeline during installation provides a frictional resistance. This contribution is calculated using equation (4.2) below.

$$F_{lb} = L_b \pi D_0 \, f_2 \tag{4.2}$$

The frictional coefficient between the lubricant fluid is estimated based on its thixotropic properties. The yield point of the lubrication fluid is the shear force required to begin to strain the fluid. This value provides an estimate of the frictional coefficient between the lubricant fluid and the advancing pipeline. Furthermore, the force at the MTBM cutting face is calculated. Pruiksma, Pfeff and Kruse recommend calculating the face support pressure by adding an applied pressure to the earth pressure. The applied pressure above minimal pressure is an additional force in excess to the horizontal earth pressure required to advance the MTBM through the soil. This calculation is shown in equation (4.3), below.

$$\sigma_{SUP} = E_0 + \sigma'_{h,min} + \mu \tag{4.3}$$

Following, the document recommends estimating the front force by multiplying the required support pressure by the area of the MTBM face, as shown in equation (4.4) below. There is a recommended mechanized face force added to the equation to account for the required thrust to push the machine into the geological formation.

$$F_f = \sigma_{SUP} \frac{\pi}{4} D_{0,m}^2 + F_{mec} \tag{4.4}$$

Calculation of the soil to pipeline interface friction for the straight sections of the tunnel alignment follows. The calculation begins by determining the buoyant weight of the pipeline with equations (4.5) and (4.6) below.

$$g_{opw} = \pi \cdot r_e^2 \cdot \gamma_{fl} \tag{4.5}$$

$$g_{eff} = g_p - g_{opw} \tag{4.6}$$

Using the effective pipeline weight, the length of pipeline that is buoyant is calculated using equation (4.7) below.

$$L_t = \begin{Bmatrix} \sqrt[4]{\frac{8EIw_{gap}}{|g_{eff}|}} & , & g_{eff} \neq 0 \\ 0 & , & g_{eff} = 0 \end{Bmatrix} \quad (4.7)$$

The amount of frictional resistance from the contact of pipeline with the soil can then be determined using equation (4.8) below.

$$\Delta F_w = f_3 \int_0^{L_b} |q(s)|\, ds \quad (4.8)$$

Next, the sections of the tunnel alignment where curvature is expected are calculated. This section uses the pipeline and soil stiffness to determine the normal force using equations (4.9) and (4.10).

$$\lambda = \sqrt[4]{\frac{k}{4EI}} \quad (4.9)$$

$$q_{max} = \frac{EI\lambda^2}{R} e^{-\pi/4}\, sin(\frac{\pi}{4}) \quad (4.10)$$

Then, using equations (4.11) and (4.12) below, the frictional force at the beginning of the bend can be determined.

$$a = \left|\frac{g_{eff}}{q_{max}}\right|, if\ a > 1\ set\ a = 1 \quad (4.11)$$

$$\Delta F_w^{bend} = \frac{f_3 EI\lambda}{R}(0.85a - 1.0903)(a - 1) \quad (4.12)$$

For the final step in the soil pipe interface friction calculation within a curved alignment, capstan forces are included. A diagram demonstrating the capstan principle is shown in Figure 4.6, and calculated using equations (4.13) and (4.14), below.

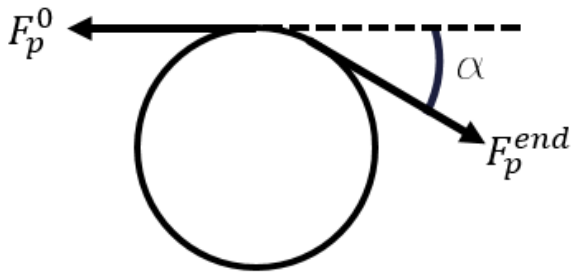

Figure 4.6: Diagram showing the capstan principle used to calculate the frictional resistance in a curved tunnel alignment.

$if\ g_{eff}R > F_p^0$

$$F_p^{end} = \frac{c_1}{f_3} + \left(F_p^0 - \frac{c_1}{f_3}\right) e^{-f_3\alpha} \quad (4.13)$$

where, $c_1 = \pi D_0 f_2 R + f_3 R g_{eff}$

$if\ g_{eff}R \leq F_p^0$

$$F_p^{end} = \frac{-c_1}{\mu} + \left(F_p^0 + \frac{c_1}{\mu}\right) e^{f_3\alpha} \quad (4.14)$$

where, $c_1 = \pi D_0 f_2 R - \mu R g_{eff}$

The underlying principle of these equations is that if the pipeline is buoyant, the soil reaction is decreased, and the soil to pipeline interface friction is also decreased. The last part of the

calculation method considers an additional frictional force due to pipe buckling in contact with the soil along the tunnel wall. As shown below, equation (4.15) provides the calculation of friction from pipeline buckling.

$$F_{buckle} = f_3 \frac{4LF^2}{\pi^2 EI} w_{gap} \quad (4.15)$$

Summation of the formulae above yields the total required thrust force, as demonstrated by equation (4.16) below.

$$\mathrm{F} = F_R + F_{lb} + F_f + F_p^{end} + F_{buckle} \quad (4.16)$$

Traditionally, calculation of the total thrust force occurs for each of the changes in tunnel alignment geometry, i.e. at each point of transition between curved or straight sections. An illustration showing the points along the tunnel alignment where the force is calculated in practice is shown on Figure 4.7, below.

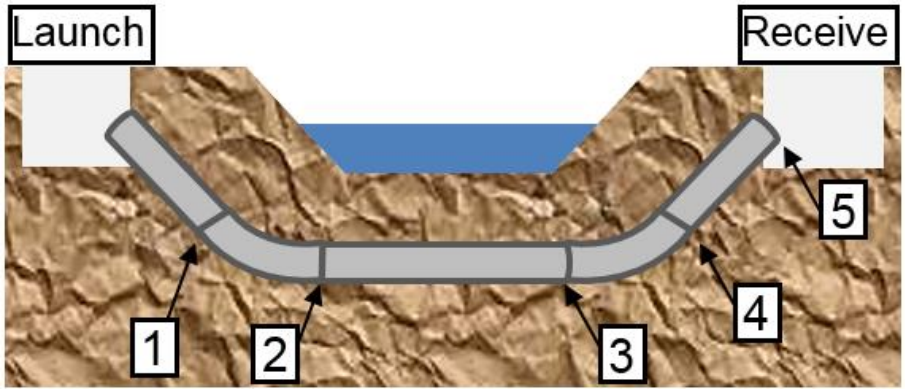

Figure 4.7: Illustration showing the points where the total required thrust force is calculated along the tunnel alignment using current practice.

Calculating the estimated thrust in this way produces five (5) points along the entire alignment to establish the estimated thrust envelope. This research includes calculations at more frequent

intervals (< 1m) to capture the effect of the changing overburden height throughout the tunnel alignment. This change to the analysis is further described in section 4.4.

4.2.1 Sensitivity Analysis

Using the method recommended above (Pruiksma, Pfeff, & Kruse, 2012), a sensitivity analysis was completed to establish which parameters have a substantial effect on the result. The parameters that have been evaluated were chosen to represent prominent coefficients or constants and soil parameters within the equations. These parameters include:

- Roller Friction Coefficient (f_1)
- Lubrication Friction Coefficient (f_2)
- Soil to Pipeline Interface Friction Coefficient (f_3)
- Applied Pressure Above Minimal Pressure (E_0)
- Soil Stiffness (k)
- Horizontal Earth Pressure Coefficient (K)
- Soil Unit Weight (γ)

The sensitivity analysis included generating a spider diagram to assess which parameters have more impact on the result.

The spider diagram uses a tunnel geometry containing both a straight section and two curved sections in attempt to create a “typical” alignment. It is acknowledged there are many configurations of tunnel geometry, and the geometry influences the thrust force components. However, the tunnel alignment used in this analysis is representative of a typical DPI alignment.

The constant and the average manipulated variables used in the spider diagram are shown below in Table 4.1 and Table 4.2, respectively.

Table 4.1: Constant parameters used during sensitivity analysis

Constant Parameter	Magnitude
Tunnel Length (L_b)	100 m
Vertical Depth (*h)*	7 m
Alignment Radius (*R*)	1100 m
MTBM Diameter *(D_T)*	1,110 mm
Pipeline Diameter *(D_o)*	1,066.8 mm
Pipe Stiffness (*EI*)	1,971.5 MN/m^3

Table 4.2: Manipulated parameters used during sensitivity analysis

Manipulated Parameter	Nominal Magnitude
Roller Friction Coefficient (f_1)	0.10
Lubrication Friction Coefficient (f_2)	50 N/m^2
Soil to Pipeline Interface Friction Coefficient (f_3)	0.20
Soil Stiffness (*k*)	20 MPa
Applied Pressure Above Minimal Pressure (E_0)	50 kPa
Horizontal Earth Pressure Coefficient (*K*)	1.0
Soil Unit Weight (γ)	18 kN/m^3

The sensitivity of each parameter to the final total estimated thrust was found using the constant variables and varying the manipulated parameters from the nominal values. The chart in Figure 4.8, below, shows the sensitivity of each manipulated parameter in the form of a spider diagram.

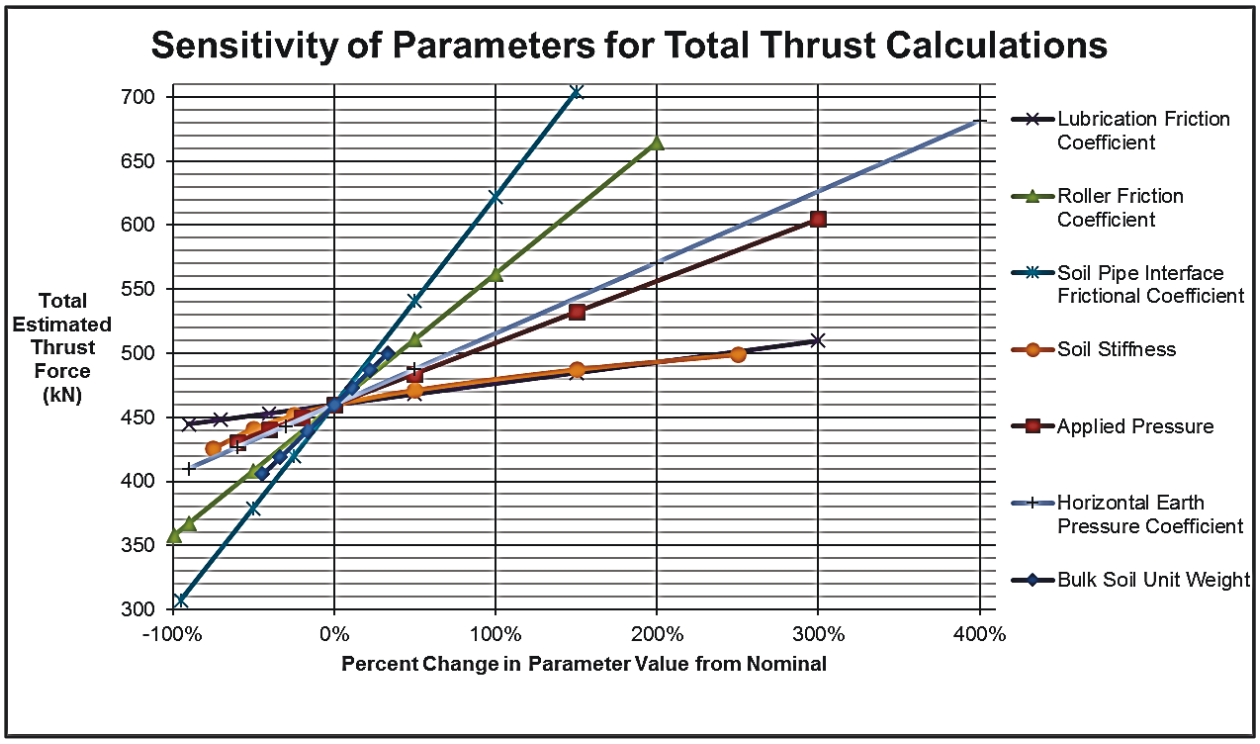

Figure 4.8: Spider diagram showing the sensitivity of the manipulated variables in the estimated thrust force calculation as recommended by Pruiksma, Pfeff, & Kruse (2012).

The soil to pipeline interface and roller frictional coefficients have the largest sensitivity in the calculation. The soil unit weight also has a large sensitivity to modification; however, the range of realistic values is small (< 50% change from average), reducing this parameter's relative significance. The applied pressure above minimal pressure and horizontal earth pressure coefficient are the next most sensitive parameters and have a large range of realistic values, according to this analysis. The lubrication frictional coefficient and soil stiffness values have the least significance on the total thrust force.

4.3 DATA ACQUISITION

4.3.1 Sensor Assessment

There are different types of MTBMs used by contractors working on various projects. While reviewing the case study information discovery that data supplied by these machines have sensors at different locations necessitated consideration during analysis.

The thruster, situated stationary on surface, measures the total thrust force required to advance the MTBM, position of the thrust cylinders during each “push”, and rate of advance. Figure 4.9 below is a photo of a thruster during construction and shows the location of the sensors.

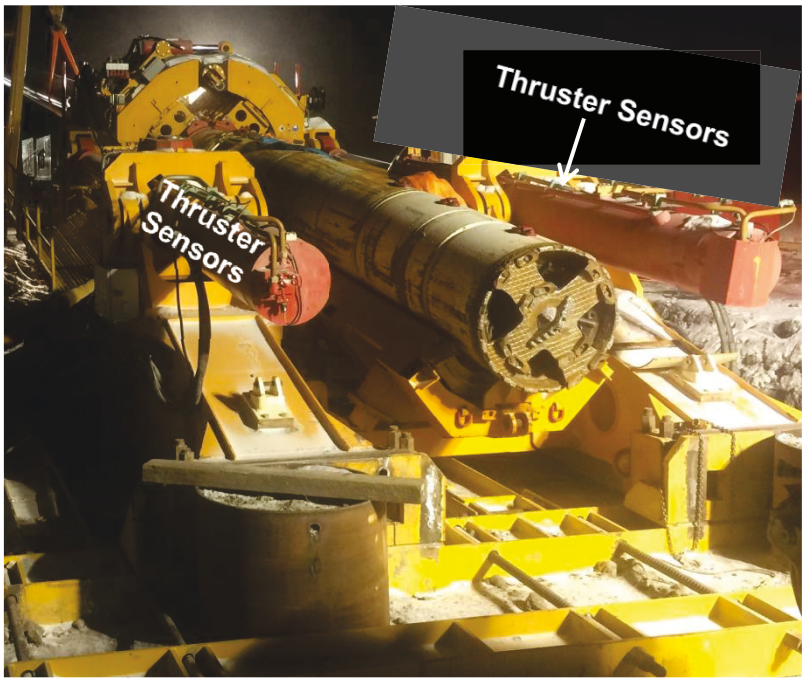

Figure 4.9: Photo showing the thruster and the location of the sensors that record the pressure data. Photo taken by the author.

The thrust force is applied by the hydraulic cylinders. A pressure transducer in the thruster cylinders measure changes in fluid pressure as the force is applied, which is then converted to an equivalent force using software developed by Herrenknecht. Sensors located on the cylinders of the thruster measure the position of the cylinders during each “push” and the advance rate. Data measured at the thruster is used to evaluate the total thrust force during construction, and to ensure maximum thrust thresholds are not exceeded. For this reason, the data provided by the thruster is considered accurate for the purposes of evaluating the current state of practice calculation method.

Sensors located on the MTBM can measure face pressure, force on the steering cylinders, torque, and face rotation. Figure 4.10 below shows the locations of the sensors on the MTBM.

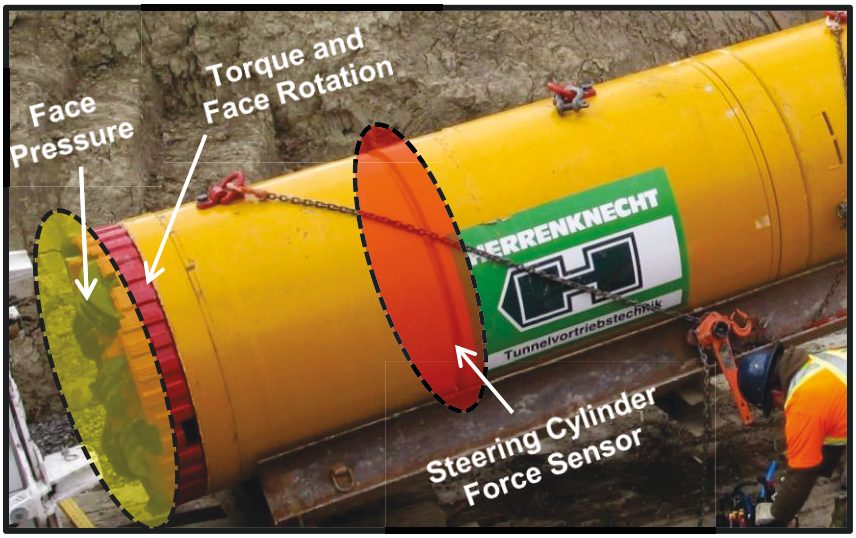

Figure 4.10: Photo showing the front of the MTBM and the location of the sensors. Photo used with permission by Darcy MacDonald of CCI Inc.

As shown in Figure 4.10, the front of the MTBM contains the sensors monitoring steering cylinder force, torque, face pressure, and face rotation speed. The steering cylinder sensor comprises a pressure transducer measuring changes in fluid pressure. The main function of the steering cylinders is to guide the MTBM along the designed alignment. Their secondary function is to provide an indication of the amount of force at the front of the MTBM. Therefore, in areas of curved alignment, higher pressure in the cylinders may be due to guidance, rather than soil reaction at the MTBM face. This data is considered sufficiently accurate for demonstrating the amount of force on the MTBM face. The assumption that the force on the steering cylinder is indicative of the force on the MTBM face has been made previously, in the work of Sharma, Snider, Williamson, & Brown in 2014, and also by Pfeff D. in 2013, when she completed a review of various DPI construction projects.

4.3.2 Sensor Data Output

The analysis used two primary situation types during the case studies; Type I and Type II. Also obtained was a third situation, Type III data; however, measurements taken had much less frequency than in the two primary situations. Both Type I and Type II situations include data from the thruster and the MTBM. Information provided by the thruster for Type I situations includes thrust force, rate of advance, tunnel length, and cylinder stroke position. Information provided by the MTBM for these same situations includes face rotary pressure, face rotary speed, face pressure, and lubrication pressure.

Type II situations also include information from both the thruster and the MTBM, but there were differences in placement of the sensors providing measurements. Information from the thruster in Type II situations include thrust force, rate of advance and tunnel length and information from the MTBM in these same situations include steering cylinder force, face rotary speed, and face rotary

pressure. Type III data combines information from the thruster, including tunnel length, rate of advance, and total thrust, with face pressure data obtained from the MTBM. As mentioned previously, Type III data is not as detailed as the other two primary data types. Table 4.3 below show the types of data that were obtained for each case study.

Table 4.3: Data types obtained for each case study

	Type I	Type II	Type III
Case Study 1	√		
Case Study 2			√
Case Study 3	√		
Case Study 4		√	

4.3.3 Methods of analysis

After extensive analysis of the case study data, the author established methods to assist in completing the research objectives. Different methods of analysis were required, based on the types of data obtained, to achieve research goals. Studying the contribution of the contact force at the cutting face of the MTBM required quantifying the frictional resistance along the alignment. Quantification of frictional resistance uncoupled from the reaction of face contact force in DPI construction methods has not yet been achieved for realized case study data.

The author considered two methods for assessing measurements of the frictional resistance using both types of data. Method I subtracts face pressure information at the MTBM from the total thrust data for specific tunnel lengths, or the entire alignment. Staheli (2006) utilized this method in her work determining frictional resistance in case studies during conventional micro-tunnelling construction projects. The difference of the force contribution of the face pressure and the total

thrust force enables assessment of the amount of frictional resistance along the length of the tunnel. In the case of Type II data, subtracting the steering cylinder force measured at the articulation joint of the MTBM from the total thrust data, quantifies the frictional resistance. Assumptions made by this methodology that could skew the results may include:

- The face pressure/steering cylinder sensor is correctly quantifying the amount of pressure acting on the cutting face;
- There are no influential factors between the thruster and MTBM face, other than frictional resistance, which affect the total thrust force;
- The face pressure or steering cylinder force is a measure of the total force at the MTBM cutting face, and no other forces are acting on the cutters.

Information obtained from the equipment manufacturer suggest that the force at the steering cylinders is influenced by curvature in tunnel alignment, a short section of friction between the cutting face and the articulation joint, and the force on the MTBM cutting face. The type II data is evaluated from relatively straight sections in attempt to limit the amount of outside error from tunnel alignment curvature, and the frictional effect between the cutting face and the articulation joint is considered to be small (generally less than 1.5 m length), therefore the assumptions listed for using a method 1 evaluation are considered valid for assessing the force at the MTBM cutting face.

The second method used to quantify the amount of frictional resistance incorporating all types of data, considered Method II, examined specific sections where the face was not in direct contact with the native soil. Such instances include examining data while the MTBM and lift section lowers through an open tunnel, or the MTBM exits into the receiving shaft/excavation, where there is an

absence of soil pressure on the cutting face. Assumptions made while analyzing data using this methodology include:

- The magnitude of the pipe weight that acts in the direction of thrust assumes densities and geometries which may influence the result;
- The face is fully clear of any native soil.

Finally, assumptions that may influence either methodology for all data types include:

- Thruster data is accurately demonstrating the force transferred to the pipe by the thruster;
- Amount of surface area in contact with the tunnel sidewall is constant while assessing frictional effects;
- The surface area is purely in contact with lubrication bentonite, purely in contact with native soil, or a combination of contact with both lubrication bentonite and native soil.

It is anticipated that geometric change of the tunnel alignment has a significant effect on the load distribution of the soil to pipeline interface. Therefore, in an effort to limit the error from these assumptions, shorter sections of data were reviewed. Evaluating shorter sections allow less time for changing interface load distribution conditions.

The face pressure data provided by the MTBM in Type I situations is rounded to the nearest ten kilopascals (0.1 bar). The rounded face pressure values produce gaps in information with missing data. The missing information provides uncertainty, for assessment of specific magnitudes in the data, however it is considered reliable when analysing general trends in relation to the other MTBM parameters.

In light of the preceding considerations, Method I and Method II were used for Type II data, while Method II only was used for Type I data. Type III data was reviewed in a general sense; however, because of the data acquisition frequency and the missing information in portions of the alignment as discussed above, the data was considered unreliable to review specific results.

4.4 COMPARING THE CURRENT STATE OF PRACTICE CALCULATION METHOD TO REALIZED THRUST AND EVALUATING DIFFERENCES

4.4.1 General

Information obtained from each case study is compared with the current state of practice calculation method (Pruiksma, Pfeff, & Kruse, 2012). Typically, a designer would calculate the total estimated thrust at changes in alignment geometry to establish the required envelope. Using this method provides five data points, assuming there are no horizontal curves, to generate the envelope. For this research, envelopes that are more detailed were required; therefore, it was necessary to perform thrust calculations at a frequency less than one meter. Analysis at this frequency generated more data points, establishing a better comparison to the information obtained from the case studies.

4.4.2 Comparison of Calculation to Realized Thrust

4.4.2.1 The Flat Typical DPI

The amount of total thrust was recorded during the Flat Typical DPI crossing. This information has been compared to the current state of practice calculation method (Pruiksma, Pfeff, & Kruse, 2012). The evaluation includes comparing the total realized thrust to the theoretical calculation using drained and undrained soil properties. The comparisons for both the drained and undrained analyses are shown on the charts in Figure 4.11 and Figure 4.12, respectively, below.

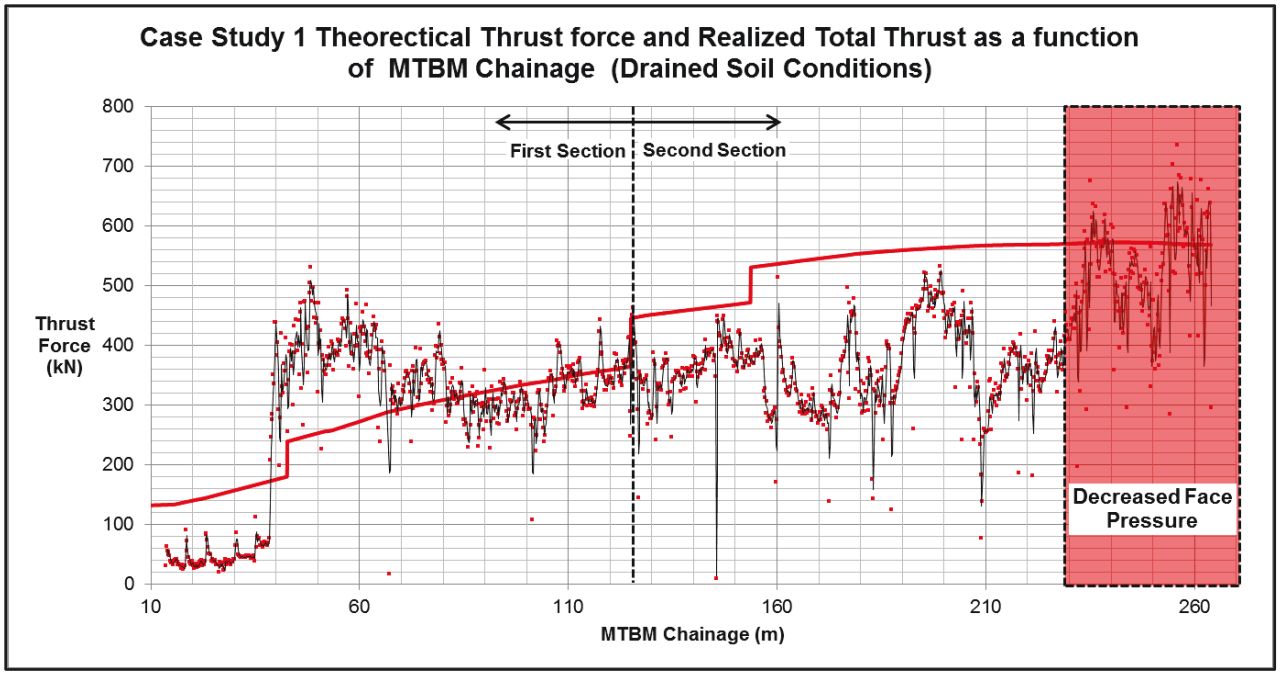

Figure 4.11: Comparison of theoretical total thrust force calculation and realized total thrust force in drained soil conditions for the Flat Typical DPI crossing.

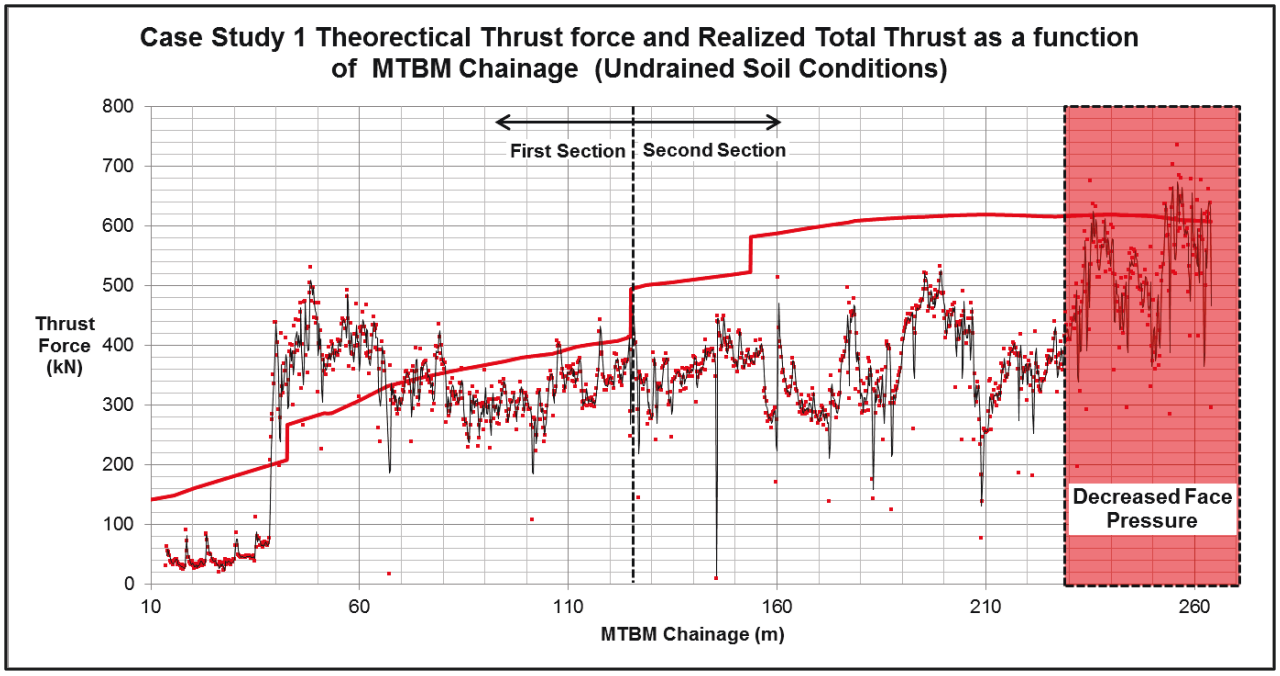

Figure 4.12: Comparison of theoretical total thrust force calculation and realized total thrust force in undrained soil conditions (K=1) for the Flat Typical DPI crossing.

Data acquired from the project showed the thrust force necessary to advance the tunnel was somewhat constant, varying between 235 kN and 510 kN, an average of about 330 kN, for most of the tunnel drive. On average the percent error of the estimation to the realized data for the drained and undrained analyses were 51% and 68%, respectively.

At a drive length of 230.6 m, the thrust forces increased to a maximum thrust force of nearly 640 kN and averaging about 520 kN. The tunnel crown is at an elevation of approximately 204.5 m, geodetic, at this location and the face pressure of the MTBM decreases from between 20 kPa and 30 kPa to less than 10 kPa. Daily construction reports confirm the decrease in face pressure and note that the face pressure remained low for the remainder of the tunnel drive to recover lost fluids. There were no considerable changes shown in the torque data, suggesting the soil through the tunnel alignment was consistent. This observation agrees with the geotechnical information

at the tunnel alignment location. Additionally, in contrast to the model where the frictional force of the pipeline tunnel sidewall predicates the anticipated thrust (Pruiksma, Pfeff, & Kruse, 2012), the Flat Typical DPI case study demonstrated that required thrust force does not substantially increase with tunnel drive length.

4.4.2.2 The Trail DPI

The amount of total thrust was recorded during the Trail DPI crossing. Comparison of this information to the recommended calculation (Pruiksma, Pfeff, & Kruse, 2012) using drained and undrained soil conditions to evaluate the estimated total thrust are shown on the charts in Figure 4.13, and Figure 4.14, below.

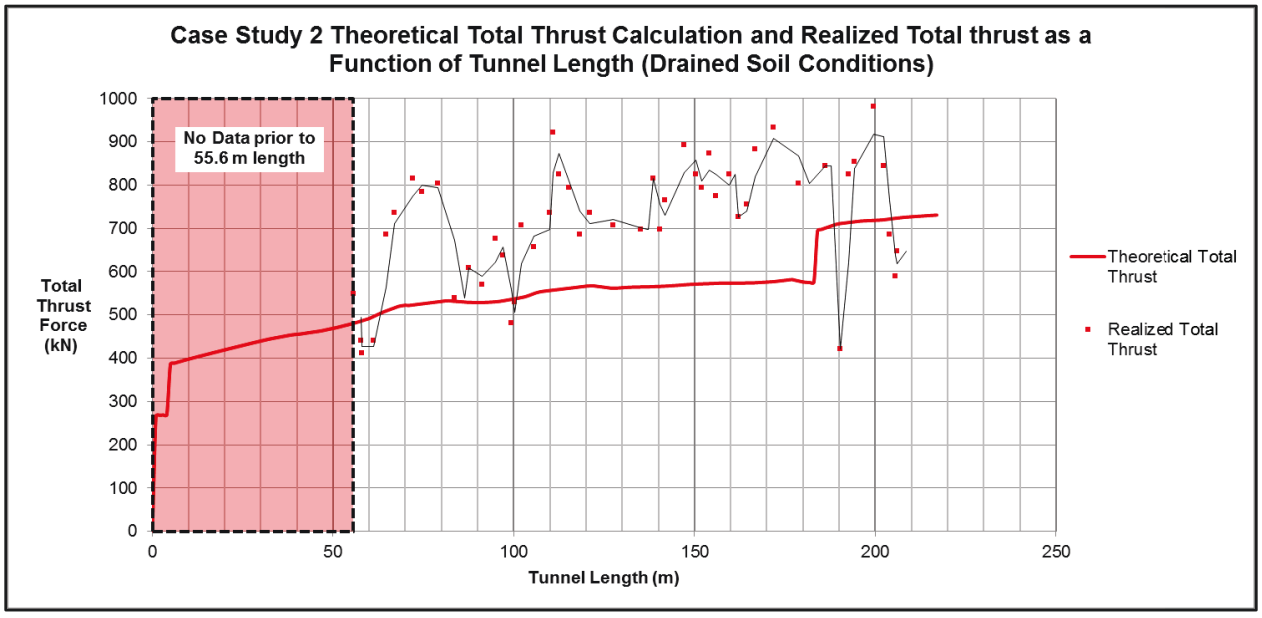

Figure 4.13: Comparison of theoretical total thrust force calculation and realized total thrust force in drained soil conditions for the Trail DPI crossing.

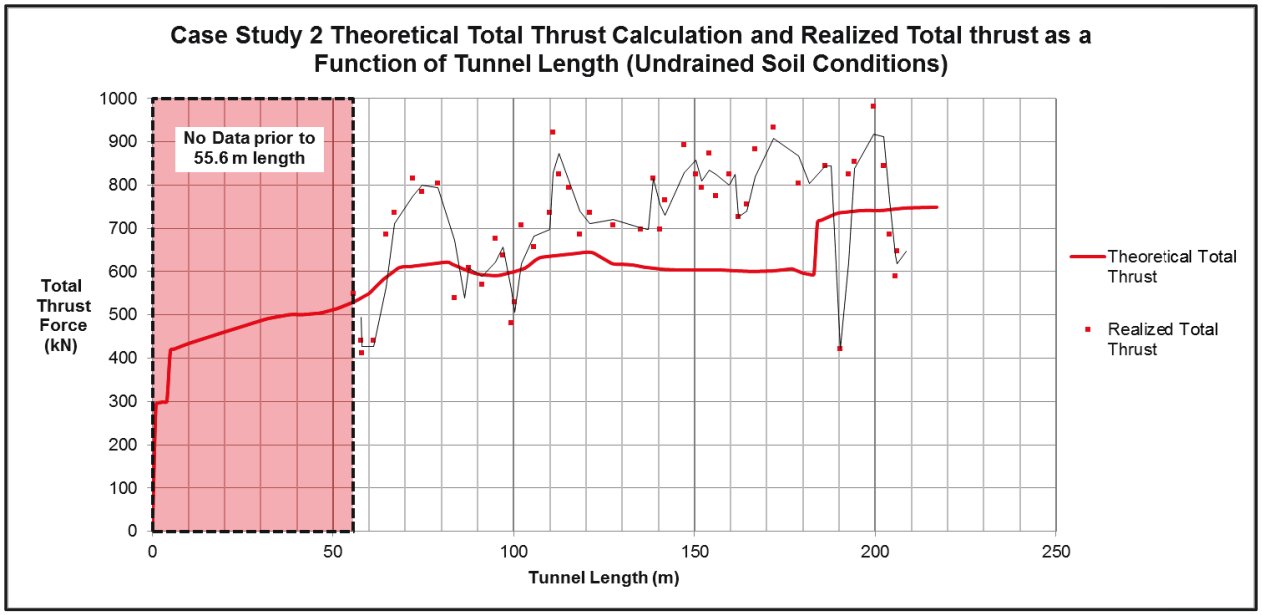

Figure 4.14: Comparison of theoretical total thrust force calculation and realized total thrust force in undrained soil conditions (K=1) for the Trail DPI crossing.

As shown on the above charts, the estimated total thrust force has under predicted the realized total thrust for much of the tunnel drive in both the drained and undrained soil analyses. The average percent errors of the calculated total thrust in the drained and undrained analysis were under predictions of 17% and 9%, respectively.

It is interesting to note that at tunnel lengths of 65 m and 110 m, the amount of soil overburden height increases, and the realized total thrust also increases. This supports the notion that earth pressure has a large effect on the total thrust force. However, according to the large magnitude of the realized thrust force at those locations, the effect of the overburden height could be even larger than previously expected.

The information obtained from the Trail DPI showed a strong correlation between increasing length and increasing total thrust force. This demonstrates that the frictional component of the

total thrust is likely the most dominant. The author postulates that efficient mass lubrication was not achieved in this case study, and the reduction of frictional resistance from the bentonite fluid within the overcut was limited. Therefore, the soil to pipeline interface friction coefficient is the most dominant component of the total required thrust force.

4.4.2.3 The LLR DPI

The total thrust force was recorded during the entirety of the LLR DPI crossing. The theoretical thrust force using the methodology recommended by Pruiksma, Pfeff, & Kruse (2012), and compared to the realized total thrust force during construction. The comparison was made using undrained behaviour within the silty clay, nearest the DPI launch and receiving pits, and drained behaviour in the silt and sand soil in the middle of the tunnel alignment due to the complexity of the geological conditions. The chart in Figure 4.15 below shows the comparison between the theoretical and realized thrust force.

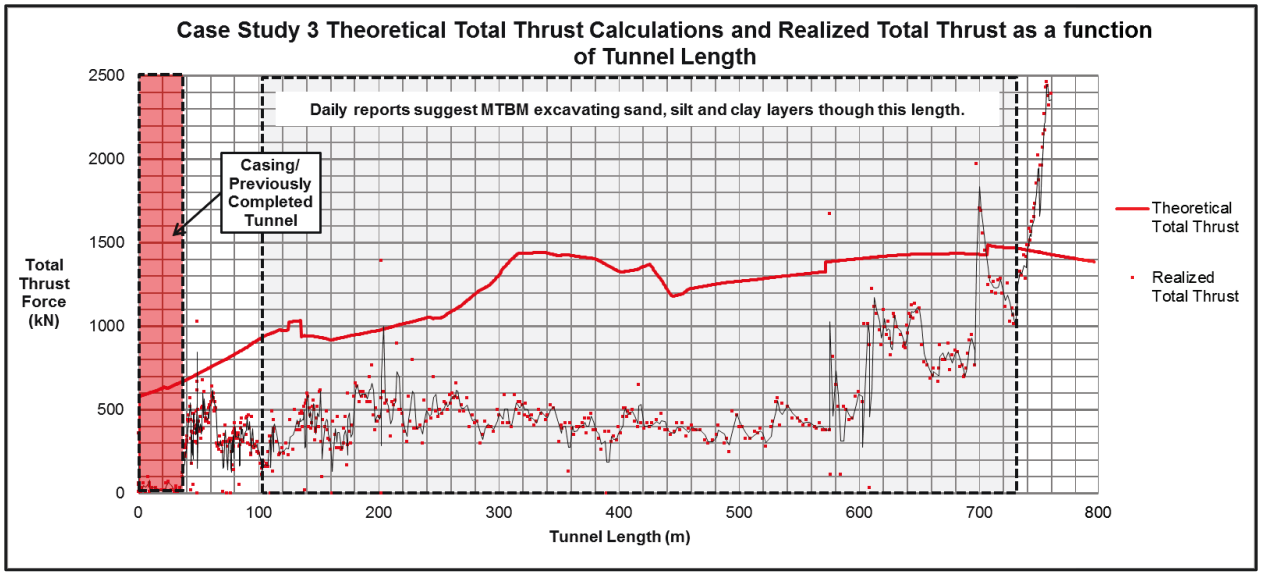

Figure 4.15: Comparison of theoretical total thrust force calculation and realized total thrust force in undrained cohesive soil conditions (K=1) and drained granular soil conditions for the LLR DPI crossing.

As Figure 4.15 demonstrates, the theoretical thrust force was much larger than the realized thrust force for much of the tunnel drive. The average percent error of the calculated thrust for the crossing was calculated to be greater than 319%. Other than a few anomalies throughout, the realized thrust force in the final 30 to 40 m of the tunnel drive is the only area which exceeds the theoretical calculation.

It is of interest that the beginning of the exponential rise in realized total thrust around tunnel length 580 m corresponds to the change of geometry in the tunnel alignment. This suggests that a substantial change in the mechanism of resistance could be contributing to the thrust force as the final vertical curve begins. In combination with other coupled factors, the occurrence of plowing could explain the exponential increase observed in total thrust force. As additional normal stress is applied to soil to pipeline interface, the contact area increases, decreasing the frictional

coefficient. Plowing occurs at high normal stress when the maximum number of soil particles are in contact with the pipeline interface, a bi-linear frictional envelope forms, and the interface frictional coefficient increases (Staheli, 2006). Additional research is required to prove this observation.

4.4.2.4 The Spirit DPI

The total thrust was recorded for about 190 m of the 261m long tunnel alignment (73%). However, additional force measurements were made at the MTBM steering cylinders for the entire tunnel alignment. The force measured at the steering cylinders represents the force on the MTBM cutting face, a small amount of frictional resistance (negligible), and additional pressure from changes in tunnel alignment.

The calculated total thrust and cutting face force were estimated using both drained and undrained geotechnical parameters and compared to the realized values during construction. The charts in Figure 4.16 and Figure 4.17, below, show comparisons using drained and undrained parameters, respectively.

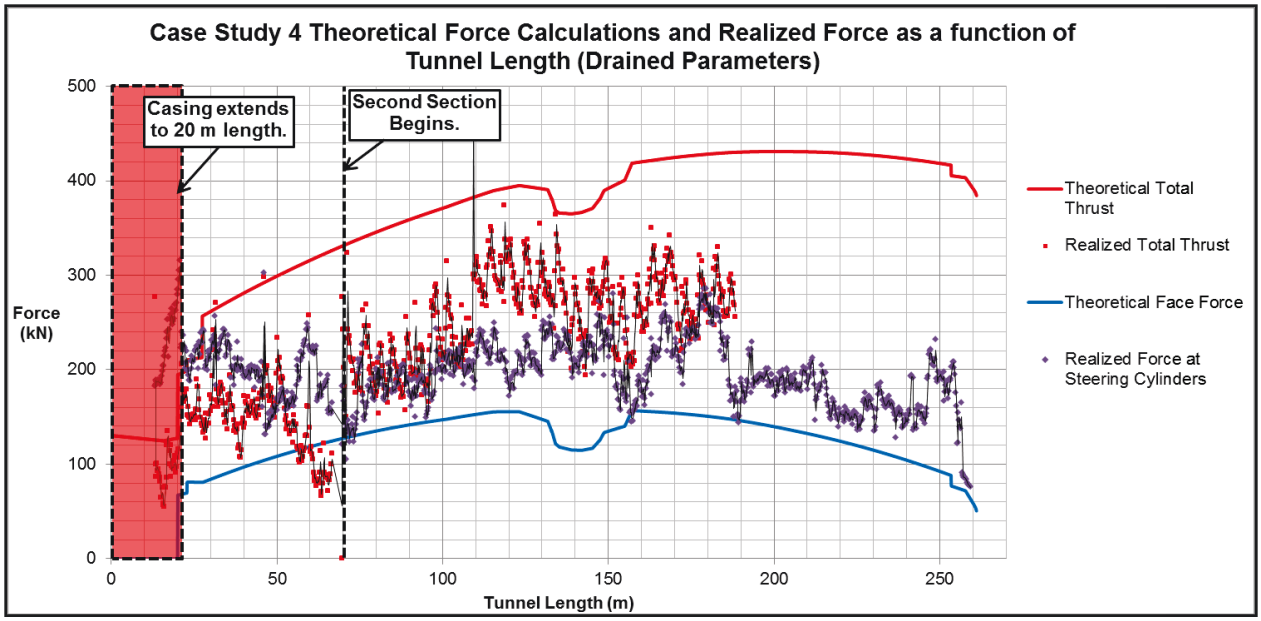

Figure 4.16: Comparison of theoretical total thrust and face force calculation to realized total thrust force and steering cylinder force assuming drained soil conditions for the Spirit DPI.

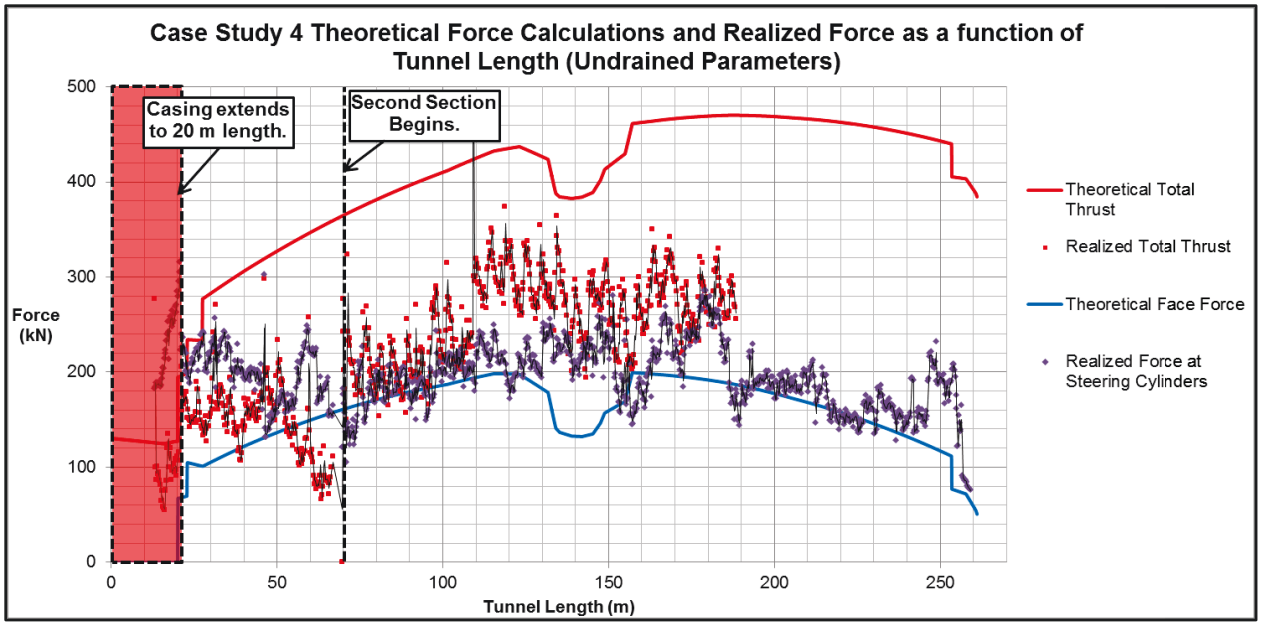

Figure 4.17: Comparison of theoretical total thrust and cutting face force calculation and realized total thrust force and steering cylinder force assuming undrained soil conditions (K=1) for the Spirit DPI.

As shown on the charts above, the total thrust force calculation over predicts the realized thrust while the cutting face force calculation under predicts the realized force on the steering cylinders during construction. The average percent error of the total thrust force calculation was 63% and 78% for drained and undrained soil conditions, respectively. Additionally, the average percent error for the front cutting face force calculation was under predicted by 30% and 13% for the drained and undrained soil conditions, respectively. As the cutting face force under predicts the realized force while the total thrust calculation over predicts the realized thrust, much of the error occurs in the frictional contribution to the total thrust. Using the undrained soil condition seems to correlate better with the face force calculation.

4.4.3 Evaluation of the Current State of Practice Calculation Performance using Percent Error Analysis

Data from four DPI case studies was reviewed and the information obtained was used to compare the calculated thrust and face force to the realized total thrust and face force during construction. To quantify the differences between the calculations and the realized values, a percent error analysis of each data point was completed, and the averages compiled. The intent of this analysis is not to complete comprehensive statistics on the data, but rather use average percent error to provide an indication if the data shows over or under prediction of the total required thrust calculation. The figures shown in the previous sections for each case study can be used to assess the accuracy and precision of the calculation at specific locations along the tunnel alignment. Table 4.4, shown below, summarizes the information obtained from the percent error analysis.

Table 4.4: Summary of average percent error of calculation model to realized forces during construction for all four case studies reviewed.

Case Study	Soil Type Analysis	Average Percent Error		Under/Over Prediction	General Soil Conditions
		Total Thrust Force	Steering Cylinder Force		
1	Drained	51%	-	Over prediction	Firm to Stiff Cl
1	Undrained	68%	-	Over prediction	Firm to Stiff Cl
2	Drained	17%	-	Under prediction	Stiff to Very Stiff, Cl (TILL)
2	Undrained	9%	-	Under prediction	Stiff to Very Stiff, Cl (TILL)
3	Drained	319%	-	Over prediction	Stiff Cl, Silt, Sand
4	Drained	63%	-	Over prediction	Stiff CH
4	Drained	-	30%	Under prediction	Stiff CH
4	Undrained	79%	-	Over prediction	Stiff CH
4	Undrained	-	13%	Under prediction	Stiff CH

All four case studies reveal there is error associated with the calculated total thrust and force at the cutting face, and the average percent error varied greatly, ranging from an over prediction of 319% to an under prediction of 9%. It should be noted that data from Case Study 2 was the only under prediction, however, complications during construction and the interval of the data make it unreliable relative to the other case studies. Therefore, the three case studies with the most reliable data sets (Case Studies 1, 3, and 4) have been used during the analysis completed in Chapter 5.

4.5 SUMMARY

After extensive review of the current state of practice for estimating the required total thrust and comparison to case study realized thrust information, the following conclusions were obtained:

- There were errors associated with predictions using the current state of practice calculation method for each of the four case studies.
- The frictional contribution to the total thrust is the main source of error in overestimation of the total thrust. This error was evidenced during the analysis of Case Study 4, where the cutting face force had under predicted, and the total thrust over predicted, the realized values. Frictional resistance is quantified as the difference between the two calculations; therefore, frictional resistance may be the primary source of error in that scenario. Other comparisons using both the force at the steering cylinder and the total thrust should be completed to confirm this finding.
- In all four cases, assumptions made about the soil conditions (drained or undrained) used in the analysis had a significant effect on the calculated force values. The undrained soil

condition compared better with the data obtained for the force at the MTBM face (Case Study 4). Additional information should be obtained to confirm this finding.

- The location of the final vertical arc had significant influence on the total realized thrust force in the LLR DPI. It is postulated that the influence of the change in geometry may be attributed to a “plowing” effect (Staheli, 2006), where the interface friction coefficient increases due to an increase in normal stress. Additionally, as the normal force increases particle rearrangement occurs, and the effect of the bentonite lubrication is negated, further increasing interface friction. This trend is observed while the LLR DPI is moving through granular soil; therefore, plowing and particle rearrangement is a likely explanation for the exponential increase in thrust force.

CHAPTER 5. EVALUATING CONTRIBUTION OF THE TOTAL THRUST FORCE COMPONENTS

5.1 INTRODUCTION

This chapter describes the analysis of the thrust information recorded during Case Studies 1 3, and 4 and the adjustments that could be made to more accurately predict the thrust force during construction. The contribution of the frictional components to the total thrust force in the current state of practice calculation method were assessed and evaluated by examining segments of the realized thrust data including modification of the frictional coefficients in the calculation. Additionally, the chapter includes assessment of the contribution of the force at the MTBM cutting face to the total thrust force, then evaluates and quantifies the difference of the estimated magnitude to the realized values. The cutting face force was assessed by reviewing data obtained from the DPI case studies where changes in thrust occurred because of changes in face condition only. It should be noted that the data obtained from Case Study 3 – The Trail DPI (Type III data) was considered insufficient to evaluate in detail, so it was omitted from all following analysis. The following sections cover the assessment and evaluation.

5.2 FRICTIONAL CONTRIBUTION ASSESSMENT

After completion of the sensitivity analysis in Chapter 2, it was determined that the frictional components which have significant effect on the total calculation were the friction due to rollers and the soil to pipeline interface friction. The differing data types obtained (Type I and II) necessitated a varied analysis for each. Additionally, due to the complex coupled mechanisms of the frictional components, both the surficial (roller) and lubrication fluid frictional coefficients had to be reviewed in conjunction with one another. Finally, for Type I data, again because of the

complex coupled frictional mechanisms in the construction method, the soil to pipeline interface friction was unable to be separated from the data obtained. However, values for soil to pipeline interface friction in a mass lubrication scenario have been reviewed for conventional micro-tunnel applications, and their applicability to DPI has been assessed.

5.2.1 Type I Data Analysis

5.2.1.1 The Flat Typical DPI

The surficial frictional component of the total thrust force was evaluated by reviewing data while the MTBM was lowered through the casing. The casing was fully open, clear from soil and full of bentonite lubrication fluid, therefore it can be assumed the only resistance acting on the system was the surficial and lubrication fluid friction. The chart in Figure 5.1, below shows the section which was extensively reviewed for this analysis.

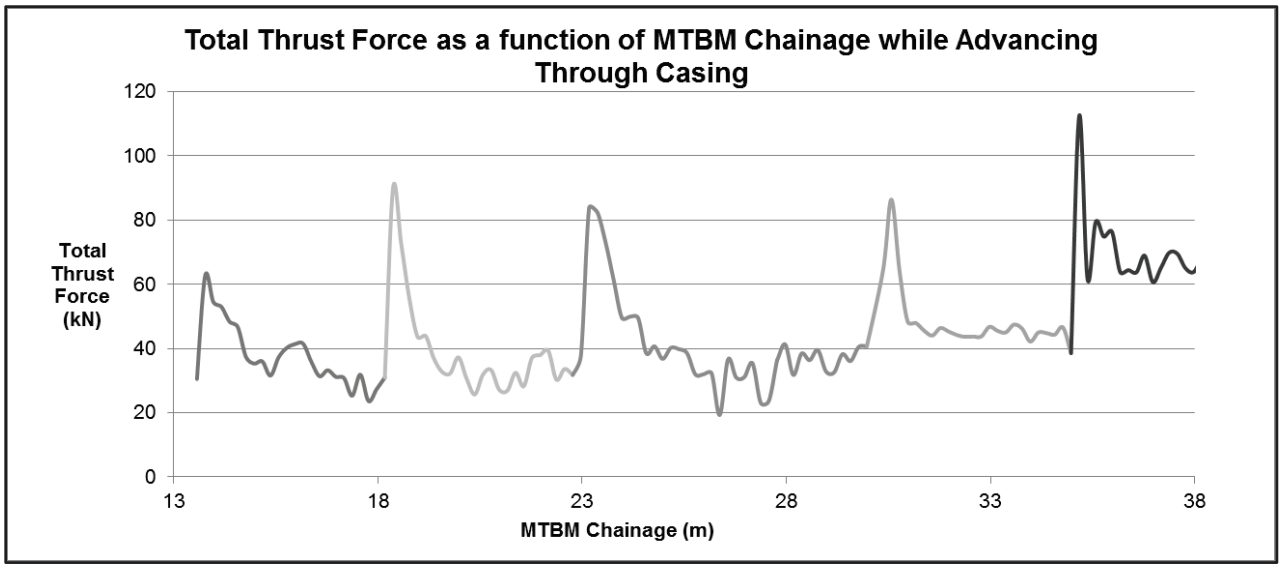

Figure 5.1: The total thrust force as a function of MTBM chainage as the MTBM advances through casing.

The chart above shows the section of required thrust force as the MTBM is lowered through the casing, from just past 13 m to 38 m of tunnel length. The data was interrupted and not recorded with accuracy during construction prior to the tunnel length of 13 m, therefore is considered unreliable. The peak thrust values in the data coincide with information showing that the thrust cylinder stroke position is at a minimum. In other words, the peak thrust forces occur at points of impending motion. Similarly, the thrust cylinder stroke position indicates that the thrust force occurring just after the peak values are representative of a dynamic system and will herein be referred to as residual frictional resistance.

As noted, this section of tunnel drive is contained within a 1524 mm (60 inch) diameter casing, filled with bentonite lubrication, and clear of soil; therefore, the frictional resistance of the surficial rollers and lubrication can be determined. The chart in Figure 5.2, below, shows the same peak and residual frictional data from Figure 5.1 separated into their respective groupings.

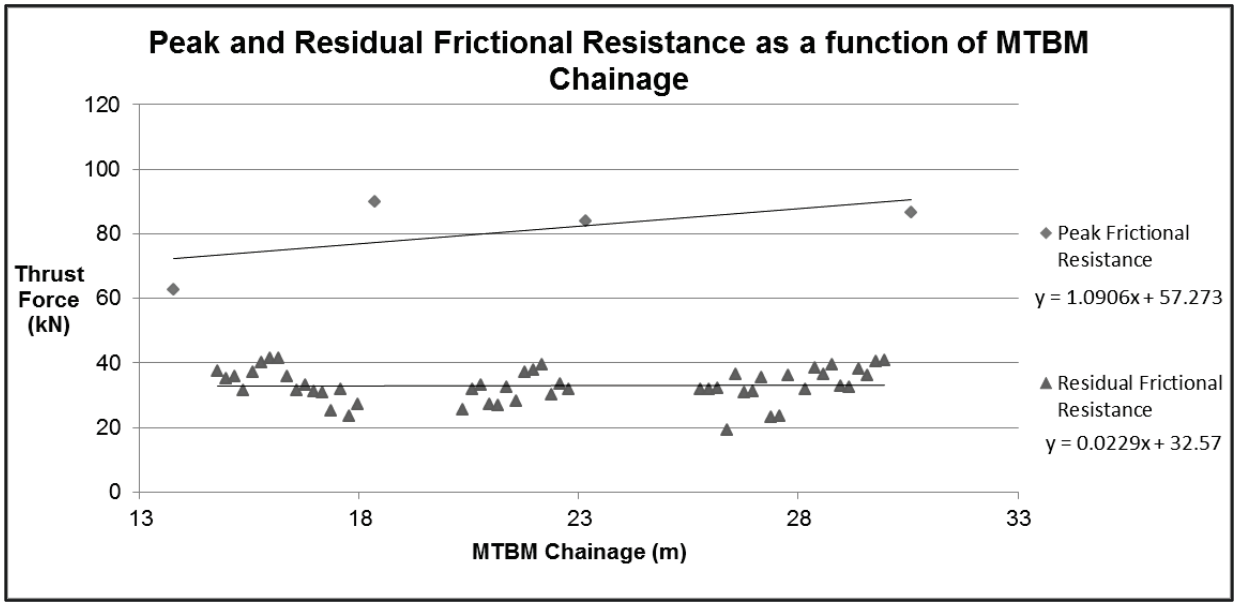

Figure 5.2: Peak and residual frictional resistance as the MTBM is lowered through the open casing.

Linear regression analysis was used to determine the peak and residual frictional resistance per length while the MTBM was lowered through the casing. Since the frictional resistance from both the lubrication and rollers are linear, the frictional coefficients can be varied so the equation matches the line of best fit for both the peak and residual data sets. Matching the frictional resistance provides the surficial (roller) frictional coefficient that best predicts the y-intercept of the linear regression equation. After obtaining the surficial frictional coefficient, the value of the lubrication frictional coefficient could be varied to establish best fit.

5.2.1.2 The LLR DPI

The LLR DPI Type I data was not recorded as frequently as the information obtained for analysis in Section 5.2.1.1, therefore an average frictional resistance combining peak and residual data was assessed. Information obtained was considered sufficient to complete the analysis on the frictional resistance data using methodology similar to that described in the previous section. The chart in Figure 5.3 below shows the total thrust information as the MTBM advances through the open casing and previously mined tunnel.

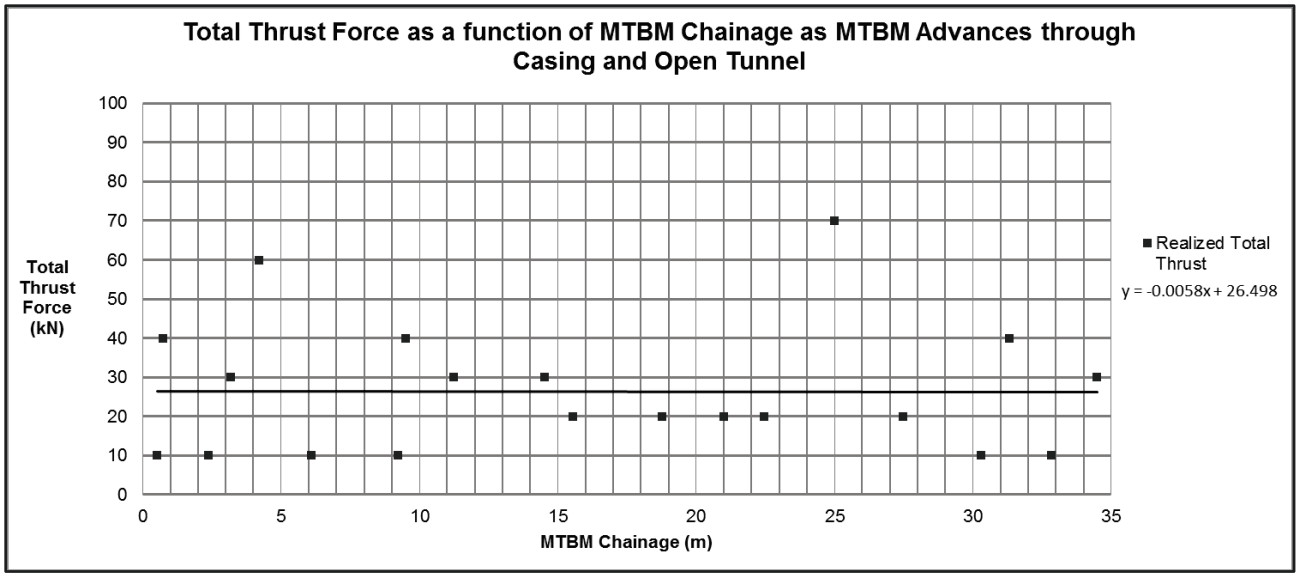

Figure 5.3: Total thrust force as a function of MTBM chainage as the MTBM advances through casing and open tunnel.

The chart shown above demonstrates the magnitude of frictional resistance as the MTBM progresses through the open tunnel. The line of best fit indicates a very slightly downward sloping trend, which at first glance seems peculiar. However, after review of the case study geometry, it was noted that the lift section sloped downward toward the launch point. In turn, this geometry would be expected to reduce the pipe weight acting on the rollers, in the location of the downward slope, thereby decreasing the total friction which is shown on the chart. Since this analysis only considers the thrust force, in a direction orthogonal to the normal force, the lower total resistance is represented within the surficial and lubrication frictional coefficients. Finally, to normalize the surficial frictional coefficient, the pipe weight in the direction of thrust for the inclined portion of the lift section was added to the realized total thrust values. The calculated value for the extra force due to pipe weight was 122.64 kN and can be considered constant for the tunnel length interval of interest. This value is substantially larger than the thrust force realized as the MTBM progressed

through the casing and open tunnel. It can therefore be concluded that the geometry of the lift section can have a large effect on the total force experienced by the pipeline and should be normalized to evaluate the thrust force. It seems, in some cases, the effect of the lift section geometry could potentially be larger than the applied force of the thruster.

5.2.2 Type II Data Analysis

5.2.2.1 The Spirit DPI

The Spirit DPI acquired information in the form of Type II data, meaning the total thrust force and the force on the MTBM cutting face were both measured. The data obtained as the MTBM progressed through the casing and beyond, to a tunnel length of 69.7 m, was heavily influenced by the geometry of the lift section (two sections, as described in Chapter 3). Data from a tunnel length of 69.7 m to 188.4 m was used for the frictional coefficient adjustment analysis.

To obtain the amount of frictional resistance along the length of the pipeline during the Spirit DPI, the force measured near the face of the MTBM was subtracted from the total thrust measured by the thruster on surface. This method of subtraction has been used previously by Sharma, Snider, Williamson, & Brown (2014) to obtain the amount of frictional resistance between the MTBM and thruster during DPI construction. On completion of this filtering process the frictional data obtained includes the pipeline to roller interface friction, pipeline to lubrication bentonite interface friction, pipeline to soil interface friction, and the pipeline weight acting in the direction of thrust. Following determination of the frictional force acting on the pipeline during tunnelling, a linear regression analysis was completed for the 118.7 m section where relatively consistent information was observed. The chart in Figure 5.4 below shows the linear regression analysis completed for this data.

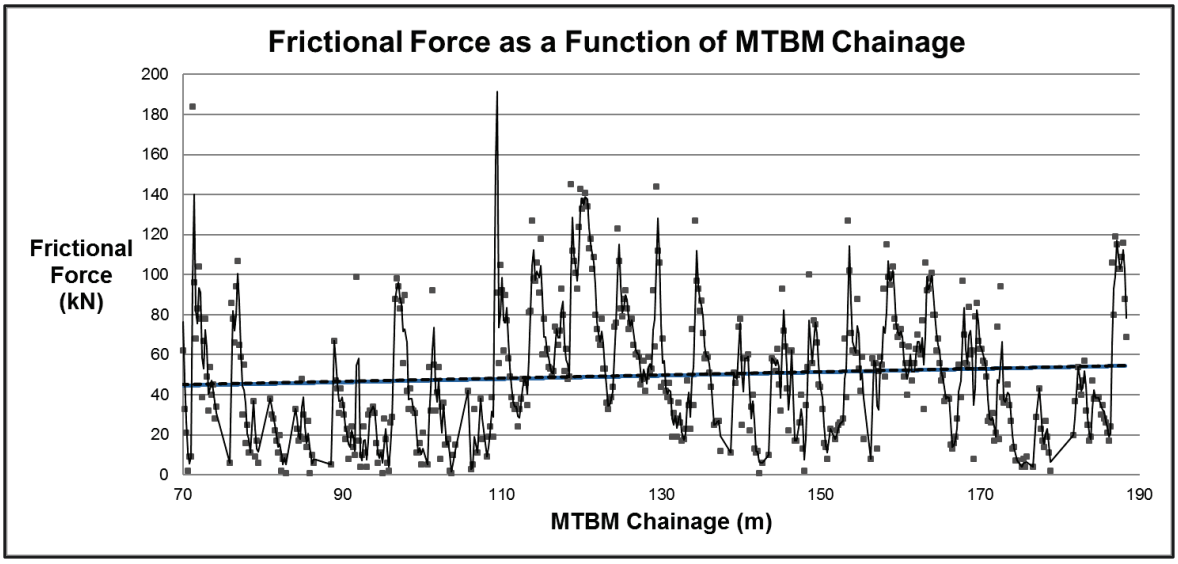

Figure 5.4: Chart showing the frictional force as a function of MTBM Chainage from 69.7 m to 188.4 m. The frictional force in the chart was obtained as the difference between the force on the steering cylinders and the total thrust force.

Using the linear regression information in the chart above as a basis, the roller to pipe, lubrication bentonite, and soil to pipeline interface frictional coefficients were modified in the current state of practice DPI calculation and matched to the line of best fit. The negative values shown in the chart above are attributed to the pipeline weight acting on the steering cylinders as the thruster carriage is pulled backwards to begin the next push. After fitting the linear regression data with the average magnitudes for the same 118.7 m long section of the calculation, all three frictional coefficients were obtained.

5.3 EVALUATION OF FRONT CUTTING FACE FORCE CONTRIBUTION

5.3.1 Evaluation of Change in MTBM Cutting Face Conditions

Analysis to determine the magnitude of the front cutting face force contribution to the total thrust force was completed for each data type. Consistent throughout each of the three case studies, the total thrust force increased as the MTBM exited the casing or open tunnel and began mining in situ soil. The sections of the tunnel alignment where the force on the face of the MTBM was examined in Case Studies 1, 3 and 4 are shown below on the charts in Figure 5.5, Figure 5.6, and Figure 5.7, respectively.

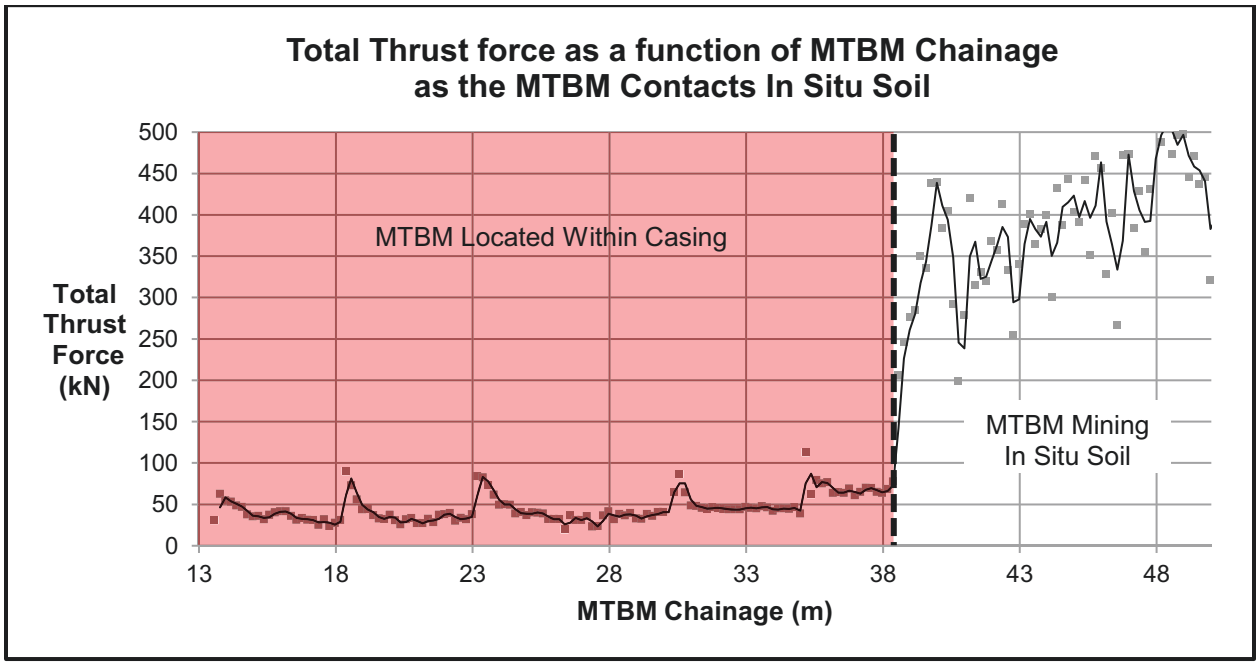

Figure 5.5: Total thrust as a function of MTBM chainage as MTBM contacts in situ soil during construction of the Flat Typical DPI.

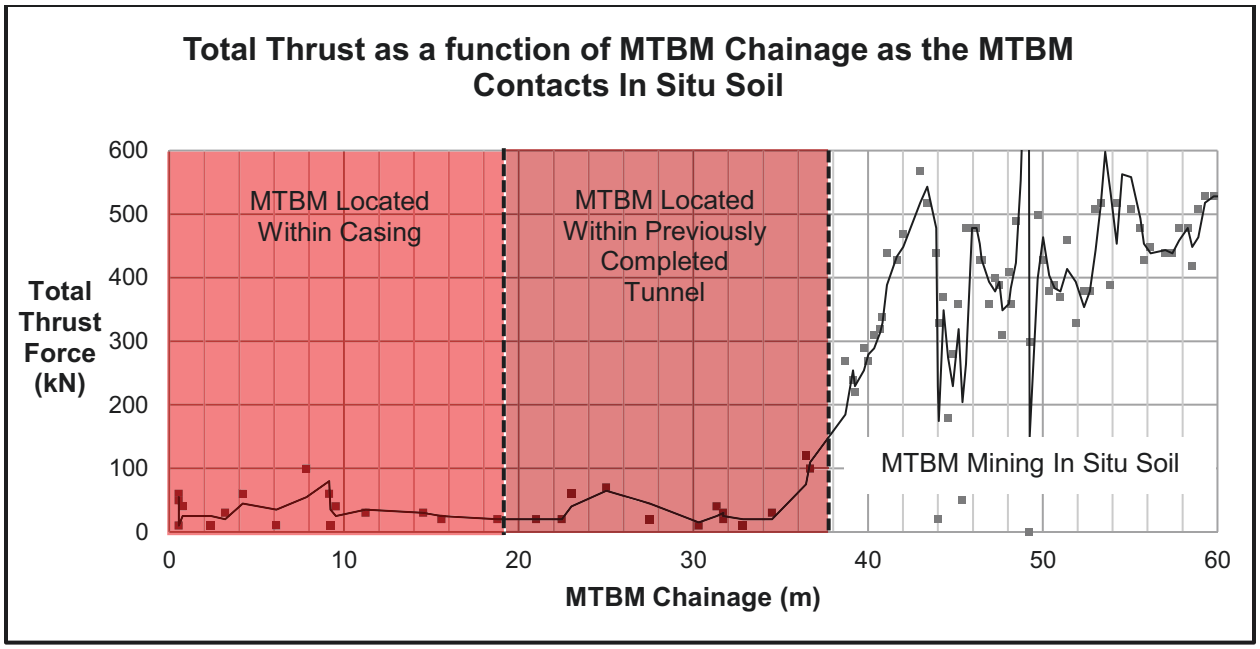

Figure 5.6: Total thrust vs MTBM chainage as it contacts in situ soil during the LLR DPI.

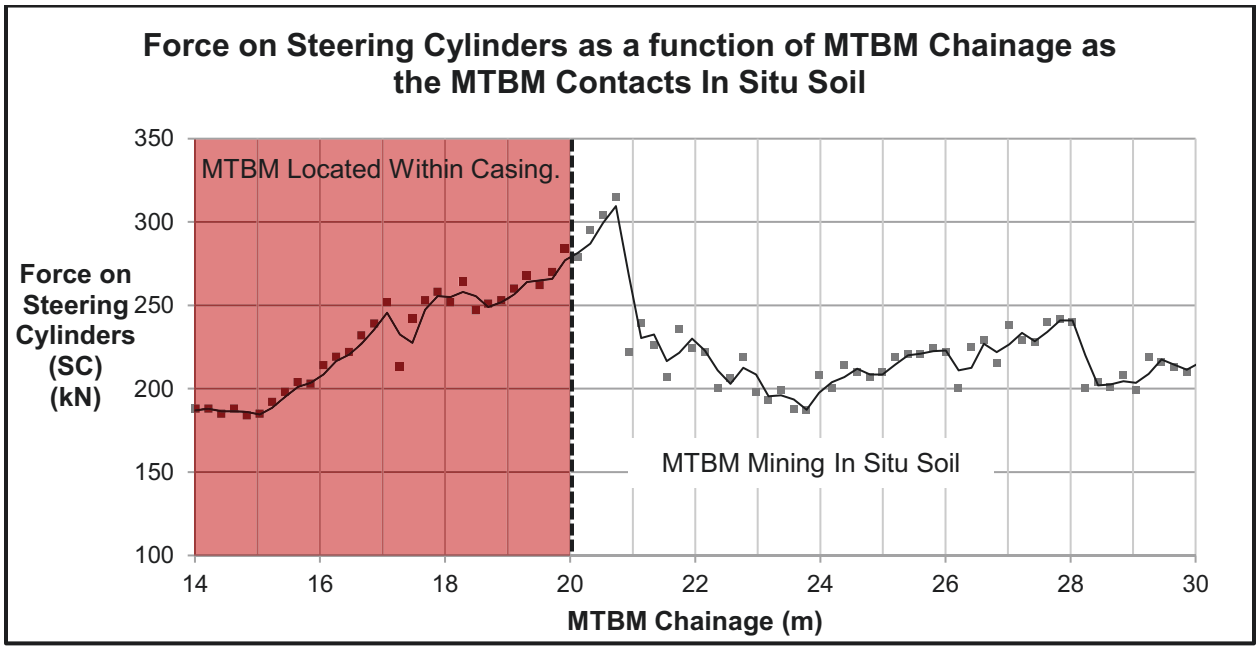

Figure 5.7: Force on Steering Cylinders (MTBM Cutting Face) vs MTBM chainage as it contacts in situ soil during the construction of the Spirit DPI.

The charts above show a substantial increase in force on the MTBM face as contact with native soil ensues. Other than the change in soil conditions at the MTBM cutting face, there were no other substantial changes in tunnelling conditions during this portion of the alignment. Therefore, an assessment can be made based on the difference in the initial (while in casing) and final (while in native soil) total thrust force, and on the final force on the steering cylinders only, to estimate the magnitude of the force exerted on the MTBM cutting face by the in-situ soil. Using this methodology, the magnitude of front cutting face force was determined to be between 300 kN and 450 kN in the three case studies reviewed. These values are substantially larger than the estimated face force using horizontal earth pressure at similar depths, which range from 91.0 kN to 158.8 kN.

Additionally, on the Spirit DPI, the force as the MTBM exited into the receiving pit was evaluated. The force on the steering cylinders dropped considerably after the exit of the MTBM, as shown by the chart in Figure 5.8 below.

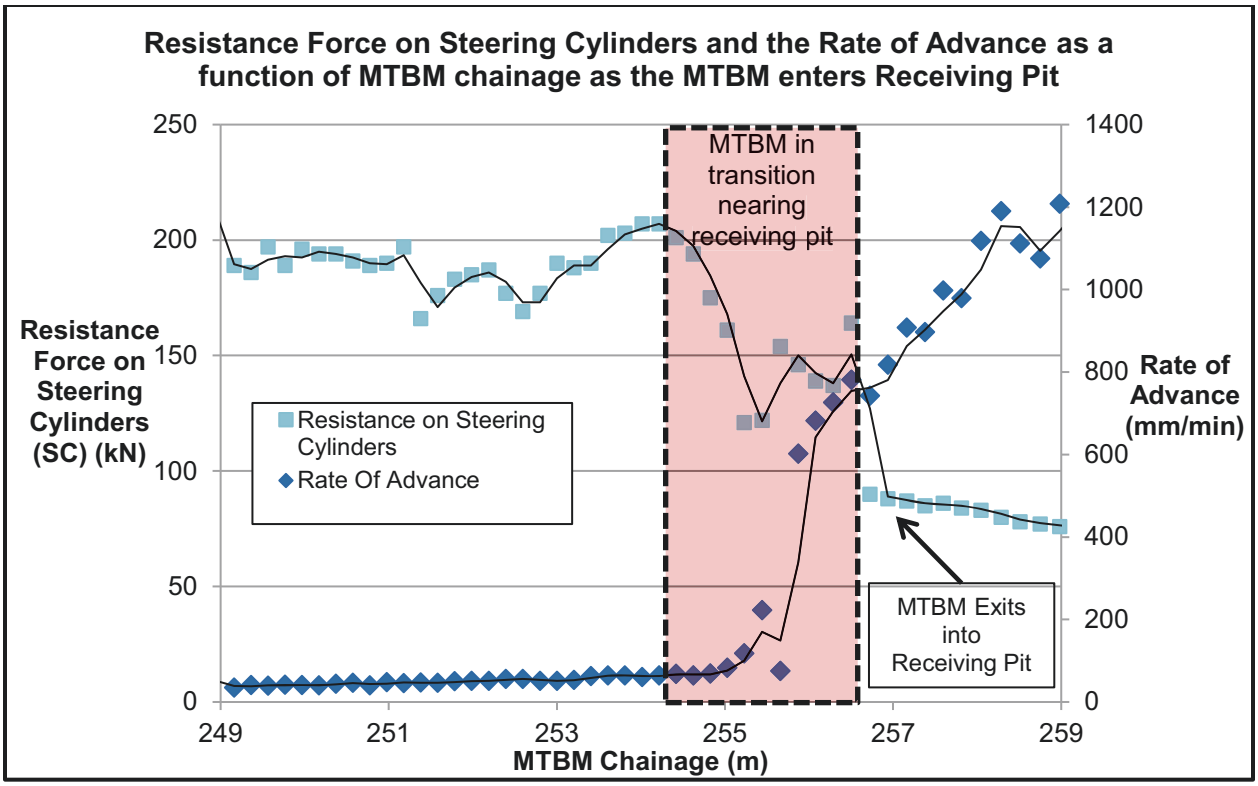

Figure 5.8: Force on Steering Cylinders (MTBM Cutting Face) vs MTBM chainage as it exits from native soil into receiving pit on completion of the construction of the Spirit DPI.

As shown in the chart above, the force on the steering cylinders is about 207 kN just prior to the MTBM exit into the receiving pit. This value is much larger than the expected face force, estimated using the expected horizontal earth pressure at a similar depth, which is calculated to be about 104.1 kN.

The rate of tunnel advance (ROA) is also shown on the chart to reinforce that the MTBM did exit into the receiving pit. The data reveals that the rate of advance is relatively constant, and low, until the MTBM exits. The advance rate then increases substantially and becomes less predictable as the MTBM is disassembled. However, information conferred by the data is only of interest during the constant rate of tunnel advance, and therefore can be considered reliable.

5.3.2 Effect of Support Pressure on Total Thrust

Additional effort was made in this research to evaluate the effect of face support pressure on the total thrust force. Nearing the end of the tunnel alignment during the Flat Typical DPI the face support pressure was decreased substantially to recover lost slurry. The total thrust force increased as a consequence of this decreased face pressure. This trend is shown on the chart in Figure 5.9, below.

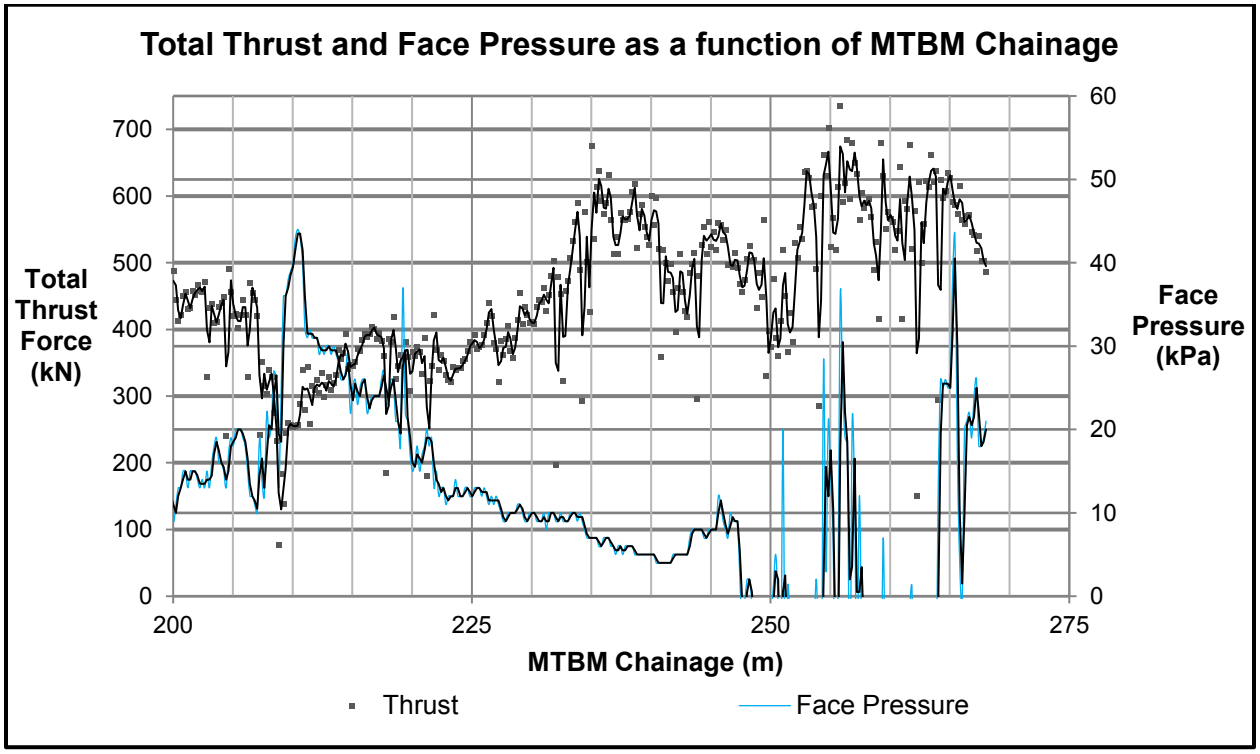

Figure 5.9: Total thrust force and face pressure vs MTBM chainage during the final portion of the Flat Typical DPI Alignment.

As shown in the above chart, at an MTBM chainage of about 220 m, the face pressure drops considerably from nearly 25 kPa to nearly nothing, and the total thrust increases from 350 kN to nearly 600 kN. This inversely proportional relationship between the face pressure and total thrust

does not agree with the fundamentals of the front cutting face force equation in the current state of practice calculation method.

5.4 SUMMARY

This chapter reviewed specific sections of the DPI case study alignments to assess and evaluate both the frictional contribution and the front force at the MTBM cutting face. The following summarizes the chapter:

- The frictional contribution of the roller pipeline, and lubrication pipeline interfaces were evaluated by examining the realized thrust data within the casing for two case studies. The coefficients of friction were determined using linear regression to best fit the data to the equations referenced from the current state of practice calculation method;
- The frictional contribution of the soil pipeline interface was evaluated using a linear regression analysis to best fit the data obtained for a straight section of the pipeline alignment within clayey soil. The linear regression was fit to the soil to pipeline frictional resistance equation for the straight tunnel alignment as referenced in the current state of practice calculation to determine the realized frictional coefficient.
- The front cutting face force was obtained just as the MTBM exited the casing in three case studies. At this location a large increase in total thrust force occurs and can be attributed strictly to the front force at the MTBM cutting face because of the changing condition at that location. Additionally, the magnitude of front cutting face force was assessed for a single case study as the MTBM exited into the receiving pit.
- Review of the realized face pressure data obtained from the MTBM in a single case study suggests that decreasing face pressure increases the required thrust force. This inversely

proportional relationship does not agree with the front cutting face force contribution in the current state of practice calculation.

CHAPTER 6. RESULTS AND DISCUSSION

6.1 INTRODUCTION

The results of the evaluation of the thrust force in DPI construction are discussed in this chapter. The current state of practice for calculating thrust force has been reviewed and compared with case study information obtained for this research. The analysis completed in Chapter 4 revealed that the current state of practice calculation method had not predicted the realized total thrust accurately. To predict the realized total thrust more accurately, evaluation of the interface friction coefficients and the force at the MTBM cutting face was completed. The following sections discuss the results of the parameter assessment

6.2 INTERFACE FRICTION COEFFICIENTS - RESULTS

Following the evaluation discussed in the previous chapters, coefficients of interface friction for the pipeline to rollers (surface) and pipeline to lubrication bentonite were determined based on the case study data available. Due to data availability, as discussed in Chapter 3, the soil to pipeline interface friction coefficient was only determined for Case Study 4. Information displayed in Table 6.1 below shows the interface coefficient adjustment suggested by the analysis completed throughout the previous chapters.

Table 6.1: Interface friction coefficients obtained from the evaluation of thrust force.

Case Study	Surface Coefficient ([ ])	Lubrication Coefficient (N/m^2)	Soil Coefficient ([ ])	Comments
1 (Residual)	0.0375	65.0	N/A	Very reliable data, flat topography near behind thruster, able to match the data very well.
1 (Peak)	0.0660	380.0	N/A	Distinct peak frictional resistance values were observed within the data obtained.
3	0.00530	20.0	N/A	A sloped lift section had a large effect on lowering the frictional coefficients.
3 (Normalized)	0.0292	45.0	N/A	Frictional coefficients normalized by increasing the required total thrust by the pipe weight in the direction of thrust for the length of sloped lift section.
4	0.0303	7.0	0.0450	Only second section coefficients were analyzed as a large downslope skewed result for first pipeline section. The differences in steering cylinder thrust and total thrust were used as a basis for the coefficient adjustment.

6.2.1 Surficial Friction Coefficient

The Case Study 1 (residual), Case Study 3 (normalized), and Case Study 4 surficial frictional coefficients range from 0.0292 to 0.0375, which are substantially smaller than the recommended value of 0.1. This is the recommended value for pull sections in HDD applications, similar in mechanism to the DPI lift section. The DPI lift sections generally have much gentler geometry changes, which likely contribute to the lower values obtained in this study. Additionally, the recommendation in HDD has been formed as an industrial “rule of thumb” and literature supporting this value for rolling friction during HDD could not be substantiated. Typical coefficients of rolling friction were listed for quenched steel to quenched steel and mild steel to mild steel of 0.01 to 0.05 mm, respectively by Wen & Huang (2018). The values obtained from Wen & Huang

(2018) should be divided by the radius of the roller, which further decreases the estimated roller friction coefficient. Additionally, the largest roller friction coefficient suggested by Wen & Huang (2018) for steel to steel contact is 0.5 mm. When this value is divided by the radius of the typical roller system in DPI projects (4”), the frictional coefficient is calculated as 0.0025. As there are four wheels per roller unit the total roller frictional resistance from this calculation is about 0.01. This value generally agrees with the coefficients obtained through this research. It should be noted that these frictional values are highly dependent on the condition of the equipment used during construction.

Results also indicate that:

- The peak coefficient of friction obtained for the roller pipe interface during Case Study 1 is nearly double the residual value.
- The uncorrected coefficient of surficial friction for Case Study 3 is extremely small, which reflects the large effect the geometry of the lift section behind the pipe thruster has on the frictional resistance.

6.2.2 Lubrication Friction Coefficient

The Case Study 1 (residual), Case Study 3 (normalized), and Case Study 4 lubrication friction coefficients range from 7.0 N/m^2 to 65.0 N/m^2, which agree well with the recommended value of 50 N/m^2 (Pruiksma, Pfeff, & Kruse, 2012).

The peak lubrication friction coefficients measured during Case Study 1 and the uncorrected value in Case Study 3 is 380 N/m^2 and 20 N/m^2, respectively. The peak lubrication friction coefficient is substantially higher than the residual value (nearly six times). It is expected that this large increase is caused by thixotropic properties of the fluid. Static bentonite lubrication fluid sets and becomes

extremely viscous. The fluid experiences shear strain in the moment of peak thrust, then the fluid thins and shear strength decreases, allowing the pipeline to move through the fluid more easily (residual).

6.2.3 Soil to Pipeline Interface Friction Coefficient

The soil to pipeline interface friction value was measured through the analysis of Case Study 4. The value obtained was 0.045, which is substantially smaller than the recommended value of 0.2 (Pruiksma, Pfeff, & Kruse, 2012). This obtained value is extremely low, though not unrealistically so. Experimental research completed by Namli & Guler in 2017 suggests that the interface friction can be decreased by up to 90% by using bentonite lubrication. This supports findings from Staheli (2006), which used case study information during pipe jacking construction with mass lubrication. Additionally, it is expected that the pipeline “floats” in the lubrication bentionite within the tunnel (Pfeff D. , 2009), especially while surrounded by cohesive soil with low permeability. This “floating” effect is thought to lead to considerably less fricitonal resistance. In light of the above, it is clear that the soil to pipeline interface friction coefficient obtained from this research is realistic for DPI construction in clayey soil.

6.3 FORCE AT THE MTBM CUTTING FACE - RESULTS

Following the evaluation discussed in the previous chapters, the total force at the cutting face of the MTBM was determined based on the available case study data. The information in Table 6.2 below shows the values of the measured force on the MTBM cutting face obtained during construction, and the expected force calculated.

Table 6.2: Measured values of force on the MTBM cutting face obtained from the evaluation.

Case Study	Depth (m)	Calculated Face Force (kN)	Realized Face Force (kN)	Comments
1	3.3	108.6	350	Force obtained as MTBM exited casing into native soil. Force decreases by 150 kN after 23 m.
3	6.1	158.8	450	Force obtained as MTBM exited casing into native soil. Force decreases by 200 kN after 19 m.
4a	2.8	91.0	315	Force obtained as MTBM exited casing into native soil, then decreased by 115 kN after 15 m.
4b	3.8	104.1	207	Force obtained as MTBM exited into receiving pit.

The force values measured range from 207 kN to 450 kN, much higher than the estimates made from the recommended calculation (Pruiksma, Pfeff, & Kruse, 2012). However, the expected trend is observed in Case Studies 1, 3, and 4a, where the force at the MTBM face increases with depth. This observation suggests that the horizontal earth pressure component of the calculation is a large contribution to the result, and the discrepancy in the measured and calculated values could be due to assumptions of the horizontal earth pressure coefficient used in the calculation. Use of an undrained (K=1) or passive earth pressure condition in the current state of practice calculation increases the force at the MTBM cutting face, thus more closely predicting the realized force. As well, the discrepancies in the calculated and realized values could be uncertainty in the applied pressure above minimal pressure value.

Additionally, the force on the MTBM cutting face decreased by 43% after 23 m, 44% after 19 m, and 37% after 15 m in Cases Studies 1, 3, and 4a, respectively. The observed decrease in force could be attributed to a “zone of optimization” where the operator of the MTBM adjusts the machine parameters to achieve a more efficient mining operation. The observed decrease in force

gives credence to the notion that the applied pressure above minimal pressure term influences the result. Integrating face pressure, slurry flow rate, torque, or a combination of the controlled machine parameters and soil properties into the applied pressure above minimal pressure may give a better prediction of the force at the MTBM cutting face. Evidence that the applied pressure above minimal pressure can be estimated using the controlled machine parameters and soil properties was observed during the Flat Typical DPI, where a lowered face pressure near the end of the alignment resulted in an increased total thrust force. This observation does not agree with theory when a constant value is used, therefore, a variable applied pressure above minimal pressure is expected to have better agreement with the realized data.

6.4 COMPARING CURRENT STATE OF PRACTICE CALCULATION TO REALIZED THRUST USING RESULTS OF THE DATA ANALYSIS

The data analysis completed in the previous sections provide values of roller to pipeline, soil to pipeline and lubrication to pipeline interface frictional coefficients and recommend increasing the force at the MTBM cutting face by use of undrained (K=1) or passive (K>1) earth pressure conditions. Active (K<1) earth pressure conditions have continued to be used for granular soil. Additionally, the soil to pipeline interface friction coefficient for the Spirit DPI was the only value obtained in this research, therefore, that value was obtained as a “proxy” for the other case study comparisons. Figure 6.1, Figure 6.2, and Figure 6.3, below, show the comparison between the calculated and realized thrust information using the recommendations from earlier in this chapter.

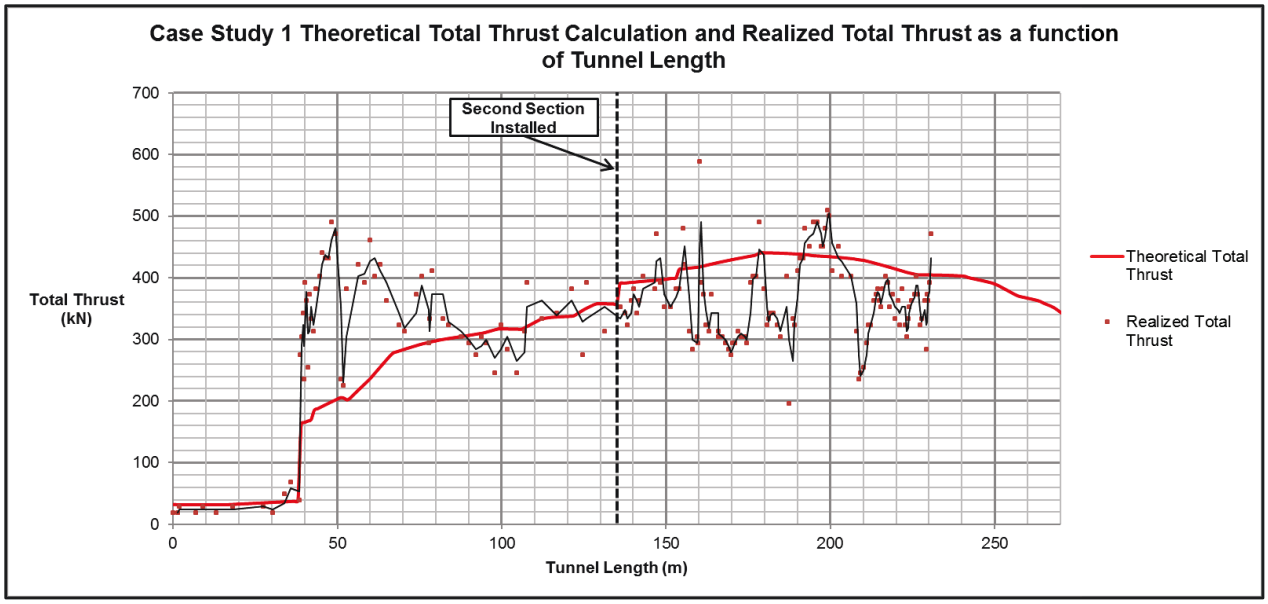

Figure 6.1: Comparison of the calculated and realized total thrust during The Flat Typical DPI using the results obtained. (f_1=0.0375, f_2=65.0 N/m^2, f_3=0.0450, K=2.46, E_0=0 kPa)

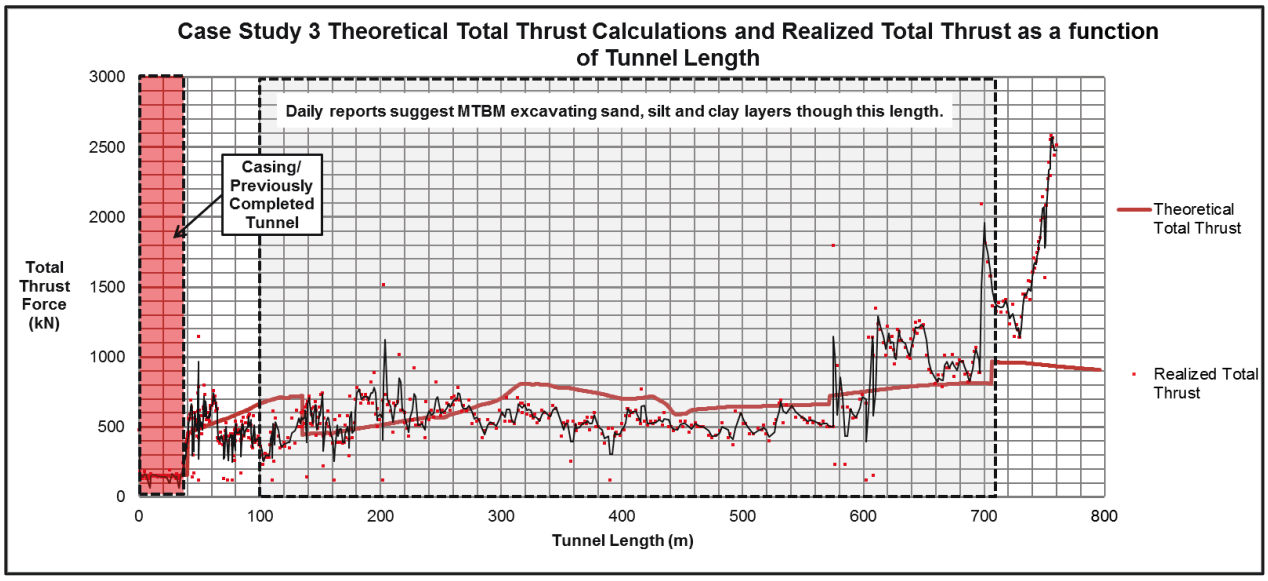

Figure 6.2: Comparison of the calculated and realized total thrust during The LLR DPI using the results obtained. (f_1=0.0292, f_2=45.0 N/m^2, f_3=0.0450, K=1, $E_{0(clay)}$=200 kPa, $E_{0(sand)}$=100 kPa)

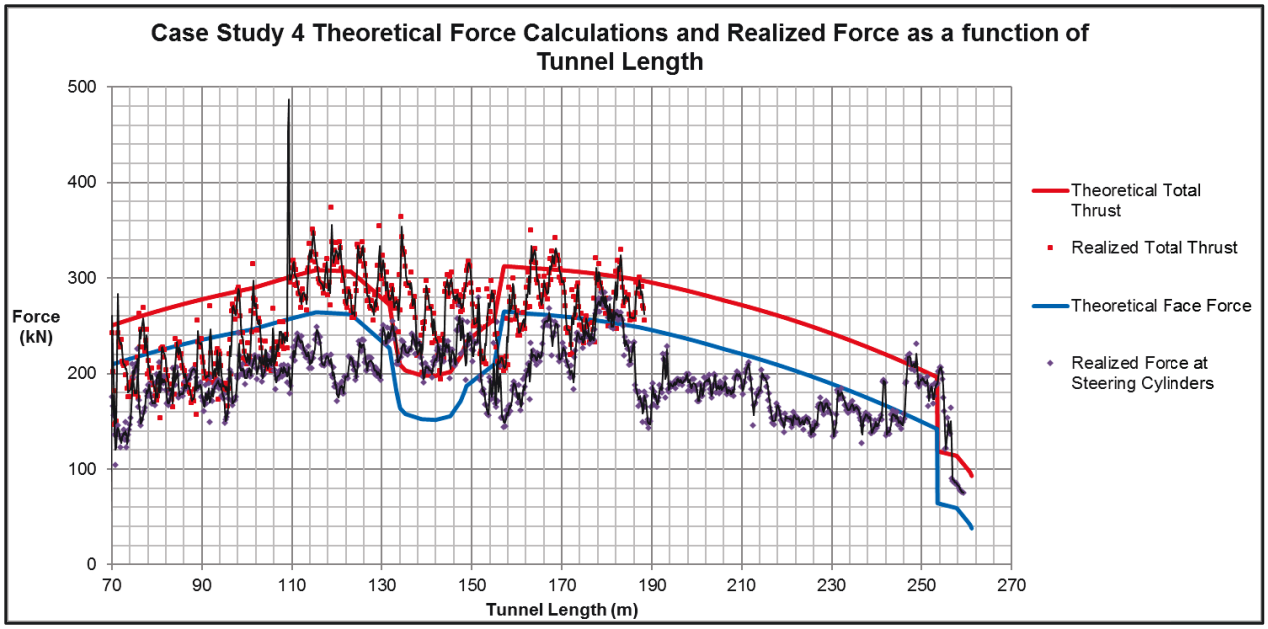

Figure 6.3: Comparison of the calculated and realized total thrust during The Spirit DPI using the results obtained. (f_1=0.0302, f_2=7.0 N/m^2, f_3=0.0450, K=1.83, E_0=50 kPa)

The charts shown above demonstrate the fit using the results obtained earlier in the chapter. A better fit of the calculated to the realized thrust magnitudes is obtained by using the reduced frictional coefficients and an undrained (K=1) or passive (K>1) earth pressure condition. The applied pressure above minimal pressure was estimated in each scenario to obtain the best fit to the realized data. As noted, it is expected that a variable applied pressure above minimal pressure value would establish the best correlation with realized total thrust force during DPI construction.

6.5 SUMMARY

The realized thrust data obtained during the construction of three DPI projects provided measurable quantities to evaluate and compare with the recommended calculations. There are distinct differences between the realized data and the recommended calculation determined from this evaluation. The main conclusions from this analysis are as follows:

- Lubrication bentonite frictional coefficient ranges from 7.0 N/m to 65.0 N/m for the normalized and residual cases, agreeing in general with the recommended value of 50 N/m (Pruiksma, Pfeff, & Kruse, 2012).
- Surficial (roller) frictional coefficient ranged from 0.0216 to 0.0375 for the normalized and residual cases, which doesn't agree with the recommended value of 0.1 (Pruiksma, Pfeff, & Kruse, 2012). However, the values obtained in this research are in the range of typical rolling friction values from other industries, depending on the radius of the roller (Wen & Huang, 2018). After consideration to the radius of the roller, the values suggested from Wen & Huang (2018) agree with the values obtained form this research.
- Soil to pipeline interface friction coefficient measured from the Spirit DPI (Case Study 4) was 0.016, substantially lower than the recommended value of 0.2 (Pruiksma, Pfeff, & Kruse, 2012). It is expected that this discrepancy can be attributed to the application of the lubrication bentonite, where the interface friction could decrease as much as 90% (Namli & Guler, 2017) (Staheli, 2006). Additionally, there could be a "floating" effect of the pipeline within the tunnel (Pfeff D. , 2009) which further decreases the interface friction.
- Front cutting face force on the MTBM was measured ranging from 207 kN to 450 kN, substantially higher than the recommended range of 91.0 kN to 158.8 kN (Pruiksma, Pfeff, & Kruse, 2012) for the same locations along the tunnel alignment.
- Passive earth pressure coefficient increases the front force at the MTBM cutting face, which ultimately provides better agreement with the realized data.
- The measured front face force on the MTBM reduced by 37% to 44% after tunnelling 15 m to 23 m through native soil, suggesting that there is a "zone of optimization" where the operator adjusts the controlled machine parameters to ensure mining is most efficient. The

reduction in force could be reflected in a variable applied pressure above minimal pressure value based on machine parameters and soil properties.

- Using the parameters obtained in the chapter, the current state of practice calculation provides a relatively good fit to the realized thrust force data, allowing designers to more closely predict the required total thrust force during DPI construction.

CHAPTER 7. CONCLUSIONS AND RECOMMENDATIONS

7.1 SUMMARY

In this thesis, the current state of practice (Pruiksma, Pfeff, & Kruse, 2012) for calculating the required thrust force during DPI construction in clayey soil was assessed and evaluated using field-based comparison to data obtained from case studies. Using the trenchless pipeline installation method, developed by Herrenknecht, whereby a micro-tunnel boring machine is connected to a section of pipeline and thrust through soil or rock has proven to be beneficial. Among the many benefits of this method, successful completion of pipeline installations in all soil types has been why this construction practice had gained prominence industry wide.

To further the knowledge of DPI and reinforce the benefits of using such a method, it was imperative to review journal articles and documents pertaining to both tunnelling and DPI subjects. A document that was reviewed compiled by Pruiksma, Pfeff, & Kruse detailed the total thrust force calculation method. As part of this literature, ABAQUS finite element software was used to determine that five mechanisms contribute to the total thrust force, which can be grouped into the front force at the cutting face force and frictional effects.To examine the force at the MTBM cutting face, articles written by authors such as Zizka and Thewes (2016), Jancsecz & Steiner (1994), Babendererde & Elsner (2014) that discuss the required face pressure during tunnelling were reviewed. The authors found that the amount of face pressure required to stabilize the face is generally smaller than one would anticipate, and best explained by the theory of arching (Terzaghi, 1936). Frictional contributions are the other component of the total thrust force. These contributions include pipeline to roller, pipeline to lubrication fluid, and pipeline to soil interface frictional effects. Interface shear characteristics investigated by Iscimen (2004), and results

published by Bennet and Cording (2000), Marshall (1998) and Staheli (2006) show that residual friction angle of the dry soil in contact with the pipe should be used to establish frictional resistance. Additionally, Staheli suggests that up to 90% of reduction in soil to pipeline interface friction can be achieved using mass lubrication similar to the lubrication method used in DPI; results that were verified by Namli & Guler (2017). Finally, observations during case studies by Pfeff (2013) had indicated that frictional effects for DPI in cohesive soil are less than granular soil. The literature reviewed during this research, with the purpose of evaluating the total thrust force during DPI, allowed useful information to be compiled from both tunnelling and DPI topics; all of these assisted in the assessment.

In addition to researching articles by others, it was considered beneficial to also review case studies relative to the evaluation and assessment of the calculation method to estimate total thrust force during DPI. Review of four DPI case studies provided a basis for evaluation of the current state of practice calculation in the research. The information obtained during DPI construction included a description of the project, evaluation of the geotechnical conditions, and construction considerations. Review of the four case studies was a key component in the assessment of the calculation method used to estimate total thrust force in DPI construction.

Extensive review of the current state of practice provided insight into the components that may affect the final estimate of the total thrust. This method uses four frictional based equations, and one equation calculating front cutting face force to determine the total thrust force. Sensitivity analysis revealed that surficial (roller) friction and soil to pipeline interface friction were the most sensitive parameters in the calculations for the frictional component, while for the front cutting face force component they were the horizontal earth pressure coefficient and applied pressure above minimal pressure. Drained and undrained soil properties were investigated to evaluate their

significance to the final estimate of total thrust force. Findings from the comparison of the current state of practice calculated result to the realized data indicate that the calculation over predicted the total thrust force in three case studies (51% to 319% error), and under predicted in one (9% to 17% error). However, the data used for the under prediction was considered less reliable due to issues with data acquisition, including measurement frequency and an unexpected rise in the upper bedrock surface influencing construction. The steering cylinder force, considered the force at the cutting face of the MTBM, was obtained during a single case study; the calculation under predicted the realized force with 13% to 30% error.

A thorough evaluation of the most sensitive parameters was completed to establish a better fit to the realized total thrust data. The frictional resistance was evaluated by measuring the realized thrust to overcome the surficial (roller) friction and friction from the lubrication bentonite as the MTBM was lowered through the casing, then modifying the coefficients of friction to fit the data. The analysis indicates that the frictional coefficient of the rollers ranged from 0.0216 to 0.0375, and the lubrication bentonite frictional coefficient ranged from 30.5 N/m to 65.0 N/m. Due to the different data types obtained from the various machines included in the analysis, the soil to pipeline interface friction coefficient was determined during one case study only. Information from the single analysis showed the coefficient of friction that best fit the data was 0.016, much lower than the recommended value of 0.2. It is expected that this lower value obtained from this analysis reflect findings from Namli & Guler (2017) and Staheli (2006), where mass lubrication decreased the soil to pipeline interface friction by up to 90%. Pfeff D. (2009) suggested that the pipeline “floats” in the tunnel, further decreasing the effect of soil to pipeline interface friction.

The force on the MTBM cutting face was also assessed by reviewing the thrust force as the MTBM exited the casing and entered in situ soil. Results from this analysis indicate that the force at the

MTBM cutting face range from 207 kN to 450 kN, substantially higher than the calculated values at the same locations in the alignment. Use of the passive earth pressure coefficient increases the front cutting face force, thus providing a closer agreement between calculated and realized total thrust values. Additionally, the data shows that the force decreases by 37% to 44% after tunnelling through native soil for 15 m to 23 m. It is expected that there is a “zone of optimization” during which the operator optimizes machine parameters, and consequently the force on the MTBM cutting face will decrease. The reduction in force suggests that the force on the MTBM cutting face is highly dependent on machine operation parameters and could be calculated based on a combination of these operational conditions, as well as soil properties.

7.2 CONTRIBUTIONS OF THESIS

The main contributions of this thesis to the studied subject are as follows:

- The current state of practice for estimating the required thrust force generally over predicts the realized thrust when the recommended frictional coefficients (Pruiksma, Pfeff, & Kruse, 2012) are used, resulting in a conservative final estimate. (Chapter 3)
- Undrained soil analysis captures the force at the MTBM cutting face more reliably than the drained soil analysis in clayey soil. (Chapter 3)
- The contribution of both surficial and soil to pipeline interface friction to the total required thrust force is over estimated when using the recommended frictional coefficients (Pruiksma, Pfeff, & Kruse, 2012). (Chapter 4)
- The recommended bentonite lubrication frictional coefficient agrees well with the realized data. (Chapter 4)

- The front cutting face force is under estimated when compared to the realized data obtained during the case studies. (Chapter 4)
- The front cutting face force is highly dependent on the operational parameters of the MTBM. (Chapter 5).

7.3 CONCLUSIONS

This research has increased our understanding of Direct Pipe Installation™ (DPI) construction methods in clayey soil conditions by completing the research objectives reviewed in Chapter 1. The main conclusions of this thesis are outlined below:

- The current state of practice for estimating total thrust force during DPI construction was reviewed and evaluated, and the parameters which have the greatest influence on the result were determined. The current state of practice calculation method uses principles from HDD and Micro-tunnel design principles to estimate the total thrust. The magnitude of total thrust estimated by the calculation is a sum of the interface friction and the force at the MTBM cutting face. The parameters in the calculation which have the greatest influence on the result are the soil to pipeline interface friction coefficient, roller to pipeline interface coefficient, horizontal earth pressure coefficient, and the applied pressure above minimal pressure;
- The estimate of total thrust force was compared to the total thrust force realized during construction and the discrepancies have been evaluated. Findings indicate that the magnitude of thrust force estimated using the current state of practice outlined by Pruiksma, Pfeff, & Kruse in 2012 generally over predicts the realized total thrust data when using the recommended frictional coefficients while tunnelling in clayey soil conditions. The

discrepancies between the calculation and the realized magnitudes ranged from an under prediction of 9% to an over prediction of 319% when evaluated using average percent error analysis.

- The contribution of the frictional component of the estimated total thrust force was assessed and evaluated including modification of the frictional coefficients in the calculation. This thesis indicates that the frictional contribution is over estimated using the recommended frictional coefficients and that the magnitude of the frictional coefficients have an immense effect on the calculated value. The research suggests that these coefficients could be reduced substantially, potentially by an order of magnitude, resulting in a better prediction of the total thrust force.
- The contribution of the force at the MTBM cutting face to the total thrust force was assessed, and the differences in magnitude from the realized data during DPI construction were evaluated and quantified. The findings indicate that the amount of force on the MTBM cutting face is under estimated in clayey soil using the current state of practice calculation method and drained soil parameters, as recommended. Using undrained soil conditions in the analysis provides a better estimate, albeit still an underestimate, of the force on the MTBM cutting face. Using a passive horizontal earth pressure condition increases the front cutting face force providing a better estimate of the realized thrust force obtained in this research. Additionally, the applied pressure above minimal pressure should be calculated to accomplish a more accurate estimate of the force on the MTBM cutting face. Findings suggest that the applied pressure above minimal pressure could be estimated based on a combination of undrained soil properties and MTBM operational parameters.

7.4 RECOMMENDED FUTURE RESEARCH

There are multiple areas touched on by this thesis which require additional research. Recommendations for the main items that require additional research are outlined below:

- Verification of the pipeline to roller interface friction coefficients using experimental methodology. A large scale experiment could be completed to assess the frictional resistance of different roller configurations. Additional data for the frictional resistance of the pipeline to roller interface would assist in not only DPI, but other trenchless pipeline installation methods as well.
- Verification of the pipeline to soil interface friction during DPI construction in a mass lubrication scenario. Experimental design that can separate the soil to pipeline interface friction from the other complex coupled mechanical processes present during DPI would be helpful in further examination of the total required thrust force. Additionally, introduction of the bentonite lubrication into this experiment would assist in understanding the influence the lubrication has on the total thrust force in DPI.
- Empirical correlation of the applied pressure above minimal pressure with the MTBM controlled parameters and soil properties by collecting more data from the steering cylinders of the MTBM during DPI construction projects. Collecting the machine and geotechnical information for additional case studies would assist in assessment of their influence. Numerical modelling to confirm the empirical correlation of the value of the applied pressure above minimal pressure should also be completed.
- Specific research outlining the geometry and orientation of the cutters on the MTBM face and their effect on controlled machine parameters (torque, total thrust force, etc.) in both

granular and cohesive soils should be completed. The correlation of type and orientation of the cutters with controlled machine parameters could provide invaluable information about the amount of thrust force required during DPI construction. The undrained shear strength of clayey soils should be incorporated into the design of this type of research.

- Numerical modelling, experimental, and field-based studies on the effects of the vertical geometry of tunnel alignment on the total thrust force would be invaluable for estimating the total thrust force in DPI construction. The additional resistance to thrust because of geometric change in the tunnel alignment has been shown to contribute significantly to the total required thrust force. More information in this area would allow better prediction of the maximum thrust force needed during DPI construction, ultimately providing a better prediction of stress on the pipeline.

REFERENCES

Anagnostou, G., & Kovari, K. (1994). The Face Stability in Slurry-shield-driven Tunnels. *Tunnelling and Underground Space Technology No.2*, 165-174.

Babendererde, T., & Elsner, P. (2014). Keeping the face support in soft ground TBM tunnelling. In C. Yoo, S. Park, B. Kim, & H. Ban, *Geotechnical Aspects of Underground Construction in Soft Ground* (pp. 531-537). London: CRC Press.

Bennett, D., & Cording, E. J. (2000). Jacking Loads & Ground Deformations Associated with Microtunneling. *No-Dig 2000 Conference* (pp. 19-35). Anaheim: North American Society for Trenchless Technology.

Hollmann, F., & Markus, T. (2012). Evaluation of the Tendency of clogging and separation of fines on shield drives. *Geomechanics and Tunnelling 5*, 574-580.

Iscimen, M. (2004). *Shearing Behavior of Curved Interfaces.* Atlanta: Georgia Institute of Technology.

Jancsecz, S., & Steiner, W. (1994). Face support for a large mix-shield in heterogeneous ground conditions. *Proc Tunnelling'94* (pp. 531-550). London: Chapman and Hall.

Marshall, M. A. (1998). *Pipe-Jacked Tunnelling: Jacking Loads and Ground Movements.* Oxford: Magdalen College, University of Oxford.

Namli, M., & Guler, E. (2017). Effect of Bentonite Slurry Pressure on Interface Friction of Pipe Jacking. *Journal of Pipeline Systems Engineering and Practice*, 04016016.

Pfeff, D. (2009). The Direct Pipe Method - Latest Developments in Pipeline Construction (Paper B-2-03). *International No-Dig Show* (p. 7). Toronto: North American Society (NASTT) and International Society for Trenchless Technology (ISTT).

Pfeff, D. (2013, 10 15). *Method Statement, Direct Pipe.* Schwanau: Herrenknecht.

Pfeff, D. (2013). *Overview of Thrust Forces Needed on Realized Direct Pipe Projects.* Herrenknecht AG.

Pruiksma, J., Pfeff, D., & Kruse, H. (2012). *The calculation of the thrust force for pipeline installation using the Direct Pipe method.* Deltares/National Institute Unit Geo-engineering.

Sharma, J. R., Snider, A., Williamson, A. R., & Brown, C. R. (2014). A New Milestone for an Emerging Technology: Longest Direct Pipe Crossing in North America. *Proceedings of NASTT's 2014 No-Dig Show.* Orlando, Florida: North American Society for Trenchless Technology (NASTT).

Sivrikaya, O., & Togrol, E. (2006). Determination of undrained strength of fine grained soils by means of SPT and its application in Turkey. *Engineering Geology, Volume 86, Issue 1*, 52-69.

Staheli, K. (2006). *Jacking Force Prediction: An Interface Friction Approach Based On Pipe Surface Roughness.* Atlanta: Georgia Institute of Technology.

Terzaghi, K. (1936). Stress Distribution in Dry and Saturated Sand above a Yielding Trap-Door. *International Conference of Soil Mechanics, Vol. 1* (pp. 307-311). Cambridge: ISSMGE.

Uesugi, M., & Kishida, H. (1986, December). Frictional Resistance at Yield Between Dry Sand And Mild Steel. *Soils and Foundations, 26*(4), 139 to 141.

Wen, S., & Huang, P. (2018). *Principles of Tribology.* Hoboken, NJ: John Wiley & Sons Inc.

Zizka, Z., & Thewes, M. (2016). *Recommendations for Face Support Pressure Calculations for Shield Tunnelling in Soft Ground.* Deutscher Ausschuss fur unterirdisches Bauen e. V. (DAUB)/German Tunnelling Committee (ITA-AITES).